Heme-Containing Oxygenases

Masanori Sono,* Mark P. Roach, Eric D. Coulter, and John H. Dawson*

Department of Chemistry and Biochemistry, University of South Carolina, Columbia, South Carolina 29208

Received May 1, 1996 (Revised Manuscript Received August 13, 1996)

Contents

* To whom correspondence should be addressed.

S0009-2665(95)00050-1 CCC: $25.00

I. Introduction

A. Chemical Properties of Dioxygen[1−4]

Dioxygen (O_2) serves two essential functions in aerobic life. It is both a terminal electron acceptor and a biosynthetic reagent. It is this latter role for dioxygen that will be the focus of this review: the incorporation of one or both of the oxygen atoms of dioxygen into organic substrates by heme enzymes. These dioxygen-utilizing reactions involve the cleavage of the oxygen−oxygen bond and are very energetically favorable, i.e., exothermic. Despite this strong thermodynamic driving force, the chemical reactivity of dioxygen with organic molecules at ambient temperatures is intrinsically low. If this were not the case, dioxygen would spontaneously oxidize organic compounds and would therefore be harmful or even fatal rather than useful for living things. The low kinetic reactivity of dioxygen is due to its triplet ground state; i.e., it is a diradical having two unpaired electrons. The molecular orbital energy level configuration of triplet dioxygen is $(1s\sigma)^2(1s\sigma^*)^2(2s\sigma)^2(2s\sigma^*)^2(2p\sigma)^2(2p\pi)^4(2p\pi x^*)^1(2p\pi y^*)$.[1] The two oxygen atoms share six electrons in their 2p orbitals and the two unpaired electrons reside in the two degenerate antibonding $2p\pi x^*$ and $2p\pi y^*$orbitals, leaving O_2 with a formal bond order of two. The lowest orbital available to accept an electron is an antibonding orbital.

Although dioxygen has a triplet ground state, essentially all stable organic compounds are singlets; i.e., all of their electrons are paired. Direct reactions between triplet and singlet molecules to yield a singlet product is a spin-forbidden process because chemical combination reaction rates are much faster than spin inversion rates. Such reactions can proceed via the spin-allowed, but highly energy-requiring formation of an unstable triplet intermediate, followed by slow spin inversion to form a singlet product. Thus, only easily oxidizable singlet organic molecules are able to react with triplet dioxygen by first forming resonance-stabilized (one-electron oxidized) radicals. Reduced flavins (RH_2), for example, are thought to react with triplet dioxygen via initial formation of a caged radical pair (a triplet complex), followed by spin inversion to singlet products (eq 1).[4]

$$XH_2 + O_2 \rightarrow [XH^{\bullet} + HO_2^{\bullet}] \rightarrow XH{-}O_2H \quad (1)$$

Although singlet oxygen is more readily reactive (free of spin restrictions) than triplet dioxygen, a considerable amount of energy is required for the spin inversion from the triplet state to the singlet state. Of the two singlet states of O_2, the lower energy one has both electrons in one of the antibonding π^* orbitals and is 22.5 kcal/mol above the triplet state. Triplet O_2 can be converted to the singlet state with light in the presence of a photosensitizer.

In contrast to the inherent difficulty of triplet dioxygen reacting with singlet organic molecules, it will react readily with organic radicals ($R^{\bullet}$), i.e., doublets (eq 2). Another way to overcome the high

$$R^{\bullet} + O_2 \rightarrow RO_2^{\bullet} \quad (2)$$

kinetic barrier inherent to the reactions of triplet O_2

Masanori Sono was born in Nagasaki Prefecture, Japan. He graduated from the University of Tokyo with B.S. (1970), M.S. (1972), and Ph.D. (1975) degrees in pharmaceutical sciences. He began studying heme proteins with Professor Toshio Asakura at the University of Pennsylvania as a pre- and postdoctoral research associate working on heme modifications and reconstitution of hemoglobin and myoglobin (1972–1977) and then as an instructor with Professor Osamu Hayaishi at the Kyoto University, Japan, studying the functional properties of heme-containing oxygenases (1977–1980). Moving back to the United States in 1980, he has continued studying heme enzymes with Professor John H. Dawson in the Department of Chemistry and Biochemistry at the University of South Carolina, currently as Research Associate Professor. His major research interests focus on spectroscopic and mechanistic aspects of heme-containing oxygenases and peroxidases including cytochrome P450, chloroperoxidase, indoleamine 2,3-dioxygenase, and recently, nitric oxide synthase.

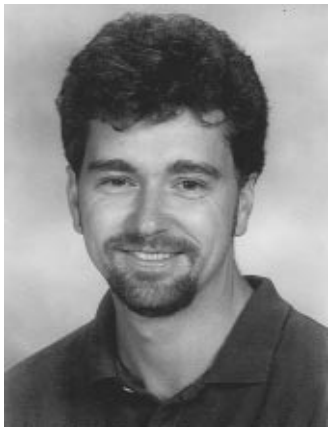

Mark P. Roach, a fourth year graduate student in the Department of Chemistry and Biochemistry at the University of South Carolina, was born in Montreal, Canada, in 1970. Prior to joining Professor John Dawson's research group, he spent four years at Mount Allison University in Sackville, NB, Canada, where he received his B.Sc. in chemistry in 1992. He is currently engaged in cytochrome P450 model studies and investigations of structure and function relationships in novel peroxide-dependent halogenating and dehalogenating heme enzymes isolated from marine sources. Following graduation, he plans to pursue postdoctoral studies at a yet-to-be-determined location. (Coming soon to a lab near you.)

Eric D. Coulter was born in Belfast, Northern Ireland, in 1969. He obtained his B.Sc. in biological chemistry from the University of Ulster at Coleraine, Northern Ireland, in 1991. He is currently finishing his Ph.D. thesis research under the direction of Professor John Dawson in the Department of Chemistry & Biochemistry at the University of South Carolina. His research interests include the mechanism of action of cytochrome P450, heme-protein reconstitution, and the application of magnetic circular dichroism and electron paramagnetic resonance spectroscopy to study heme systems. He will be pursuing postdoctoral studies in the laboratory of Professor David Ballou in the Department of Biological Chemistry at the University of Michigan.

John H. Dawson was born in Englewood, NJ, in 1950 and attended Columbia University where he majored in chemistry and received an A.B. degree in 1972. In 1976, he received his Ph.D. degree in chemistry with a minor in biochemistry from Stanford University where he worked with Professors Carl Djerassi and Bruce Hudson. He was next a National Institutes of Health Postdoctoral Fellow with Professor Harry Gray in the Chemistry Department at the California Institute of Technology. In 1978, he joined the Chemistry and Biochemistry Department at the University of South Carolina with a joint appointment in the School of Medicine. He was promoted to Professor and named Carolina Distinguished Professor in 1986. Earlier this year, he returned to CalTech on sabbatical as a Visiting Associate in the Beckman Institute with Professor Gray. His research interests focus on the structure and function of oxygen and peroxide activating heme iron enzymes and on the application of spectroscopic methods, especially magnetic circular dichroism, to probe their coordination structure.

is to utilize a transition metal ion such as iron or copper as the cofactor in enzymes that carry out biological oxidations. Transition metals in the appropriate oxidation states are able to react directly with triplet O_2 to form dioxygen adducts that can participate in reaction pathways leading either to the incorporation of oxygen atoms into organic substrates or to the oxidation of the organic substrates.

Because of the key role played by dioxygen and its reduced forms in biological oxidation processes, the four stepwise one-electron reductions of dioxygen to water are illustrated in Figure 1. The standard redox

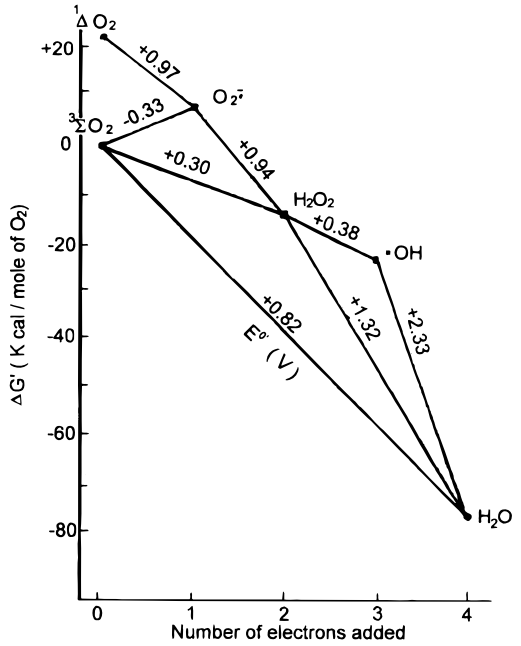

Figure 1. Free energy changes and standard reduction potentials (pH 7.0, 298 °C) for reduction of ground-state dioxygen ($^3\Sigma O_2$) to various oxygen species. The standard state used here is unit pressure (i.e., $[O_2] = 0.25$ mM) rather than unit activity ($[O_2] = 1$ M).[1d] Adapted from ref 1a.

potential at pH 7.0 and 298 K ($E^{\circ\prime}$, V) and free energy change ($\Delta G^{\circ\prime}$, kcal/mol) for each electron addition step are also indicated.

B. Discovery and Classification of Oxygenases

Prior to 1955, it was thought that the sole role of dioxygen in biological systems was as an electron acceptor in dioxygen-utilizing oxidase or dehydrogenase reactions. It was in that year that Mason[5] and Hayaishi[6] independently demonstrated by $^{18}O_2$ labeling that one or both oxygen atoms of dioxygen can be directly incorporated into organic molecules following enzymatic oxidation of 3,4-dimethylphenol by phenolase and catechol by pyrocatechase, respectively. The enzymes that incorporate oxygen atoms from dioxygen in such reactions were designated as "oxygenases" by Hayaishi.[7] It is now known that oxygenases are extensively distributed in nature throughout the plant, animal, and microorganism kingdoms.

The oxygenases can be further classified into two categories, monooxygenases and dioxygenases, depending on whether one or both oxygen atoms from dioxygen are incorporated into substrate (eqs 3 and 4),[7] where XH and AH_2 represent substrate and an

monooxygenase:

$$XH + {}^*O_2 + AH_2 \rightarrow X(^*O)H + H_2{}^*O + A \quad (3)$$

dioxygenase:

$$XH + {}^*O_2 \rightarrow X(^*O_2)H \quad (4)$$

electron donor, respectively. Monooxygenases require two electrons to reduce the second oxygen atom of dioxygen to water. Thus, monooxygenases are sometimes called "mixed-function oxidases" or "mixed-function oxygenases" since they function as both oxygenase and oxidase. The two electrons can come from a reducing agent like NADH (external mo-

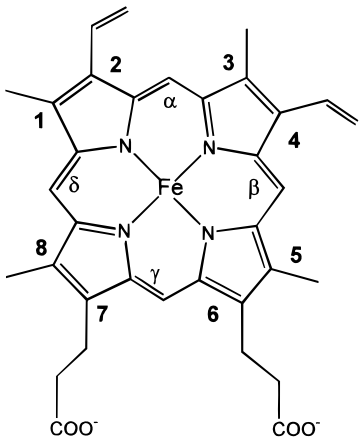

Figure 2. Structure of protoheme IX (iron protoporphyrin IX, heme *b*).

nooxygenase) or from the substrate itself (internal monooxygenase). Similarly, dioxygenases are subcategorized into intermolecular and intramolecular classifications depending on whether the two oxygen atoms are incorporated into separate substrates or into a single molecule. Clearly, the terms mono- and dioxygenase relate only to the stoichiometry of the oxygen incorporation reaction and not to the mechanism of dioxygen activation.[2,6]

C. Structure and Reactivity of Heme Iron-Bound Dioxygen[8]

The most common heme prosthetic group is protoheme IX (iron protoporphyrin IX, heme *b*) (Figure 2). It is the prosthetic group found in all of the heme enzymes to be discussed in this review. The role of the heme group in these oxygenases varies from case to case depending on the nature of the heme proximal ligand, the heme environment, and the substrate. Many of the heme-containing oxygenases go through a ferrous−dioxygen complex as a key intermediate in their catalytic reaction cycles. Consequently, the electronic structure of this species will be considered here in some detail.

The ferrous high-spin state (d^6, $S = 2$) state of heme iron can reversibly form a complex with triplet O_2 yielding a low-spin complex that is generally described as either $Fe^{2+}O_2$ or $Fe^{3+}O_2^{\bullet-}$ or a resonance hybrid of these two forms ($Fe^{2+}O_2 \leftrightarrow Fe^{3+}O_2^{\bullet-}$) (see Figure 4 in ref 8a and Figure 2 in ref 8b for their qualitative molecular orbital schemes). For the $Fe^{2+}O_2$ structure, π bond formation is possible by back donation from a ferrous ion orbital (e.g., d_{xz}) to the empty π_{O_2}* orbital. The $Fe^{2+}O_2$ complex is a singlet. Transfer of one electron from iron to the bound dioxygen yields the ferric−superoxide structure, $Fe^{3+}O_2^{\bullet-}$. An unpaired electron on the superoxide resides in its antibonding π orbital (π_{O_2}*), while a second unpaired electron is in a nonbonding iron orbital (d_{xy}). In either resonance structure, ferrous dioxygen or ferric superoxide, the complex is *diamagnetic*; there are no unpaired electrons in the former case and the two unpaired electrons are considered to be spin-coupled in the latter. The actual electronic structure may involve partial electron transfer from iron to bound dioxygen, i.e., $Fe^{(2+\delta)+}O_2^{\delta-}$.

In the case of cytochrome P450 and secondary amine monooxygenase, the ferric superoxide structure may be the best description since the enzyme heme-bound dioxygen is ultimately reduced by two electrons to the level of peroxide, O_2^{2-}. Coordination of dioxygen to ferrous heme and subsequent one-electron transfer from iron to oxygen can be thought of as the first reduction of dioxygen in this process. For indoleamine and tryptophan dioxygenases, however, the ferrous dioxygen structure may be a more accurate description of their reactivity. Further reduction of the heme-bound dioxygen is not part of their reaction cycles. However, the complex formed between ferrous heme iron and triplet O_2 must be a singlet for reasons previously described. The bound dioxygen is not singlet O_2 but can react by an ionic mechanism to give products that are similar to those that would be produced by the reaction of singlet O_2.[1,2]

II. Cytochrome P450 (P450)

A. Background[9−24]

Shortly after the discovery of oxygenases by Mason and Hayaishi, Garfinkel[25] and Klingenberg[26] independently described the presence of a CO-binding pigment in liver microsomes which exhibited an unusual absorption band maximum near 450 nm in the ferrous−CO minus ferrous difference absorption spectrum. Six years later, Omura and Sato[27] identified this unusual pigment as a heme protein containing protoheme IX (Figure 2) and assigned it the name "cytochrome P450" despite the absence of knowledge about its function. The unusual spectral properties of P450 were first attributed by Mason[28] to the coordination of a sulfhydryl sulfur atom to the heme iron of the enzyme. A particularly important breakthrough occurred in 1963 when Estabrook and coworkers demonstrated a catalytic role for the pigment in the C-21 hydroxylation of 17-hydroxyprogesterone by adrenal cortex microsomes.[29] This was accomplished through measurement of a photochemical action spectrum generated by monitoring the reversal of CO inhibition of the enzyme activity by light as a function of wavelength. The observed maximum reversal of CO inhibition at 450 nm connected the enzymatic activity with the absorbance of the P450 pigment. Liver microsomal P450 is now known to exist in multiple forms and to play important roles in the hydroxylation of endogenous, physiological substrates as well as a tremendous range of drugs and other chemicals foreign to organisms (termed "xenobiotics"). In fact, exposure to certain xenobiotics leads to induction of particular P450 proteins. Furthermore, over 450 different P450 enzymes are now known to exist. They have been found in virtually every mammalian tissue and organ as well as in plants, bacteria, yeast, insects, and so on. A nomenclature system has been developed to relate each P450 sequence based on their structural homology.[30] These P450 enzymes catalyze diverse types of reactions as illustrated in Figure 3.

With the exception of microbial P450s, the majority of P450 enzymes are membrane-bound, being associated with either the inner mitochondrial or the endoplasmic reticulum (microsomal) membranes. In fact, the majority of the physiological substrates such as steroids and fatty acids as well as xenobiotic

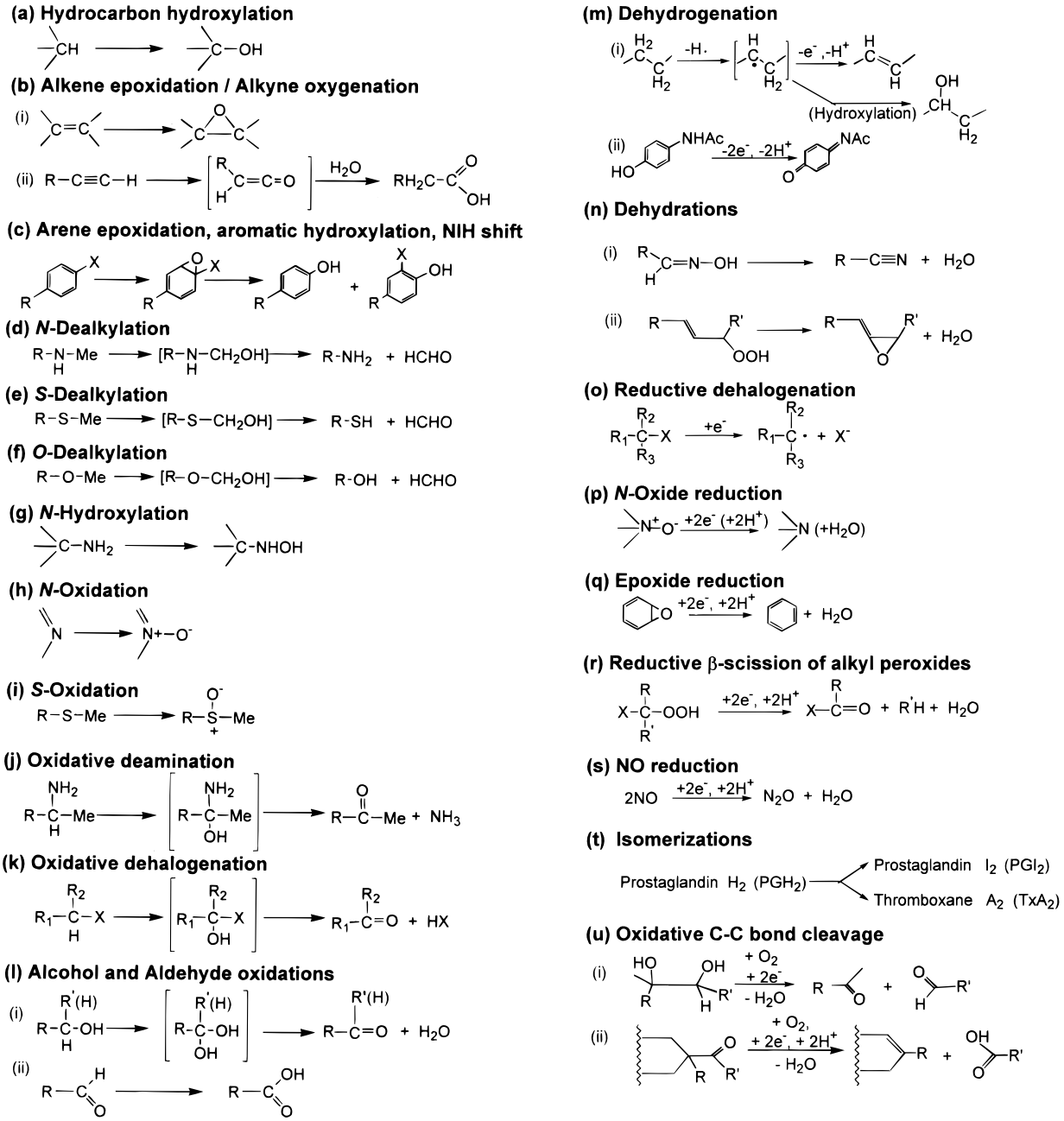

Figure 3. Schematic summary of the diverse P450-catalyzed reactions discussed in this review. See text (especially section IIK) for references (for reactions *l* - *u*).

molecules that react with P450 are highly hydrophobic as well. Oxygenation of membrane-trapped xenobiotics by nonconstitutive liver microsomal P450s to yield partially water soluble derivatives for excretion from the body has been called "membrane detoxification". In contrast to these highly beneficial roles, P450 has a "bad" side in its ability to convert certain otherwise unreactive xenobiotics to highly reactive, electrophilic metabolites which alkylate DNA, thereby accounting for their carcinogenicity.[31]

Initial efforts to release the membrane-bound P450s from the membrane by detergent solubilization led to loss of monooxygenase activity as well as a shift of the characteristic 450-nm absorption peak to 420 nm in the difference absorption spectrum. The inactive form of P450 was thus termed "cytochrome P-420" by Omura and Sato.[27] Subsequently, successful solubilization and purification of the active forms of the P450 proteins and the associated electron transport components were achieved for the mitochondrial and liver microsomal P450 monooxygenases, initially by Estabrook and Coon and their respective co-workers.[29,32] A soluble, camphor-inducible, bacterial P450 monooxygenase (P450-CAM) system was discovered in *Pseudomonas putida* by Gunsalus and co-workers.[33] Being soluble, it was quickly possible to purify this P450 in large quantity. As a result, many important mechanistic and spectroscopic investigations of P450 as well as the first successful X-ray crystallographic analysis have been carried out with P450-CAM.[19,34]

B. Electron Transport Systems[15,32]

In catalyzing monooxygenation reactions, P450 is able to utilize either NADH or NADPH as the electron donor (eq 5). However, the two electrons

$$RH + O_2 + NAD(P)H + H^+ \rightarrow ROH + H_2O + NAD(P)^+ \quad (5)$$

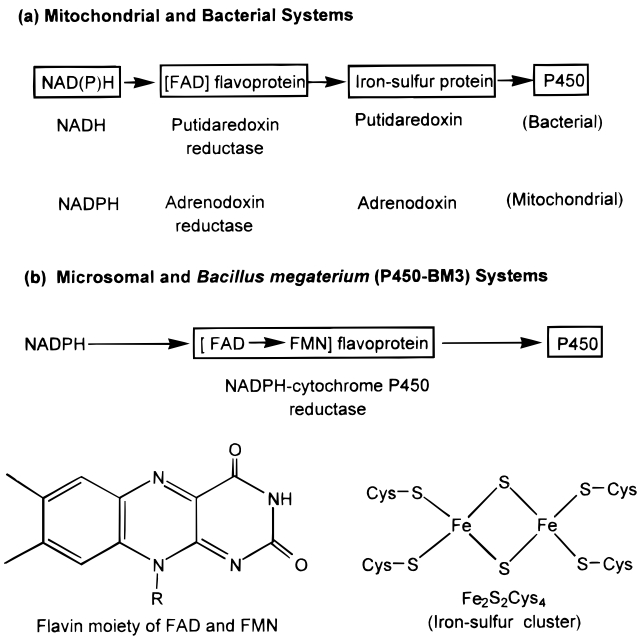

Figure 4. Electron donors and transport pathways for the mitochondrial and bacterial (a) and for the microsomal and *Bacillis megaterium* (b) cytochrome P450 systems. The structures of the flavin moiety of FAD and FMN (bottom, left) and of the $Fe_2S_2Cys_4$ cluster (bottom, right) are also shown.

derived from NAD(P)H must be transferred to P450 via electron transport protein(s). There are two types of electron transport protein systems (Figure 4), those involving flavin *and* iron−sulfur prosthetic groups and those that require only flavins.[20] Most bacterial P450s as well as mitochondrial P450 systems employ the former system in which electrons flow from NAD(P)H to an FAD-containing protein to an iron−sulfur protein to P450. In contrast, the microsomal P450 system utilizes a single flavoprotein, NADPH-cytochrome P450 reductase, which contains *both* FAD and FMN, to transport electrons from NADPH to P450. In some microsomal P450 reactions, the NADH-cytochrome b_5 reductase/cytochrome b_5 electron transport system may participate in delivering electrons.[13] Finally, a very unusual bacterial P450 from *Bacillis megaterium*, P450-BM3,[35] has been studied that utilizes the microsomal-type electron transport system (i.e., both FAD and FMN without the iron−sulfur component). Even more unusual, the protein is "self-sufficient" in that it has both the electron carrier component and the monooxygenase heme iron unit present in one large single subunit protein.[20,35] Nitric oxide synthase (see section IIK.5), a complex enzyme that contains both flavin and a P450-type heme center, is also self-sufficient.

C. Molecular Structure of P450

Poulos, Kraut, and co-workers reported the first X-ray crystal structure of a P450 enzyme, the soluble bacterial P450-CAM.[34d] Consisting of 414 amino acid residues (M_r ~45 000), the protein has a triangular shape with the heme plane nearly parallel to the plane of the triangle. The heme prosthetic group is deeply embedded in the hydrophobic interior with no significant exposure of the heme to the protein surface. The identity of the proximal heme iron ligand as a cysteine had been established based on earlier spectroscopic work.[9] The crystal structure demonstrated that the specific cysteine that is bound to the heme iron is Cys-357. Four P450 crystal structures have now been published including those for the heme domain of P450-BM3,[36] P450-TERP,[37] and P450-eryF,[38] the latter two being bacterial P450s that hydroxylate α-terpineol and erythronolides, respectively. The overall structures of camphor-bound ferric P450-CAM and of the heme-containing domain of ferric P450-BM3 are shown in Figure 5. Comparisons of the structures of these four P450s have been extensively discussed by Poulos[19] and by Peterson,[20] as well as the relationship between the structures of these soluble bacterial P450s and those of membrane-bound eukaryotic P450s, in the latter review.

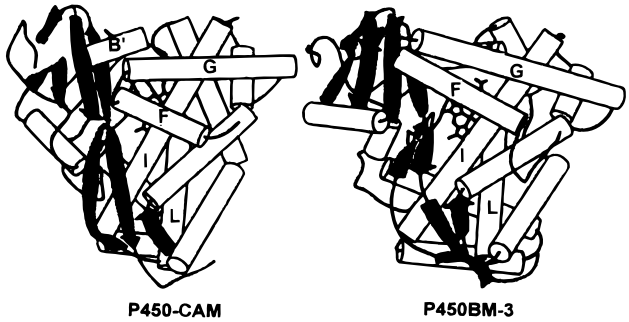

Figure 5. Schematic representation of the crystal structures of camphor-bound ferric cytochrome P450-CAM (left) and of the heme domain of substrate-free ferric cytochrome P450-BM3. Helices are indicated by cylinders and β structure by shaded ribbons. Taken from ref 19 based on data presented in refs 34a and 36.

The binding of camphor to ferric P450-CAM is accompanied with the displacement of five to six water molecules that fill the camphor pocket prior to substrate binding. Except for Tyr-96, which forms a hydrogen bond to the C-2 carbonyl group of camphor, the camphor-binding pocket is lined with nonpolar amino acid residues. Positioning of the substrate is conferred through hydrophobic interactions such as that between its C-8 and C-9 methyl groups and the isopropyl side chain of Val-295.

Comparison of the amino acid sequences of P450-CAM and of many mammalian P450 proteins has revealed two regions of sequence similarity. One region is that containing the Cys proximal ligand. A second region of sequence conservation is that corresponding to Thr-252 of P450-CAM, which is located on helix I and can directly contact the dioxygen molecule in the P450−O_2 complex.

D. Reaction Cycle of P450

1. Reaction Cycle and Intermediates

The monooxygenation reaction catalyzed by *P. putida* P450-CAM[9,18,33] in the hydroxylation of (1*R*)-camphor is given in eq 6.

The P450 reaction cycle involves four well-characterized and isolable states[9,15] (**1**−**4** in Figure 6). The resting form of the enzyme is a six-coordinate low-spin ferric state, **1**, with water (or hydroxide) as the exchangeable distal ligand *trans* to the proximal cysteinate. Substrate addition generates the five-coordinate high-spin ferric state, **2**, which has a vacant coordination site that will ultimately be

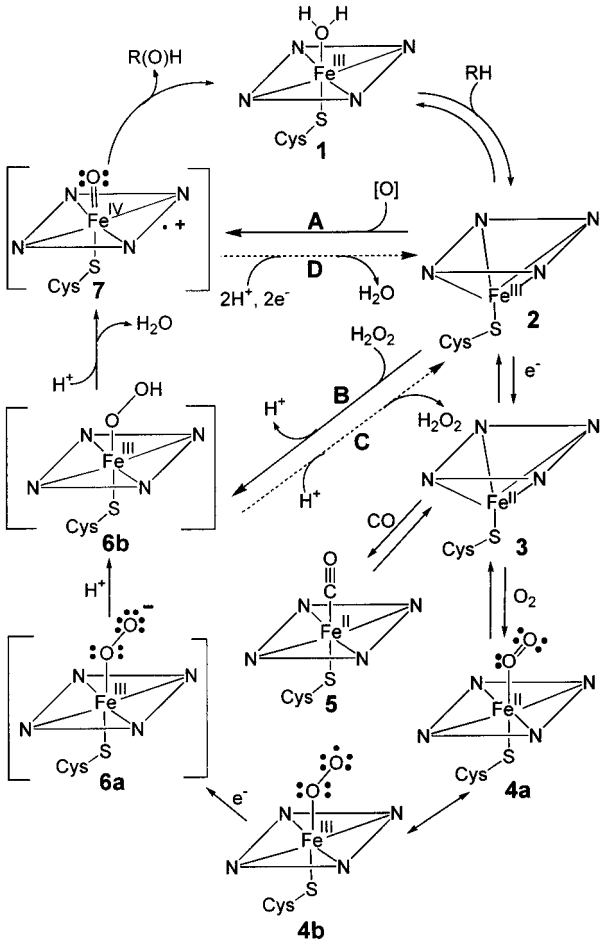

Figure 6. Catalytic cycle of cytochrome P450 including postulated structures of putative intermediates. RH represents the substrate and R(O)H the product. The diatomic porphyrin macrocycle is abbreviated as a parallelogram with nitrogens at the corners. States **6a**, **6b**, and **7** are hypothetical intermediates whose structures have not been established. Structures **1**, **2**, and **7** are neutral (the dot and the positive charge on **7** indicated the radical state and electron deficiency of the π-electron system of the porphyrin ring), while the overall charge on structures **3**, **4a**, **4b**, **5**, and **6b** is −1 and on intermediate **6a** is −2. Two artificial ways of turning over the enzyme are indicated: path A involves the addition of various single oxygen atom donors to state **2** to generate **7** and path B is for the addition of H_2O_2 to **2** to form **6b**. Two modes of uncoupling electron and oxygen transfer, C and D, are also shown.

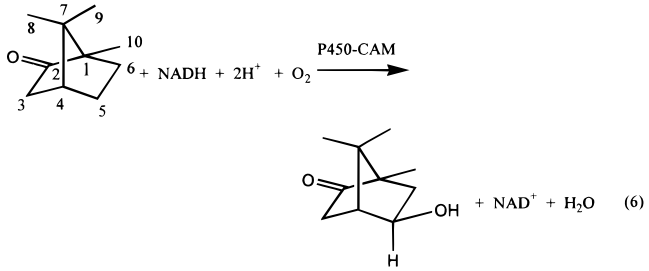

(6)

available for dioxygen binding. Conversion of the ferric iron from low to high spin results in a significant increase in the redox potential ($E°'$) of the enzyme heme (−330 to −173 mV vs NHE). Thus substrate binding facilitates electron transfer from reduced putidaredoxin ($E°'$= −196 mV) to the ferric P450 heme to generate the five-coordinate high-spin deoxyferrous state, **3**. Dioxygen then binds to the ferrous enzyme heme iron to form the oxyferrous complex, whose valence structure can be presented either as the ferrous−O_2, **4a**, or as the ferric−superoxide, **4b**, complex as described above. CO addition to **3** yields the ferrous−CO inhibitor adduct, **5**, with its characteristic absorbance peak near 450 nm.

P450 states **1**−**5** have all been isolated in stable form and have been extensively studied with UV−visible absorption, electron paramagnetic resonance (EPR), magnetic circular dichroism (MCD), resonance Raman, proton nuclear magnetic resonance, Mössbauer, and extended X-ray absorption fine structure (EXAFS) spectroscopies.[9] X-ray crystal structural analysis of P450-CAM states **1**, **2**, and **5** have further established the structures of these P450 species.[19,34] It was the spectroscopic studies on these P450 intermediates and of parallel model porphyrin complexes that convincingly established the presence of the cysteinate axial ligand in the heme iron coordination structures of P450 states **1**−**5** (see refs 9a and 9b and references cited therein). Axial coordination by cysteinate accounts for the unusual spectroscopic properties of ferrous−CO P450 and its other derivatives.[9,36]

Addition of the second electron to **4**, the-rate limiting step in the cycle,[39] is proposed to yield a ferric peroxide adduct, **6a**, which can be protonated to give a hydroperoxide complex, **6b**. A second protonation of that same oxygen then leads to heterolytic O−O bond cleavage releasing water and generating the proposed oxo−ferryl ($O=Fe^{IV}$) porphyrin radical intermediate, **7**, which is equivalent to the high-valent iron−oxo intermediate of peroxidase enzymes called compound I. The mechanism of formation and properties of this reactive P450 species will be discussed further below. Intermediate **7**, sometimes represented as $(FeO)^{3+}$, is the most likely candidate for the "reactive oxygen" form of P450 that hydroxylates unactivated hydrocarbon substrates. The P450 reaction cycle is completed when **7** transfers an oxygen atom to the substrate, presumably by an oxygen rebound mechanism,[16] to give the alcohol product and to regenerate **1**.

2. Short Circuit or Peroxide Shunt

Numerous oxygen atom donors can replace the two electrons (NADH or NADPH) and O_2 which are required for the normal catalytic cycle and react directly with **2** via a "short circuit" or "peroxide shunt"[12,21,32] path (labeled A) to generate oxygenated products likely through **7**. These oxygen atom donors include alkyl peroxides, peracids, sodium chlorite, sodium periodate, and iodosobenzene (also called iodosylbenzene). Interestingly, these same "artificial" oxygen donors are able to convert ferric peroxidase heme enzymes to compound I.[17] Some P450 enzymes are able to turn over using H_2O_2 as the source of the oxygen atom,[21] presumably via short-circuit path B. H_2O_2, of course, is the natural substrate for peroxidase enzymes.

3. Uncoupling of Electron Transfer to Oxygen Transfer

With (1*R*)-camphor, the P450 cycle occurs with nearly 100% coupling[40,41] of electron transfer (**2** → **3** and **4b** → **6a**) to oxygen transfer (**7** → **1**). One mode of uncoupling electron transfer from oxygen transfer is via autoxidation of oxyferrous P450.[18] This pro-

duces superoxide ($O_2^{\bullet-}$) which disproportionates nonenzymatically to H_2O_2 and O_2 in aqueous media. This type of uncoupling is considered to be of little significance because one-electron reduction of oxyferrous P450 is usually much faster than autoxidation. Two additional uncoupling pathways have been described.[18,40,41] Protonation of **6b** on the unprotonated oxygen releases H_2O_2 generating **2** and *no* oxygenated product (path **C**, **6b** → **2**, two-electron uncoupling). Note that NADPH and O_2 are consumed in a 1:1 ratio for this uncoupling reaction. Alternatively, two-electron reduction and diprotonation of the oxo group in **7** yields a second H_2O (path D, **7** → **2**, the four-electron "oxidase" reaction), regenerates **2**, and again produces *no* oxygenated product (**7** → **2**, four electron "oxidase" uncoupling). This uncoupling reaction differs from the one described above in that O_2 and NADPH are consumed in a 1:2 ratio. It has been observed for microsomal P450 with perfluoro-*n*-hexane[42] and for P450-CAM with deuterated norcamphor[40] and with (1*R*)-5,5-difluorocamphor.[41]

Poulos has discussed the most likely causes of these latter two uncoupling reactions based on examination of the crystal structures of complexes of P450-CAM with various camphor analogs and of site-directed mutants of P450-CAM with modified substrate binding sites.[43] High substrate mobility in the active site and the presence of excess water near the heme iron have been suggested as possible explanations. Although water is the ultimate source of the protons that are required for the normal catalytic reaction, the presence of excess water in the active site could promote the various uncoupling reactions. In related work, Sligar and co-workers have thoroughly demonstrated that steric factors on the distal side of the heme strongly influence the coupling of oxygen and electron transfer in P450-CAM and the partitioning between two-electron and four-electron uncoupling.[18]

E. Cleavage of the O–O Bond of Heme Iron-Bound Peroxide

A distinguishing feature of monooxygenases is their ability to reductively cleave the O−O bond of dioxygen to generate a "reactive oxygen" species ("oxenoid reagent") capable of oxygen atom insertion into hydrocarbon substrates. In the P450 reaction cycle (Figure 6), this is accomplished by one-electron reduction of the P450−O_2 complex, **4**, to form a ferric peroxide complex ($Fe^{3+}O_2^{2-}$, **6a**) followed by protonation of the outer oxygen atom twice, first to give **6b** and then to induce heterolytic O−O bond cleavage to generate **7**. The alternative of homolytic O−O bond cleavage has frequently been discussed and is generally not thought to be involved in the normal monooxygenation process.[13]

1. "Push–Pull" Mechanism for Peroxidases

Heme-containing peroxidases also carry out heterolytic O−O bond cleavage, although they start from the ferric state and bind hydrogen peroxide to form the high-valent iron−oxo intermediate known as compound I. For cytochrome *c* peroxidase, a general "push−pull" mechanism (Figure 7) for this process has been proposed by Poulos based on the X-ray crystal structure of the enzyme.[34b] The "push" is

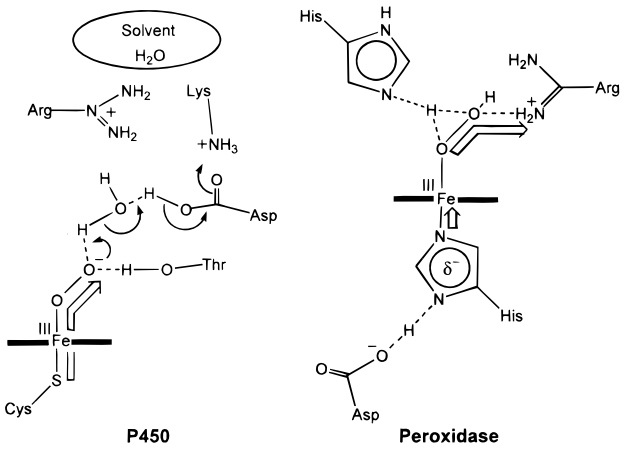

Figure 7. Schematic view of the "push−pull" mechanisms for O−O bond cleavage of an iron-bound peroxide in thiolate-ligated (left) and histidine-ligated (right) systems such as P450 and horseradish peroxidase, respectively. Adapted from refs 9b, 44, 49, and 52a (left) and 9b and 34b (right).

provided by the proximal histidine ligand whose electron donor capabilities are enhanced via hydrogen bonding to a neighboring carboxylate group, thereby increasing its imidazolate character relative to the corresponding non-hydrogen-bonded proximal histidine in hemoglobin or myoglobin. This may also help to stabilize higher oxidation states of the heme iron during catalysis. At the same time, the distal histidine accepts a proton from the oxygen atom of hydrogen peroxide that binds to the heme iron and transfers it to the other oxygen to generate a good leaving group. The distal histidine works in concert with an appropriately positioned cationic residue (protonated arginine) to facilitate heterolytic O−O bond cleavage of the iron-bound peroxide, with the latter stabilizing developing negative charge on the outer oxygen during bond cleavage. The combination of the distal histidine and arginine provide the "pull" effect (Figure 7).

2. "Push" Effects of Proximal Thiolate Ligand for P450

P450 lacks the distal machinery present in the peroxidases and has a proximal ligand different from typical peroxidases. Twenty years ago, in fact, Dawson proposed that the P450 proximal thiolate ligand serves as a strong internal electron donor to facilitate O−O bond cleavage to generate **7**.[44] Three lines of evidence for the "big push" (strong electron-releasing character) of the proximal cysteinate have been reported. First, bound distal thiolate ligands show enhanced basicity *trans* to the endogenous cysteinate of P450-CAM relative to parallel myoglobin adducts.[45] Second, significant differences have been reported for the affinities of anionic ligands to ferric P450 and myoglobin, with anionic ligands having much lower affinity for ferric P450, presumably due to the electron- releasing character of the proximal thiolate ligand.[46] More recently, Dawson and co-workers have observed shifts in the X-ray absorption energies for thiolate-ligated heme iron derivatives relative to those lacking a thiolate ligand to provide a direct measure of the strong electron-releasing nature of thiolate axial ligand.[47] Experimental support for the postulated "push" effect of the axial thiolate coordination to the ferric heme, which favors the heterolytic

O−O bond cleavage of the heme-ligated peroxides, has been provided using an axial His → Cys mutant myoglobin[48a] or a thiolate-ligated iron porphyrin model system.[48b] Once the O−O bond is heterolytically cleaved, the electron-releasing axial thiolate ligand helps to stabilize the high-valent nature of **7**.

3. Proton Delivery by Distal Side Groups in P450

The "big push" of the cysteinate proximal ligand cannot, by itself, accomplish the cleavage of the O−O bond; there must also be a source of protons to enable the outer oxygen of the bound peroxide in state **6a** to leave as water. Sligar has proposed a distal charge relay involving two distal side amino acids, Thr-252 and Asp-251 in P450-CAM, to carry out the proton donation.[49] Thr-252 has been proposed to form a hydrogen bond to the heme iron-bound dioxygen moiety in **4** and **6a**. According to Sligar's proposal, Thr-252 and Asp-251 form a proton relay network that works in conjunction with two other charged amino acids to reach the surface solvent to provide a conduit for protons. Replacement of Thr-252 with Ala leads to loss of hydroxylation activity (by ∼95%) by P450-CAM without significant changes in NADH and O_2 consumption rates (i.e., with increased uncoupling).[50] Similarly, replacement of the corresponding Thr-268 with Ala for P450-BM3 results in a considerable decrease in substrate (laurate) hydroxylation (by ∼85%) and increased uncoupling.[51] Ishimura and co-workers[52] have proposed a refinement of the role of Thr-252[53] based on their studies with the "artificial" amino acids *O*-methylthreonine and *S*-methylthreonine incorporated into P450-CAM in place of Thr-252. They observeed 40% of normal activity with *O*-methyl-Thr[54a] and lack of activity with *S*-methyl-Thr[54b] and concluded that the oxygen of Thr-252 positions a water molecule to deliver protons to the iron-bound peroxide, rather than the proton on the threonine hydroxyl group serving as a direct proton donor. The ferrous-O_2 intermediate of the Thr-252Ala mutant is considerably more autoxidizable (by a factor of ∼100) than wild-type P450-CAM.[50b,52b] Interestingly, the Thr-252Ser mutant retains an efficient hydroxylation activity and a rate that are comparable to those of the wild-type enzyme.[50a,54] These results suggest that the Thr-252 residue stabilizes the ferrous P450−O_2 intermediate through hydrogen bond formation between its hydroxyl group and the distal oxygen of the bound O_2 (Figure 7). Poulos has proposed that protons are delivered during catalysis via a solvent access channel or from an internal solvent pool, i.e., protein-bound water.[19,34] On the other hand, substitution of Asp-251 with Asn[49] or Ala[54] drastically diminishes NADH and O_2 consumption rates (by ∼95%) by lowering the reduction rate of the oxy−ferrous P450 intermediate, suggesting an important role of the Asp residue in the electron transfer reaction.

F. Nature of the P450 Reactive Oxygen Intermediate

1. Oxo–Ferryl Porphyrin π-Cation Radical Species as an Electrophilic Oxygen Transfer ("Oxenoid") Reagent

The electrophilic nature of the P450 active oxygen intermediate is well-known.[9,13,16,18,21] With aliphatic hydrocarbon substrates, for example, when all the substrate carbon atoms have equal access to the active site heme iron, reaction occurs preferentially at the more electron rich tertiary C−H bonds followed by secondary and then primary sites.[13] Monosubstituted aromatic compounds are mainly hydroxylated at the *ortho* and *para* positions as expected for an electrophilic aromatic substitution reaction. These reaction patterns support the strongly electrophilic nature of the P450 active oxygen species. An oxo−ferryl ($O{=}Fe^{IV}$) porphyrin π-cation radical such as intermediate **7** in Figure 6 (formally equivalent to an oxygen atom bound to ferric iron) might well be expected to transfer oxygen (eq 7) via an electrophilic

$$O{=}Fe^{IV}(P^{\bullet+}) + RH \rightarrow Fe^{III}(P) + ROH \qquad (7)$$

(oxenoid) mechanism. Strong support for this idea has come from the functional P450 model systems developed by Groves and co-workers.[16,55] They have reported numerous examples of oxygen transfer to alkanes and alkenes from suitable oxygen donors such as iodosobenzene catalyzed by various ferric porphyrins. Of particular importance, they have been able to isolate and to spectroscopically and chemically characterize a green oxo−ferryl porphyrin π-cation radical species.[16,55] Further, they have shown that this complex is capable of oxygen transfer reactions. These results strongly support the ability of oxo−ferryl porphyrin π-cation radicals to carry out oxygen atom transfer to the organic substrates (eq 7).

2. Search for the P450 Reactive Oxygen Intermediate

Little is known about intermediates beyond oxy-P450 in the O_2-dependent cycle. In 1976, Coon, Ballou, and co-workers[56] used rapid kinetics to detect two intermediates upon mixing of photoreduced rabbit liver microsomal P450-2B4 with O_2 in the absence of NADPH and P450 reductase; no further information has been forthcoming concerning the identity of these intermediates. In a later study of cumene hydroperoxide-supported toluene hydroxylation by P450-2B4, Blake and Coon[57] detected two reversibly formed spectral intermediates termed C and D. The species C is involved in the hydroxylation while species D is a compound II-type, dead-end complex. However, spectral properties of both C and D are dependent on the peroxides used. Kobayashi and co-workers have spectrophotometrically examined the one-electron reduction product of the ferrous−O_2 complex of 2,4-diacetyldeuteroheme-reconstituted P450-CAM at 25 °C by pulse radiolysis and found that a compound II (oxo−ferryl) rather than compound I (oxo−ferryl porphyrin cation radical)-like species is formed.[58a] In a separate study, Kobayashi and co-workers examined the addition of superoxide anion to ferrous P450-CAM.[58b] They observed an intermediate that spectrally resembles oxyferrous P450-CAM and decays to the native ferric state. A small amount of hydroxylated camphor was formed in the process. Davydov et al. have presented preliminary evidence for an EPR-detectable intermediate upon X-ray irradiation of oxyferrous P450-CAM at 77 K in the presence of camphor.[58c] Tajima et al.[59] have reported that reaction of *n*- or *tert*-butyl hydroperoxide with P450-2C11 yields a ferric low-spin species (77 K) having EPR *g* values (2.29, 2.24,

1.96) which are very similar to those of a thiolate−ferric heme−alkyl peroxide complex (2.285, 2.198, 1.959). None of these results are supportive of the postulated compound I-type intermediate of P450. On the other hand, evidence in support of an oxo−ferryl porphyrin π-cation radical (compound I-like) intermediate in the short-circuit pathway has been presented recently by Ishimura.[60] Following earlier work by Wagner and Dunford,[61] rapid-scan stopped-flow absorption spectroscopy was used to study the interaction of camphor-free ferric P450 with an artificial oxygen donor, *m*-chloroperbenzoate.[60] They reported preliminary evidence for the appearance of a species with an absorption spectrum that closely resembles that of chloroperoxidase compound I: a thiolate-ligated oxo−ferryl porphyrin π-cation radical.[62]

3. Analogy to Chloroperoxidase Compound I

Chloroperoxidase is an unusual heme enzyme isolated from the marine fungus *Cardariomyces fumago* by Hager and co-workers[63] that functions as a peroxidase, a catalase, or halogenation catalyst. Extensive spectroscopic similarities to P450 support the conclusion that chloroperoxidase also has a cysteinate proximal ligand.[9] That conclusion has recently been confirmed with X-ray crystallography by Poulos and co-workers.[64] Chloroperoxidase forms a spectroscopically detectable and isolable compound I intermediate. Is this chloroperoxidase derivative a good model for the P450 active oxygen intermediate? In general, peroxidase compound I intermediates function as oxidants rather than as oxygen atom donors. Substrate oxidation occurs at the heme edge, and the iron-bound oxo group is shielded from the substrate to prevent oxo transfer.[65] In the case of P450, the substrate is bound in close proximity to the deeply buried heme and oxo transfer is the dominant reaction. With chloroperoxidase, both peroxide-dependent oxidations and oxo transfer with alkenes, sulfides, and alkylamines ("peroxygenations") occur.[65] Thus, chloroperoxidase compound I seems to be a good reactivity model for the P450 reactive oxygen intermediate. The major factor that differentiates the functions of these two thiolate-ligated heme proteins appears to be the difference in their active site protein structure, which controls substrate accessibility to the iron−oxo group or to the heme edge.[65]

On the other hand, evidence against the involvement of a thiolate-ligated oxo−ferryl porphyrin π-cation radical intermediate in the P450 reaction cycle also exists. White compared the oxidative reactivity of several P450 enzymes with that of peroxidase enzymes and concluded that if both enzyme mechanisms involve an oxo−ferryl intermediate, then these species are somehow very different in both their mode of formation and reactivity.[66] Characterization of the active oxygen intermediate in the P450 reaction cycle remains one of the most challenging areas of P450 research.

4. Postulated Candidates for the P450 Reactive Oxygen Intermediate

While it is often presumed that the P450 "reactive oxygen" intermediate is a peroxidase compound I-type species with a thiolate ligand, **7,** there are at least two other reasonable resonance formulations for such a complex (Figure 8). Calculations by Loew and co-workers[67] have suggested that the P450 active oxygen species is an oxygen-based radical, **7a**. The most generally accepted mechanism for hydrocarbon oxygenation by the P450 active oxygen species, the oxygen rebound (see section IIG), is initiated by hydrogen atom abstraction; that reactivity is consistent with at least some radical character on the oxo oxygen. A resonance structure having an iron-bound sulfur radical, **7b**, has also been proposed.[32,42] This structure is based on the premise that the sulfur ligand is easier to oxidize than the porphyrin macrocycle. Until the P450 active oxygen intermediate is actually observed, the discussion about its electronic structure is really more speculation than substance.

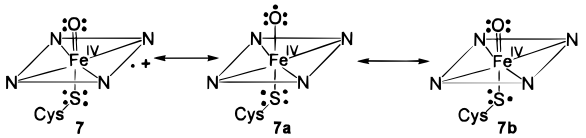

Figure 8. Three different resonance structures proposed for the putative P450 active oxygen intermediate.

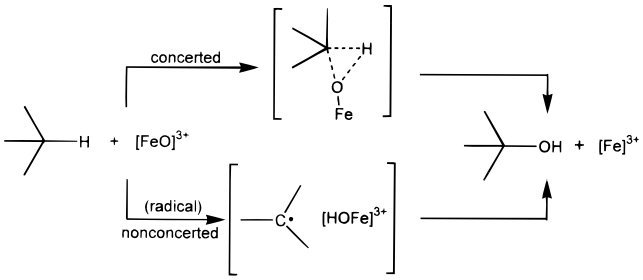

Figure 9. Schematic illustration of the concerted and nonconcerted (radical) mechanisms for hydrocarbon hydroxylation by P450. $[FeO]^{3+}$ and $[Fe]^{3+}$ represent the active oxygen P450 species (state **7**) and resting ferric P450 (state **1**), respectively.

G. Mechanism of Alkane Hydroxylation

The mechanism of P450-catalyzed hydroxylation of unactivated hydrocarbons (Figure 3a) was initially proposed to follow a concerted insertion pathway (Figure 9, top) based on the frequent retention of stereochemistry and very small apparent kinetic isotope effects ($k_H/k_D < 2$).[68] In the late 1970s, however, more sophisticated investigations of these same two mechanistic parameters, stereochemistry and isotope effects, provided new information that led to the opposite conclusion: the mechanism is a two-step abstraction and recombination process (Figure 9, bottom). Very recently, a new set of experiments has drawn the radical mechanism into question. The evidence in favor of the radical mechanism and the recent results challenging that conclusion will now be presented.

1. Isotope Effects

The hydroxylation of hydrocarbons by monooxygenase enzymes is a reaction in which a C−H bond is broken and an oxygen atom is inserted to produce an alcohol, C−O−H. If the breakage of the C−H bond is the rate-limiting step in the reaction, replace-

ment of the hydrogen with deuterium can lead to a change in the rate. This change is referred to as the kinetic isotope effect. The magnitude of the isotope effect provides information about the mechanism by which the C−H bond is broken provided that C−H bond breakage is rate limiting.

Early studies of the kinetic isotope effect for P450-catalyzed hydroxylations gave relatively low values ($k_H/k_D < 2$) that were cited as evidence for a concerted "oxene" insertion mechanism.[69] In 1977, however, Hjelmeland et al.[70] demonstrated for the first time that the isotope effect for benzylic hydroxylation was much larger ($k_H/k_D > 11$) than had ever been reported previously. This result was followed quickly by a similar study of aliphatic hydroxylation by Groves et al. in which an isotope effect of comparable magnitude was reported.[71] The difference between the earlier investigations and those of Hjelmeland[70] and of Groves[71] was that the latter studies determined the isotope effect in an *intra*molecular manner. The earlier, *inter*molecular isotope effects were determined by simply measuring the rate of hydroxylation of a particular substrate and then remeasuring the rate when the site of hydroxylation was deuterated. When C−H bond breakage is *not* rate limiting, however, this method gives a low value. In those cases, it is said that the isotope effect has been masked. The intramolecular isotope effect method involves examining a molecule with two symmetrically related C−H sites, one of which is proton-bearing and the other deuterated. In such a molecule, the only step that will be sensitive to deuteration will be the step in which the C−H bond is broken. The fact that such a large isotope effect was observed by Hjelmeland[70] and by Groves[71] was cited as evidence in favor of a mechanism involving complete breakage of the C−H bond during catalysis. Lack of carbocation rearrangements (see below) and the extremely low acidity of typical aliphatic C−H bonds argued against mechanisms involving carbocations and carbanions, respectively. This suggested a two step radical mechanism involving (i) abstraction of a hydrogen atom at the C−H site of reaction to generate a carbon radical and hydroxy radical bound to the heme iron and (ii) recombination of the two radicals to give the alcohol.

Recently, Dawson and co-workers[41] have directly observed a large intermolecular isotope effect ($k_H/k_D > 11$) for substrate C−H activation using a derivative of camphor, the physiological substrate for P450-CAM, in which the normal site of hydroxylation is blocked with fluorines.[41] They had previously shown that this substrate, 5,5-difluorocamphor, reacts almost exclusively at C-9 to form the primary alcohol at a substantially diminished rate.[72] The ratio of the independently measured rates of hydroxylation of that substrate and its 9,9,9-d_3 analog was in excess of 11. The observation of such a large isotope effect in an intermolecular study suggests that the rate-limiting step for hydroxylation of that substrate by P450-CAM has switched from electron to oxygen transfer.[41]

2. Stereochemical Scrambling

In 1978, Groves et al. observed that hydroxylation of (*exo,exo,exo,exo*-2,3,5,6-d_4 norbornane (Figure 10A) by purified liver microsomal P450 (P450-2B4) led to considerable stereochemical scrambling.[55b,71] The monohydroxylated *exo* and *endo* alcohols, a, a′, b, and b′, were formed (Figure 10A). The detection of an *endo* alcohol with only *three* deuterium atoms (b) and an *exo* alcohol with all *four* deuterium atoms (a′) showed that the reaction did not proceed with retention of stereochemistry. Stereochemical scrambling was also reported by Sligar and co-workers[73] for the hydroxylations of (5-*exo*- or (5-*endo*-d_1)camphor by P450-CAM (Figure 10B). They found that P450-CAM could remove either 5-*endo* or 5-*exo* hydrogen (deuterium) from camphor, but hydroxylation occurred only at the 5-*exo* position. It was subsequently demonstrated by Groves and Sabramanian[74] using purified rabbit liver microsomal P450-2B4 that the allylic rearrangement of double bonds was induced upon hydroxylation of (3,3,6,6-d_4)cyclohexene (Figure 10C, c vs d). White and co-workers[75] have also shown that substantial (up to 40%) stereochemical inversion (crossover) occurred in the P450-catalyzed hydroxylation of the *S* and *R* enantiomers of (1-d_1)phenylethane (ethylbenzene) (Figure 10D).

3. Mechanistic Implications Favoring the Oxygen Rebound Mechanism

The large intra- and intermolecular isotope effect and stereochemical scrambling observed for hydrocarbon hydroxylation by various P450 isozymes strongly support a two-step mechanism involving complete breakage of the C−H bond to give a discrete intermediate with a finite lifetime. Such an intermediate can in principle be either a carbon radical or carbocation, both of which are planar at the carbon center and can thus recombine with a hydroxyl radical or anion, respectively, on either side of the plane. These two mechanisms can be distinguished by the relatively large intrinsic deuterium isotope effects ($k_H/k_D = 10-14$) observed,[70,71,76] which are most consistent with a hydrogen atom abstraction (to generate a carbon radical), followed by hydroxyl radical recombination ("oxygen rebound") to form the hydroxylated hydrocarbons (Figure 9, bottom).[55b,77] This radical mechanism is also supported by the absence of skeleton-rearranged alcohol products which were expected to be generated from a carbocation intermediate when certain substrates such as norcarane (bicyclo[4.1.0]heptane)[78] and methylcyclopropane (*vide infra*) were employed for P450-catalyzed hydroxylation. Stereospecific hydrocarbon hydroxylations by P450 can be attributed to the rigid and stereospecific binding of the substrates to the particular enzyme active sites. This is especially true for bacterial and constitutive mammalian P450s, the latter of which hydroxylate specific endogenous substrates (e.g., sterols). With xenobiotic-inducible and metabolizing microsomal P450s, on the other hand, a relatively wide substrate specificity is observed, implying a loose contact with the substrates at their active sites.

4. Radical Clocks

The proposed carbon radical intermediate in the P450 cycle would not be expected to have a long enough lifetime to be directly observed. However, as initially reported by Ortiz de Montellano and co-

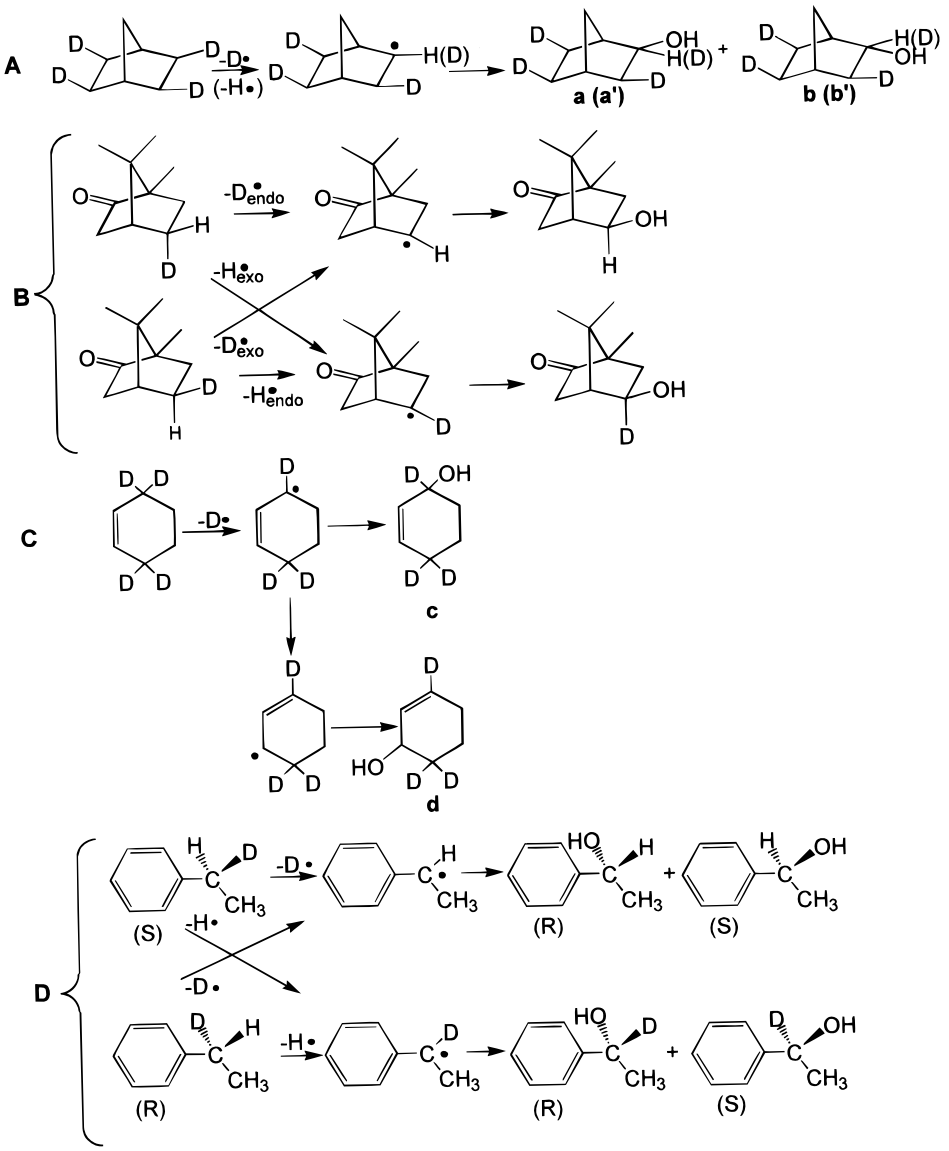

Figure 10. Illustrations of P450-catalyzed hydrocarbon hydroxylation reactions in which stereochemical scrambling occurs. (A) Reaction of P450-2B4 with (2,3,5,6-*exo*-d_4)norbornane.[71] (B) Reaction of P450-CAM with (5-*exo*- and 5-*endo*- d_1)camphor.[73] (C) Reaction of P450-2B4 with (3,3,6,6-d_4)cyclohexene.[74] D. Reaction of P450-2B4 with both enantiomers of (1-d_1)-phenylethane.[75]

workers, its existence and lifetime can be estimated using "radical clock"[78−80] substrates that have highly strained carbocyclic structures such as methycyclopropane and bicyclo[2.1.0]pentane (1,2-methylenecyclopentane) (Figure 11).[78] A carbon radical localized adjacent to the cyclopropane ring of such substrates rearranges to another ring-opened carbon radical at a known rate (k_r).[79,80] Hence, the rate of oxygen rebound (k_{OH}) can be estimated by examining the ratio of unrearranged/rearranged hydroxylated products. Methylcyclopropane (and the other simple cyclopropanes initially examined)[81] yielded only unrearranged alcohol, suggesting that the carbon radical rearrangement rate ($k_r = \sim 10^8$ s^{-1}) is relatively slow as compared with the oxygen rebound rate (k_{OH}). Alternatively, the carbon radical of bicyclo[2.1.0]-pentane has a sufficiently fast rearrangement rate (2.1×10^9 s^{-1})[78,79] to compete with the hydroxyl radical recombination rate (k_{OH}); this substrate gave a mixture of the unrearranged and rearranged alcohol products in a ratio of 1:6.5−7.[78,79] Thus, the k_{OH} value for this substrate was calculated to be 1.4×10^{10} s^{-1}.[78,81]

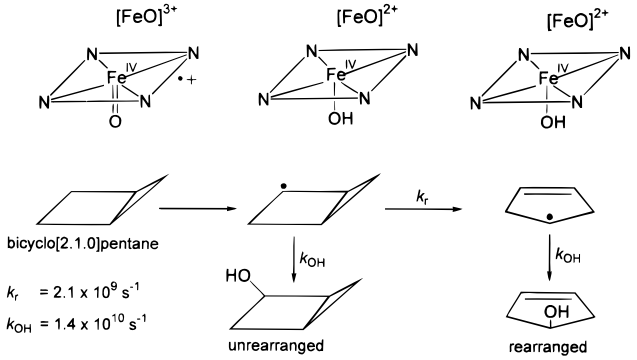

Figure 11. Use of bicyclo[2.1.0]pentane as a radical clock for P450-2B1-catalyzed hydrocarbon hydroxylation to estimate the rate of the radical rebound reaction between the substrate carbon radical and the enzyme iron-bound hydroxyl radical. The rate of the hydroxyl radical transfer reaction (k_t) is calculated from the ratio of the rearranged to unrearranged alcohol products and the known rate of the rearrangement reaction (k_r). Adapted from ref 78.

Recently, however, some researchers have reported results using faster radical clock substrates that

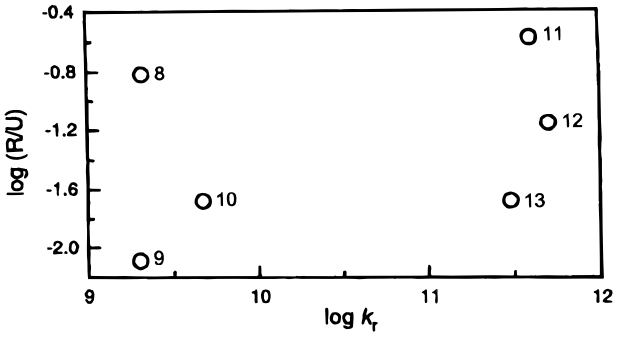

	k_r at 37°C (s^{-1})		Microsomal	
	U•	R•	[UOH]/[ROH]	"k_{OH}" (s^{-1})
8	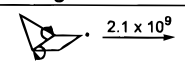		6.5-7	1.4×10^{10}
9	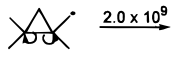		124	2.5×10^{11}
10	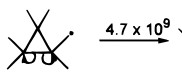		48	2.3×10^{11}
11	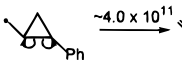		3.8	$\sim1.5\times10^{12}$
12	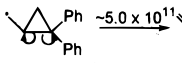		14.5	$\sim7\times10^{12}$
13	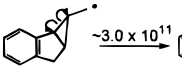		37-48	$\sim1.3\times10^{13}$

Figure 12. (Top) Plot of the ratio of rearranged (R) to unrearranged (U) alcohol products [log (R/U)] vs log k_r (k_r is the rate of ring opening of a given radical) for the P450-2B4-catalyzed hydroxylation of substrates **8**−**13**. (Bottom) Table showing the unrearranged (U•) and rearranged (R•) radicals formed during the P450-catalyzed reaction with substrates **8**−**13** along with the rate of ring opening (k_r), the [UOH]/[ROH] ratio, and the estimated oxygen rebound rate ("k_{OH}") for each substrate. Taken from refs 81 and 83 (copyrights 1993 and 1994, respectively, American Chemical Society).

challenge the radical mechanism of P450-catalyzed hydroxylations of hydrocarbons. Atkinson and Ingold[81] found that the four cyclopropane derivatives shown in Figure 12 (**9**−**12**) also gave a mixture of the unrearranged and rearranged alcohol products in various ratios upon hydroxylations catalyzed by the rabbit liver microsomes and by purified P450-2B4 (Figure 12). The k_r values for these substrates range from fast (10^9 s^{-1}) (**9** and **10**) to ultrafast (10^{11} s^{-1}) (**11** and **12**) values. Of particular note, the calculated k_{OH} values for these fast-clock substrates varied from 10^{11} (**9** and **10**) to 10^{12} s^{-1} (**11** and **12**), which are 1−2 orders of magnitude higher than the value determined for bicyclo[2.1.0]pentane (**8**). The k_{OH} values for the latter two ultrafast substrates (**11** and **12**) are unreasonably high. The possibility that steric effects at the enzyme active site might slow the radical clocks for **11** and **12** and yield overestimated k_{OH} values was considered. However, results with two systems argue against that suggestion. (i) Both enantiomers [(1*S*,2*S*) and (1*R*,2*R*)] of **11**, which are expected to interact differently with the enzyme active site, gave similar product distributions as well as apparent k_{OH} values.[82] Furthermore, (ii) the new constrained substrate **13**, which would be less likely to be subject to steric effects, also gave an incredibly high apparent k_{OH} value of $\sim1.3\times10^{13}$ s^{-1}.[83] This value was essentially equal to the rate constant for decomposition of a transition state. The plot of the ratio of rearranged (R) to unrearranged (U) alcohol products [log(R/U)] vs log k_r (Figure 12, top) clearly reveals a lack of correlation between these parameters. A linear correlation would be expected from a radical "oxygen rebound" mechanism because higher k_r values would produce more rearranged alcohol products. Actually, much less rearranged product was found for **13** than expected while the opposite is true for **8**.

5. Ionic Mechanism Involving a Carbocation Intermediate

To explain these puzzling findings, Newcomb, Hollenberg, and their co-workers have suggested an ionic mechanism.[83] Unfortunately, the previously employed radical clock substrates (e.g.; **8**−**13**) do not distinguish between radical and carbocation intermediates because both would give the same rearrangement products.[84] To overcome this problem, Newcomb and co-workers have introduced an ultrafast radical clock substrate, (*trans*,*trans*-2-*tert*-butoxy-3-phenylcyclopropyl)methane (**14** in Figure 13), as a hypersensitive probe which can distinguish between radical and carbocation intermediates on the basis of the identity of the rearranged products.[83,84] Hydroxylation of this hypersensitive probe by rat liver microsomes and by the purified microsomal P450-2B1 reconstituted system gave the unrearranged alcohol **16** with two rearranged minor products, **18** and **22**, in a molar ratio of 22:1:2.5.[84] These latter two products were derived from **14** by ring opening toward the phenyl substituent (via a carbon radical, **15** → **17)** and toward the *tert*-butoxy substituent (via a carbocation**, 20** → **21),** respectively. In addition, substantial amounts of aromatic ring-hydroxylated products (**23**) were also produced. These results led Newcomb to conclude that both radical and carbocation mechanisms were involved in the rearrangements. Variable partitioning between the radical and carbocation mechanisms would explain the wide range of k_{OH} values described above (e.g., Figure 12). They also suggested that the relatively low k_{OH} values ($<10^{11}$ s^{-1}) determined in some cases might have resulted from greater involvement of the carbocation mechanism.

Since many of the radical clock substrates examined previously yielded exclusively unrearranged alcohol products, obligatory carbocation formation can be excluded; it is known that the cyclopropylcarbinyl cation exists only in resonance with its ring-opened homoallyl cation (e.g., **20** ↔ **21**) rather than as a discrete compound.[84,85] Thus, the following two mechanisms for the carbocation formation have been suggested: (i) A radical intermediate, **15**, formed by hydrogen atom abstraction (**14** → **15**) is further oxidized to a carbocation (**15** → **20)** in competition with the oxygen rebound reaction (**15** → **16**). Alternatively, (ii) P450 catalyzes the formation of a protonated alcohol by OH^+ (not OH as indicated in ref 84) insertion into the methyl C−H bond (**14** → **19**), followed by competition between deprotonation to form the unrearranged alcohol (**19** → **16**) and loss of water to give the carbocation (**19** → **20**). This OH^+ insertion mechanism is analogous to the theoretical proposal of Bach et al.[86] for P450-catalyzed hydroxylations. The latter process, however, requires het-

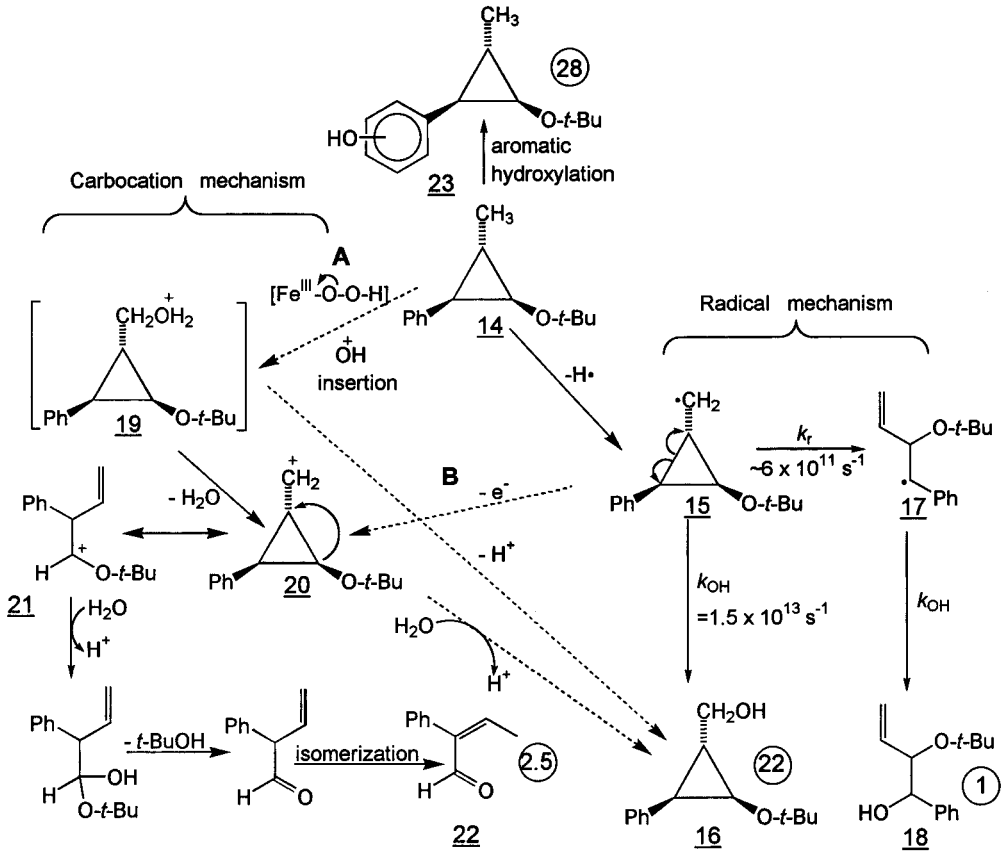

Figure 13. Pathways for the hydroxylation reaction of the calibrated hypersensitive radical probe substrate (*trans,trans*-2-*tert*-butoxy- 3-phenylcyclopropyl)methane (**14**) with cytochrome P450-2B4. Adapted from ref 84.

erolytic O−O bond cleavage of the P450 ferric peroxide (Fe^{III}−OOH) state to generate OH^+ and ferric−oxo $Fe^{III}O^{2-}$ [$(FeO)^+$] species.[84] This is opposite to the generally accepted mechanism of heterolytic O−O bond cleavage to generate compound I [Fe^{III} + oxygen atom = $(FeO)^{3+}$] and water (OH^- + H^+).

Newcomb and co-workers then re-evaluated the oxygen radical rebound rate constant as well as its mechanism. Using the ratio of the radical-derived rearranged product, **18**, to the sum of unrearranged alcohol, **16**, plus cation-derived rearranged product, **22**, which is 1:(22 + 2.5) = 1:24.5, they calculated an oxygen rebound rate constant (k_{OH}) (**15** + •OH → **16**) of 1.5×10^{13} $s.^{-1}$.[87] This value is very similar to that previously determined for the constrained radical clock substrate **13** in Figure 12. From this value, they determined the lifetime of the radical to be ~70 fs.[87]

The extremely short lifetime (<100 fs) of the radical intermediates derived from these substrates has led these researchers to propose the mechanistic sequence depicted in Figure 14, in which the progress of bond cleavage and formation are schematically described in terms of nuclear motion and energy changes. It was suggested that since the oxygen rebound process occurs at a rate (~10^{13} s^{-1}) comparable to that of a single Fe−O bond vibration, there is no activation energy, and therefore no intermediate, in that process. This is apparently contradictory to the observation that a portion (~5%) of the radical underwent rearrangement. However, these researchers postulated this to be a theoretically feasible situation, where one can consider that zero activation energy process (collapse to unrearranged product)

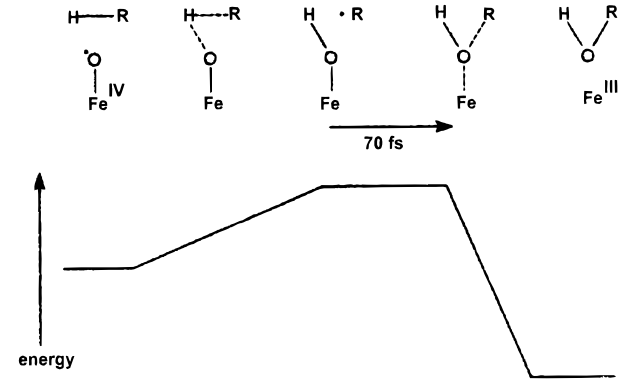

Figure 14. Sequence of nuclear motions in the cytochrome P450- catalyzed hydroxylation of alkanes proposed by Newcomb et al. The P450 reactive oxygen intermediate (**7**) is arbitrarily shown as an Fe^{IV}−oxyl radical (**7a**). Taken from ref 84 (copyright 1995, American Chemical Society).

and a small activation energy process (rearrangement) compete. Such a reaction process inevitably requires that the hydroxylation reaction is a concerted insertion as opposed to the sequential process of oxygen rebound reaction. Despite the concerted nature of the hydroxylation reaction, the short but finite lifetime of the radical indicates that nuclear motion is nonsynchronous; i.e., abstraction of the hydrogen atom from carbon must precede the formation of the C−O bond. Newcomb and co-workers[84] then concluded that a lifetime of less than 100 fs is too short for hydrogen atom abstraction to occur with a linear or near-linear C−H···O−Fe arrangement as is generally accepted for the nonconcerted oxygen rebound mechanism, but instead a "side-on" approach of the oxygen atom to the C−H bond would be required so that the oxygen atom is within bonding

distance to carbon at the moment of hydrogen atom abstraction.

6. Remaining Mechanistic Uncertainties

Although the carbocation mechanism proposed by Newcomb et al.[84] (also by Bach et al.[86]) rationalizes the above-mentioned inconsistencies with the radical mechanism, the following critical questions remain unanswered. First, is the carbocation mechanism in competition with the radical mechanism in all P450 hydroxylation reactions? If so, why do certain radical clock substrates (e.g., norcarane[77] and methylcyclopropane) not give skeletal-rearranged products as would be expected from a carbocation intermediate? Second, the evidence of stereochemical scrambling (Figure 10), which was used to exclude the concerted oxygen insertion mechanism, is contradictory to the "concerted nonsynchronous" mechanism proposed by Newcomb et al. How can these two incompatible mechanisms be reconciled? Third, the "ultrafast" radical clocks ($k_r = \sim 4 \times 10^{11}$ s^{-1}), **11** in Figure 12, were previously shown by several researchers including Ingold and Newcomb to exhibit a large primary deuterium kinetic isotope effect of ~8 for the methyl group hydroxylation.[82] This large isotope effect, as well as the values in excess of 11 described above, seem to be inconsistent with the oxygen side-on mechanism (Figure 14), which gives relatively small primary isotope effect.

Establishment of a definitive mechanism for P450-catalyzed hydroxylation of hydrocarbons, using radical clock probes in particular, requires further studies. For example, the identification of the source of the oxygen atom, either O_2 (radical mechanism) or H_2O (carbocation mechanism), incorporated in the rearranged alcohol products for such radical clock substrates as those (e.g., **8**−**13** in Figure 12) that would give identical products by the two mechanisms, should provide useful information which should be able to quantitatively demonstrate whether a cation intermediate is indeed involved.

H. Mechanism of Alkene Epoxidation[11,16,21]

The insertion of an oxygen atom into the carbon−carbon π bond of an olefin by cytochrome P450 yields epoxide products (Figure 3b.i), most often with retention of stereochemistry; e.g., epoxidation of a *cis* olefin gives a *cis* epoxide.[88,89] Although this observation is consistent with a concerted oxygen atom transfer mechanism (Figure 9, top), it is now generally agreed that the mechanism of olefin epoxidation by P450 is a stepwise process initiated by formation of a charge transfer complex (Figure 15).[11,21,90,91] From the charge transfer complex, a variety of paths ensue leading to epoxide formation, heme alkylation, or group transfer to a carbonyl-containing product. In general, the charge transfer complex undergoes electron transfer to an olefin cation radical. This can proceed to epoxide via either radical or cationic paths with branch points to the other products (Figure 15).[11,21] The observations that heme alkylation occurs with terminal olefins and that some olefins undergo substituent migration appear to be the result of a reaction pathway involving radical and/or cationic intermediates as seen in Figure 15.

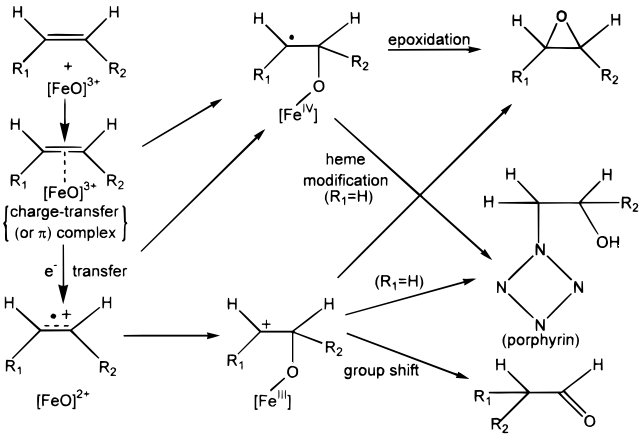

Figure 15. Schematic illustration of the mechanism of P450-catalyzed epoxidation of olefins. See text for description.

1. Suicide Inactivation by Terminal Olefins and Substituent Migration

Reaction of P450 with terminal olefins such as ethylene, propene, and 1-octene, for example, yields the expected epoxide product *as well as* heme modification (Figure 15) resulting in inactivation (destruction) of the P450 enzyme during catalysis.[91] The modified heme group has been isolated as the metal-free, green, N-alkylated porphyrin. Thus, terminal olefins are suicide substrates (or mechanism-based inhibitors) of P450.[91] For some olefin substrates, substituent migration (group shift) to the adjacent carbon occurs (e.g., trichloroethene → trichloroacetaldehyde)[92,93] along with epoxide formation. It has been shown that the epoxide products, when incubated in the P450 monooxygenase system, do not cause such N-alkylation of the heme group or group migration.[94] Thus, epoxide formation is not an intermediate step for these reactions. The N-alkylation of the heme prosthetic group suggests the formation of a carbon radical or cation intermediate generated via a pathway that is either independent of or in competition with epoxide formation. The group migration strongly argues for the formation of cationic intermediates. Attempts to prove the formation of radical or cationic intermediates by employing specially designed radical clock-type substrates (see the previous section) have been unsuccessful. For example, *trans*-1-phenyl-2-vinylcyclopropane[95] has been used as a substrate for rat liver microsomal P450-2B1 by Ortiz de Montellano and co-workers, and olefins having the *trans*-2,*trans*-3-diphenylcyclopropyl substituent[96] as substrate for an iron−porphyrin/*m*-chloroperbenzoic acid system by Bruice and /Castellino. Only the ring-unrearranged epoxide products were found as the catalytic oxidation products for both cases.

2. Radical Cation Formation

Ostovic and Bruice[90] have suggested that the radical cation formation upon one-electron oxidation of the olefin π bond by P450 (electron transfer) is an unlikely pathway because the oxidation potential ($E_{1/2}$) of the hypervalent P450 species may not be sufficiently high. On the other hand, Macdonald, Guengerich, and co-workers[97] have estimated the $E_{1/2}$ value for P450 [$(FeO)^{3+}/(FeO)^{2+}$] to be ~1.85 V [vs

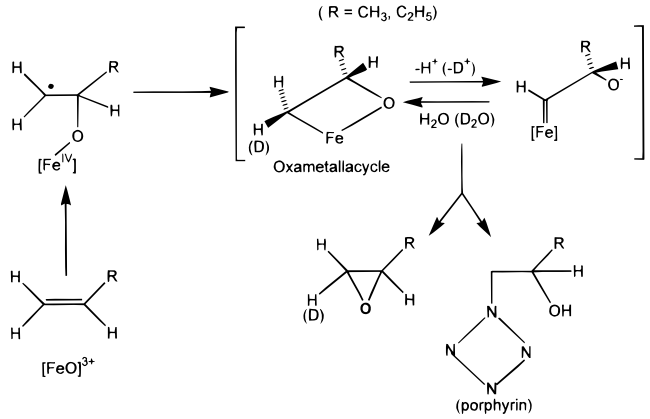

Figure 16. Mechanism proposed by Groves and co-workers for the exchange of deuterium for hydrogen during the P450-2B4-catalyzed conversion of the terminal olefins propene and 1-butene to propene oxide and 1-butene oxide, respectively. Adapted from ref 16.

saturated calomel electrode (SCE)] based on their systematic studies of P450-2B1-catalyzed oxidation (N-demethylation) of substituted *N*,*N*-dimethylanilines (*vide infra*). Since this $E_{1/2}$ value for P450 is comparable to the $E_{1/2}$ values of most of the olefins used (1.6−2.5 V vs SCE), the feasibility of the olefin free radical cation formation in enzymatic oxidations has not been ruled out by these researchers.[11]

3. Proton Exchange

An intriguing finding by Groves and co-workers[98] is that the P450-catalyzed epoxidation of 1-propene and 1-butene (but not 1-pentene and 1-octene) is accompanied by a significant exchange (85−100%) of a specific proton (or deuterium label) that is *trans* to an alkyl group (R), with a deuterium or a proton derived from D_2O or H_2O, respectively. Curiously, such proton exchange has been observed only when the enzymatic reaction is supported by NADPH/NADPH-cytochrome P450 reductase but not by the artificial oxygen donor iodosobenzene, nor in nonenzymatic metalloporphyrin model systems. To rationalize the results, these researchers have proposed a mechanism in which an oxametallacycle intermediate is formed in equilibrium with an iron−carbene adduct (Figure 16). The latter is generated by enzyme base-catalyzed stereospecific reversible removal of a proton from the former. However, because the proton exchange is limited to lower terminal olefins, the significance of the oxametallocyle formation in general olefin epoxidation mechanism is unclear.

4. Epoxidation by Metalloporphyrin Models

Model studies employing metallo(Fe, Mn, Cr)-porphyrins have suggested the initial rate-limiting formation of a charge transfer (or π) complex between an olefin and a hypervalent oxo−metalloporphyrin (Figure 15).[90] A recent paper reports that such a charge transfer complex has been detected with NMR spectroscopy.[99] The charge transfer complex can subsequently react in several ways such as to a radical cation by electron transfer, to an Fe−O-attached radical species (radical σ complex) by radicaloid addition to the π bond, or possibly, to a Fe−O-attached cation species (cation σ complex) by

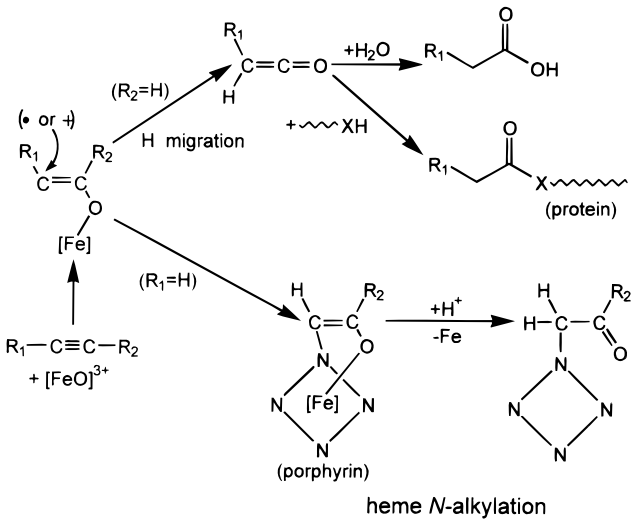

Figure 17. Schematic illustration of the mechanism of P450-catalyzed oxygenation of alkynes. See text for description.

electrophilic addition to the π bond. Either of these two σ complexes will, through competing pathways, lead to the formation of an epoxide, N-alkylated heme group, or a group-shifted carbonyl compound (from the cation σ complex).

5. Reactions of Alkynes

Alkynes are also oxidized by P450 (Figure 3b.ii) in complex pathways as outlined in Figure 17. The oxidation of terminal alkynes leads to either the formation of carboxylic acid, enzyme protein modification, or heme N-alkylation. Thus, terminal alkynes serve as suicide substrates for P450 as do terminal olefins as described above. These observations, in conjugation with deuterium labeling studies, have led to the postulation of a mechanism of terminal alkyne oxidation by P450 as schematically shown in Figure 17.[91]

I. Mechanism of Arene Epoxidation, Aromatic Hydroxylation, and the "NIH Shift"

The hydroxylation of aromatic compounds by P450 has long been considered to occur via an arene oxide (an epoxide) formation[100] (Figure 3.c). Subsequent nonenzymatic opening of the epoxide ring yields the hydroxylated product. During the course of this process, the migration of substituents (H, ^{2}H, ^{3}H, Cl, Br, etc.) occurs from the site of hydroxylation to the adjacent carbon. This process is known as the "NIH shift".[100] The postulated mechanism accounting for the NIH shift is schematically shown in Figure 18, where the epoxide ring opening proceeds through the formation of a zwitterion intermediate, followed by the group migration concomitant with the ketone formation. Subsequent enolization gives the hydroxylated arene products, which consist of one with the substituent *ortho* to the hydroxyl group and another with the original substituent lost.

An argument for the formation of a π-cation radical by direct electron transfer from polycyclic aromatic hydrocarbons to the hypervalent P450 species has been suggested by Cavalieri and co-workers.[101−103] The involvement of a single-electron transfer step in arene hydroxylations has also been suggested from

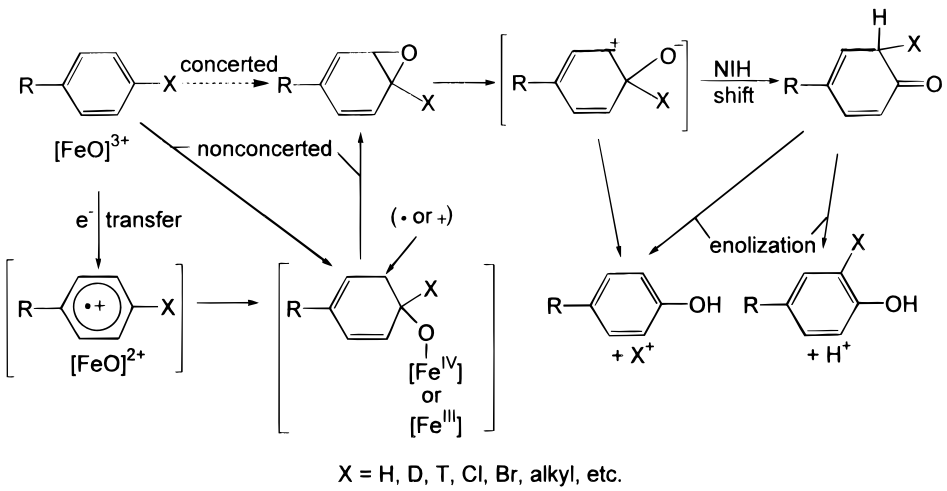

Figure 18. Schematic illustration of the mechanism of P450-catalyzed oxygenation of aromatic compounds including the NIH shift. See text for description.

the observation of a linear correlation between the rates (k_{cat}) of *meta* hydroxylation of monohalogen-substituted benzene by P450-2B1, and the σ^+ values (which correlate with the $E_{1/2}$ values for benzene) of the substituents.[104] However, a concerted oxygen atom insertion mechanism cannot be ruled out for some cases.[21] Alternative mechanisms (not shown here) have also been suggested which do not involve the epoxide intermediate but rather proceed by direct hydroxylation of the aromatic moiety.[105] Although the mechanism(s) of aromatic hydroxylations has (have) not been established unambiguously, Guengerich and Macdonald have proposed a unified common reaction scheme involving a radical σ complex or cation σ complex that may be applicable to epoxidation of both olefins and arenes.[11]

J. Dealkylation and Oxygenation of Heteroatom-Containing Substrates

1. Oxygen Source

Substrates that contain a heteroatom (X = NR, S, and O) that is alkylated ($RXCH_2R'$) have been shown to undergo dealkylation upon oxidation by P450 to yield a dealkylated heteroatom-containing compound and an aldehyde (RXH, R′CHO) (Figure 3d−f). Since the oxygen atom in R′CHO exchanges rapidly with solvent water (through the aldehyde−*gem* diol equilibrium), the origin of the aldehyde oxygen atom and the mechanism of these dealkylation reactions have been the subject of some speculation. For alkylamines, the oxygen atom has been established to come from dioxygen in two ways: (i) by rapid *in situ* reduction of the aldehyde to alcohol to prevent oxygen exchange[106−109] or, more definitively, (ii) by using *N*-methylcarbazole as a substrate, to yield a stable oxygenated product *N*-(hydroxymethyl)carbazole.[110,111] The source of the oxygen atom incorporated into the product for P450-catalyzed reactions utilizing peroxides (ROOH) or peracids [RC(O)OOH] in place of NADPH and O_2, is the respective oxygen donor.[112]

2. One-Electron Transfer Mechanism

Guengerich and Macdonald have proposed an electron transfer/deprotonation mechanism for P450-catalyzed N-dealkylation of alkylamines as follows[11,113] (Figure 19, X = NR: **24** → **25** → **26** → **28**): initial one-electron oxidation of the amine nitrogen gives an aminium cation radical, **25,** which is followed by rapid deprotonation of the hydrogen on the adjacent carbon (i.e., α-hydrogen) and internal electron transfer to yield an α-carbon-centered neutral radical, **26**. Subsequent oxygen rebound to this carbon radical gives the carbinolamine, **28**, which nonenzymatically decomposes to the final products, the dealkylated amine and aldehyde. In this pathway, the formation of the α-carbon radical does not involve direct hydrogen atom abstraction. An alternative mechanism involving direct hydrogen atom abstraction will be discussed below. In the absence of α-hydrogens, alkylamine substrates give N-hydroxylated (NOH) (Figure 3g) or N-oxygenated (N^+O^-) (Figure 3h) products upon oxygenation by P450. For example, β-naphthylamine is oxidized to 2-(hydroxyamino)naphthalene and quinidine (a tertiary amine) to quinidine *N*-oxides.[113,114] It should be pointed out that, even for those alkylamines which predominantly undergo N-dealkylations, small amounts of N-oxygenation products are also detected by sensitive assays.[115]

Peroxidases also catalyze the dealkylation of alkylamines to yield the same products as obtained with P450, but via disproportionation of the amine cation radical to form an imine cation ($RNH^+{=}CHR'$) followed by hydration (Figure 19: **24** → **25** → **27** → **28**).[113] In this case, the oxygen atom incorporated into the products is derived from medium water rather than peroxides or peracids.

In the case of sulfur-containing substrates, sulfoxides (**29**, X = S) are the predominant products even when α-hydrogens are available, e.g., dimethyl sulfide → dimethyl sulfoxide (Figure 3i). This is due to the relatively stable nature of the sulfur cation radical, **25**, as compared with the nitrogen radicals. Consistent with this mechanism (**24** → **25** → **29**), Watanabe et al.[116] found that the rates of sulfoxide formation (log k_{cat}) for a series of *para*-substituted thioanisoles were correlated with the one-electron oxidation potentials of these thioanisoles (1.26−1.85 V vs SCE) as well as the σ^+ values of the substituents. Phosphorus compounds are even more readily oxidized to phosphine oxide than sulfides to sulfox-

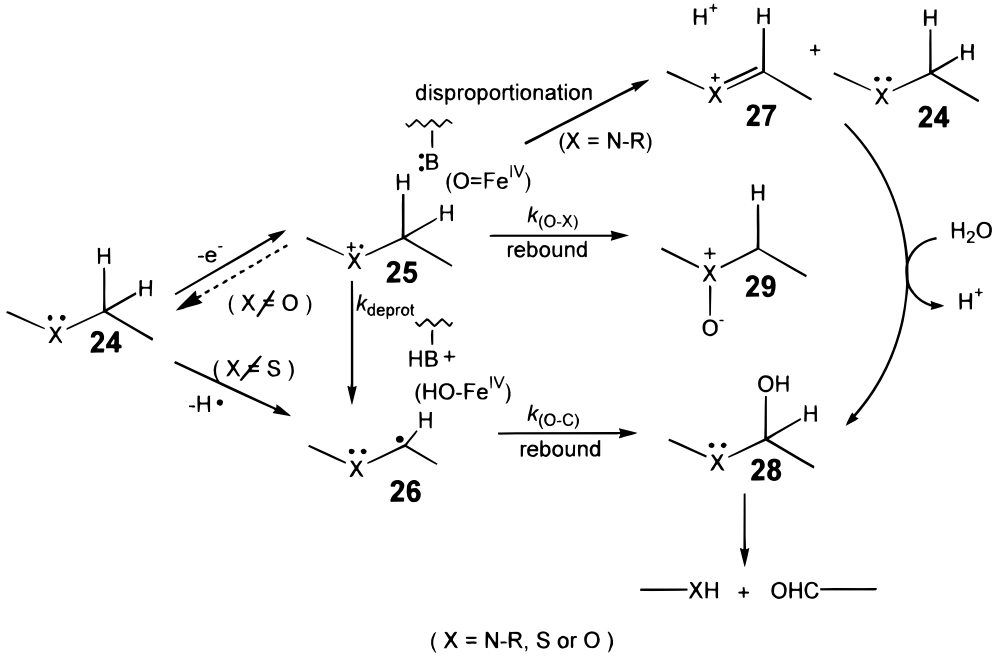

Figure 19. Schematic illustration of mechanisms of P450-catalyzed heteroatom (X) oxidation (X = NR, S) (**29**) and dealkylation (X = NR, S, O) (via **28**). The dealkylation of alkylamines catalyzed by peroxidases (involving **27**) is also shown for comparison. See text for description.

ides; phosphorus compounds have even lower oxidation potentials than sulfur compounds.

On the other hand, oxygen atom-containing substrates cannot be oxidized by P450 via the one-electron transfer mechanism due to the more electronegative nature of oxygen, which requires much higher ionization energies than nitrogen and sulfur atoms. The oxygenation of oxygen-containing substrates is therefore initiated by direct hydrogen abstraction from the α-carbon, followed by oxygen rebound (Figure 19, X = O: **24** → **26** → **28**).[11,21]

3. Isotope Effects and Their Mechanistic Implications

The N-demethylation of *N*,*N*-dimethylaniline by P450 exhibits low kinetic deuterium isotope effects in the range of 1−2.[117] This has been interpreted as being most consistent with the initial one-electron transfer mechanism as described above. On the other hand, the large kinetic deuterium isotope effects observed for O-dealkylation of 7-ethoxycoumarin (k_H/k_D = 13-14) lend support to the direct hydrogen abstraction mechanism.[74]

Although kinetic deuterium isotope effects can be used as informative mechanistic probes for P450-catalyzed hydroxylations of various substrates, it has been pointed out that isotope effects must be subject to careful interpretation. Recent studies by Dinnocenzo and co-workers[118−120] have indicated that the hydrogen atom abstraction (**24** → **26** → **28**) vs an electron transfer/deprotonation mechanism (**24** → **25** → **26** → **28**) for dealkylation of amines cannot be distinguished by the magnitude of kinetic deuterium isotope effects alone. Examples of model alkylamine hydrogen atom abstraction reactions with low isotope effects and model alkylamine cation radical deprotonation reactions with high isotope effects have been presented.[118−120] As an example of the former case, Griller and Scaiano reported an isotope effect of only 1.4 for hydrogen atom abstraction from trimethylamine (d_0 and d_9) by the *tert*-butoxy radical.[121] In an example of the latter case, proton transfer from the tertiary amine cation radical of *N*,*N*-di(4-anisidinyl)-*N*-methylamine (the estimated pK_a = 10 for the cation radical in acetonitrile) to the base quinuclidine gives a relatively large kinetic isotope effect of 7.7.[122] These findings are at odds with the premise[12] that the hydrogen atom abstraction mechanism should yield only high isotope effects (greater than 7) and that the electron transfer/deprotonation mechanism should exhibit only low isotope effects (less than 4). In fact, the relatively high isotope effect observed by Dinnocenzo and co-workers[119,122] for deprotonation of amine cation radicals may help explain the unexpectedly high isotope effects (8.7−10) observed for the oxidative N-dealkylation of *N*,*N*-dimethylaniline catalyzed by peroxidases (as well as hemoglobin and myoglobin). The iron-bound oxygen atoms in the hypervalent intermediates (compounds I and II) of horseradish peroxidase have been shown to be inaccessible for direct hydrogen abstraction from the alkylamine substrate.[64] In this case, substrate oxidations proceed through electron transfer at the heme edge.

Unlike peroxidases, the P450 enzymes lack basic residues in their active sites to serve as proton acceptors.[19] Yet, P450-catalyzed N-dealkylations exhibit low kinetic isotope effects. This has been interpreted by Guengerich and Macdonald[11b] to be due to an initial one-electron oxidation of the amine nitrogen followed by rapid deprotonation of the α-methyl group of the postulated aminium radical intermediate. Further, these authors have proposed that the P450 $[Fe^{IV}{=}O]^{2+}$ species itself (equivalent to the deprotonated form of compound II of peroxidases) may play a role of a specific base to facilitate proton transfer.[88,113]

4. Amine Cation Radical Formation

Although formation of nitrogen or sulfur cation radicals cannot readily be detected for N- and S-

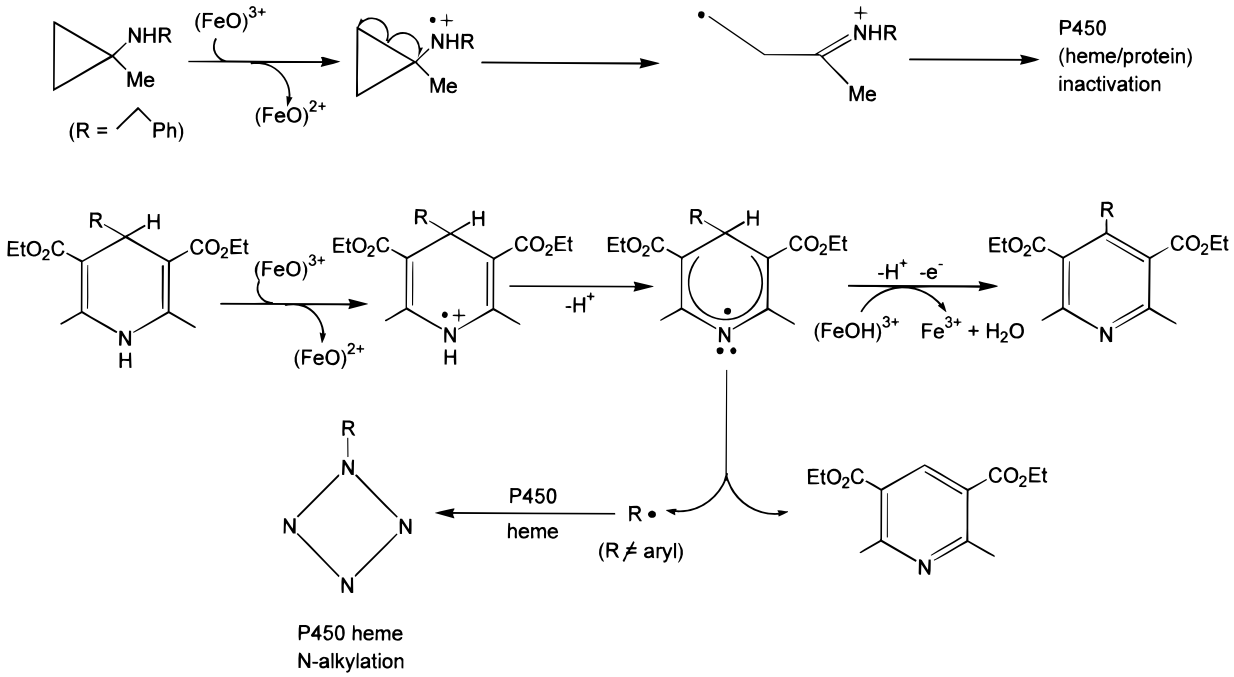

Figure 20. (Top) Reaction of P450 with cyclopropylamines leading to enzyme inactivation. See text for description. (Bottom) Reaction of P450 with 1,4-dihydropyridines leading to aromatization and enzyme inactivation. See text for description.

containing substrates, the electron transfer/deprotonation mechanism was supported by the following experimental results[11,21] (Figure 20): (i) Cyclopropylamines give ring-opened products and also cause irreversible enzyme inactivation. (ii) 4-Alkyl-1,4-dihydropyridines produce an alkyl radical which alkylates the heme group and leads to enzyme inactivation.

As for cyclopropylamine, *N*-(1-methyl)cyclopropyl-*N*-benzylamine (Figure 20, top) and its desmethyl derivative, *N*-benzylcyclopropylamine (not shown), have exhibited comparably effective enzyme inactivation as well as heme group loss. Since the formation of a cyclopropyl iminium cation (>C=N$^+$HR) is only possible for the desmethyl derivative *N*-benzylcyclopropylamine, the iminium cation has been ruled out as the major cause of the enzyme inactivation.[123,124] These results have been rationalized by proposing that the cyclopropylamines undergo one-electron oxidation to the radical cation, followed by rapid ring opening to give β-iminium methylene radical, which will alkylate either the protein or the heme group (Figure 20, top). Similarly, *N*-cyclobutylamine is not only a mechanism-based inhibitor of P450 but also gives ring-rearranged oxidation products. Thus, the same mechanism, i.e., iminium cation radical formation, can be applied to this amine as proposed for cyclopropylamines. This mechanism is also supported by the demonstration that the rates of enzymatic inactivation correlate well with the $E_{1/2}$ of a series of N- and halogen-containing cyclopropyl compounds.[123]

The aromatization of 1,4-dihydropyridines is one of the P450-catalyzed dehydrogenation reactions (Figure 3m). P450-catalyzed oxidation of 4-alkyl-1,4-dihydropyridines gives two aromatic metabolites, 4-alkyl group-retaining (i.e., 4-hydrogen removed) and dealkylated pyridines, in addition to the N-alkylated heme group (Figure 20, bottom). The alkyl group released was also spin-trapped, showing that the 4-alkyl group is eliminated as a free radical.[125] When the 4-substituent is an aryl (e.g., phenyl) group, its extrusion does not occur.[126] Instead, 4-arylpyridine derivatives are formed. The deuterium isotope effects for the removal of the 4-hydrogen for dihydropyridine aromatization are generally small,[127] arguing against the initial hydroxylation at the 4-position.

5. Effective Oxidation–Reduction Potential of the P450 Reactive Oxygen Species

To estimate the effective oxidation−reduction potential [$E_{1/2(app)}$] of the postulated hypervalent P450 species, Macdonald, Guengerich, and co-workers[97] have examined the rates (k_{cat}) of rat liver P450-2B1-catalyzed N-demethylation for a series of *para* (and one *meta*)-substituted *N*,*N*-dimethylanilines in the system supported by O_2/NADPH/NADPH-P450-reductase or by iodosobenzene. These substituted *N*,*N*-dimethylanilines had different $E_{1/2}$ values ranging from 0.74 to 1.27 V (vs SCE). From a good correlation between the log(k_{cat}) and the substrate $E_{1/2}$ values and its theoretical analysis, these researchers have concluded that the $E_{1/2(app)}$ for P450-2B1 is in the range of 1.7−2.0 V (vs SCE), i.e., ∼1.85 V. This $E_{1/2}$ value is significantly higher than the value measured for model iron porphyrins ($E_{1/2}$ = 1.0−1.8 V, vs SCE)[128,129] and that of compounds I/II of horseradish peroxidase ($E_{1/2}$ = ∼0.75 V, vs SCE).[130] To account for the abnormally high $E_{1/2}$ for P450 as compared with those for other systems, it has been suggested that the $E_{1/2(app)}$ for P450 is the sum of the intrinsic oxidation−reduction potential, $E_{1/2(int)}$, for the postulated hypervalent active center of P450 ([FeO]$^{3+}$) and a Coulombic factor [$E_{(cf)}$] that is a function of the electrostatic factors such as the charges of the enzyme oxidant and substrate.[97] P450 is distinct from horseradish peroxidase in that the former has the electron-releasing cysteine thiolate axial ligand in contrast to histidine imidazole axial ligation for the latter. In addition,

the active site of P450 monooxygenases consists of mostly nonpolar amino acid residues as compared with the presence of positively charged group(s) for peroxidases. Thus, it has been suggested that the unique chemical reactivity (and the relatively high $E_{1/2}$ value) of P450 may be attributed, at least in part, to the electronic effects of the negatively charged thiolate axial ligand.[97]

6. Direct Hydrogen Atom Abstraction Mechanism

All the data and their interpretations (including the estimation of the apparent $E_{1/2}$ values for P450) for the P450-catalyzed amine oxidations described above are rationalized on the basis of the postulated mechanism, which involves the initial one-electron oxidation of the amine nitrogen, followed by rapid removal of a proton from the α-methyl group, when available.[11,113] This mechanism has, however, recently been challenged by Dinnocenzo and co-workers, who have put forward an alternative mechanism by which amine oxidations proceed by initial direct hydrogen atom abstraction from the α-methyl group.[118−120] These researchers have proposed a new method for distinguishing between these two mechanisms of N-dealkylation which involves comparison of the isotope effect profile for a series of *para*-substituted (methyl, cyano, chloro, nitro) *N*,*N*-dimethylanilines with mechanistically defined model reactions.[118] Results obtained from reactions catalyzed by a series of six different P450s were found to match the hydrogen atom abstraction profile rather than the electron transfer/deprotonation profile in that the trend shows a linear correlation of isotope effect magnitude with electron-withdrawing ability of the *para* substituent. The electron transfer/deprotonation model reaction exhibits a bell-shaped profile with no clear correlation between the isotope effect magnitude and electronic properties of the *para* substituent.[119]

It is possible that the P450-catalyzed N-dealkylation reactions of alkylamines may involve the two mechanisms and that incidence of either mechanism in an N-dealkylation reaction might be influenced by fine-tuning of the redox potential of the amine and/or the lability of an α-hydrogen atom by the amine substituents. Obviously, more work will be necessary to determine whether only one of the two mechanisms can exclusively rationalize all the data obtained from P450-catalyzed amine oxidations.

K. Other Types of P450-Catalyzed Reactions

The wide range of reactions catalyzed by cytochrome P450 has been listed in Figure 3. The mechanism of oxygen incorporation into alkanes, alkenes, arenes, alkylamines, thioethers, and ethers, the subsequent dealkylation reactions in the latter three cases, and N-hydroxylation, N-oxidation, and S-oxidation (Figure 3, reactions a−i) has already been discussed. Several of the other reaction types listed in the figure, oxidative deamination, oxidative dehalogenation, and alcohol/aldehyde oxidations,[131,132] (Figure 3, reactions j−l) are basically oxygen transfer reactions like those already presented. In some cases (reactions j, k, and l.i), as with the dealkylation reactions, the initial hydroxylated product is unstable and nonenzymically undergoes breakdown (loss of ammonia, HX, or water, respectively) to give the final product.

1. Dehydrogenation and Dehydration Reactions

The role of P450 in dehydrogenation and dehydration (Figure 3, reactions m and n) has recently been discussed by Mansuy[24] and will not be discussed further here. The dehydration of aldoximes (Figure 3n.i) and of other substrates is not a commonly reported P450 reaction. The enzyme allene oxide synthase, which catalyzes the dehydration of lipid hydroperoxides to form allene oxides (Figure 3n.ii), has been isolated from numerous sources and is the best characterized example of P450-catalyzed dehydration.[133]

2. P450-Catalyzed Reductions

Four of the P450-catalyzed reactions listed in Figure 3 (reactions o−r) involve the reductive conversion of organic substrate. These include unusual reactions such as the reductive β scission of alkyl peroxides,[134] N-oxide reduction,[135] and epoxide reduction.[136] Although not included in Figure 3, an azoreductase activity of P450 has also been reported.[137] These reactions involve the ferrous form of the enzyme (Fe^{2+}, **3** in Figure 6) as the reactive species[12,13,134] rather than the common "reactive oxygen species" ($[FeO]^{3+}$, **7** in Figure 6). *In vivo*, these reactions would occur only under anaerobic or semi-anaerobic conditions. Since P450 is serving as an electron carrier in these reactions, it is functioning as a real "cytochrome".

Shoun and co-workers have recently isolated a very interesting P450 enzyme from the fungus *Fusarium oxysporum*[138] and designated it cytochrome P450-NOR, where NOR stands for NO reductase. P450-NOR catalyzes the anaerobic reduction of NO to N_2O (Figure 3, reaction s). Unlike all other P450 enzymes, this one involves direct reaction between NADH and P450 without requiring electron carrier proteins, although only in the presence of NO. It also has a turnover number in excess of 500/s that is considerably higher than any other known P450 enzyme. The enzyme is not inhibited by CO, suggesting that free deoxyferrous P450 is not involved in the reaction pathway. The ferrous−NO complex has also been shown not to be an intermediate in the reaction cycle.[138e] It has been proposed that the ferric−NO adduct reacts directly with NADH, serving in its usual role as a hydride donor. The enzyme has recently been crystallized.[139]

3. P450 as an Isomerase

Hecker and Ullrich have identified two unusual P450 enzymes, prostacyclin (PGI_2) synthase and thromboxane (TXA_2) synthase (Figure 3t),[140] in which the ferric heme iron is proposed to homolytically cleave the endoperoxide O−O bond of PGH_2 (see Figure 36, section V). The two enzymes differ in the direction of opening of the peroxide en route to the isomerized products. Both enzymes give rise to Soret absorption peaks close to 450 nm in the ferrous−CO state as expected for P450 enzymes. However, both function entirely in the ferric and higher oxidation

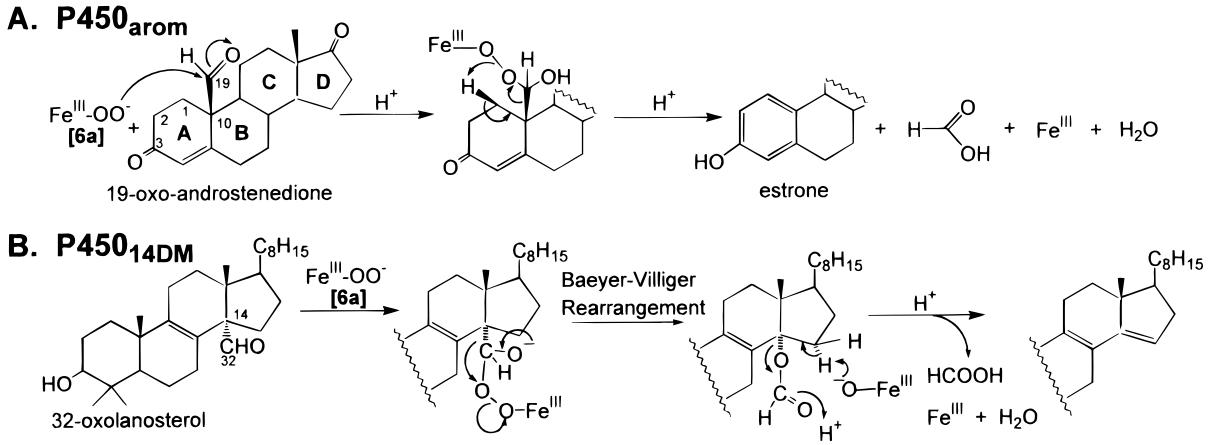

Figure 21. Proposed deformylation mechanisms for P450-aromatase (A) and P450-14DM (B). See text for description.

states and are not inhibited by CO. The catalytic cycles of these two P450 enzymes have recently been discussed in considerable detail by Mansuy[24] and will not be discussed further here.

4. P450-Catalyzed Lyase (C–C Bond Cleavage) Reactions

Cytochrome P450 enzymes play key roles in the biosynthesis of hydroxysteroids as part of the pathways for production of bile acids and steroid hormones. In contrast to the relatively nonspecific P450 enzymes involved in the metabolism of xenobiotics, the steroid hydroxylating P450s are very regio- and stereospecific. These hydroxylation reactions presumably proceed via the same mechanism of oxygen transfer described above in section IIG. An intriguing feature of several steroid-metabolizing P450s, however, is that they carry out consecutive hydroxylations ending in a lyase (C−C bond cleavage) step (Figure 3u). Four examples of P450 enzymes catalyzing such lyase reactions are described below.

(*i*) *Cholesterol Side-Chain Cleavage P450 (P450-SCC).* P450-SCC catalyzes the sequential hydroxylation of the vicinal 20 and 22 carbons of cholesterol.[141,142] After formation of the 20(*R*),22(*R*)-diol, another cycle of oxidation takes place in which a third molecule of dioxygen (and NADPH) is consumed and the $C_{20}-C_{22}$ bond is cleaved.[142] Ortiz de Montellano has recently discussed the two proposed mechanisms of C−C bond cleavage.[21]

(*ii*) *Cholesterol 17α-Hydroxylase/17,20-Lyase.* The reaction catalyzed by this P450 starts with α-hydroxylation at C-17. Next, in the lyase step, the 17-keto derivative is formed by oxidative removal of the 17-acetyl substituent. Both steps require NADPH and O_2. Possible mechanisms for the deacetylation step have been discussed by Ortiz de Montellano.[21] One feature of the proposed mechanism that will be seen again in the next two P450-lyase reactions is the suggested role of the ferric−peroxide P450 adduct (Figure 6, **6a**) as the "reactive oxygen" species in the lyase step rather than the oxo−ferryl state, **7**. The oxidative deacetylation step has recently been studied in detail by Swinney and Mak[143] and by Akhtar and co-workers.[144] The latter researchers have shown by ^2H and $^{18}O_2$ isotope labeling that the ferryl−oxo porphyrin cation species (**7**) is not involved in the reaction.[144]

(*iii*) *P450-aromatase.* The biosynthesis of the sex hormone estrone from androstenedione (see Figure 21A) (and of β-estradiol from testosterone) is carried out by aromatase by oxidative removal of the C-19 methyl group attached to carbon 10. The name "aromatase" comes from the fact that the oxidative removal of the C-19 methyl group to give the C-1, C-10 olefin is accompanied by enolization of the C-3 ketone to yield an aromatic steroid A ring. The aromatase reactions proceed via three stages whereby the methyl group is hydroxylated twice to give an aldehyde (formyl) group. Finally, in the lyase step, the formyl group is oxidatively removed as formic acid concomitant with the formation of the C-1, C-10 double bonds. Each of the three steps requires NADPH and O_2. The first two hydroxylations proceed in the normal manner of P450-catalyzed alkane and alcohol hydroxylations (Figure 3, reactions a and l.i).

The most widely accepted mechanism for the oxidative deformylation step for aromatase was initially proposed by Akhtar[145] and is illustrated in Figure 21A. It involves initial nucleophilic attack by the P450 ferric−peroxide intermediate (Figure 6, **6a**) on the carbonyl carbon of the formyl group at C-19 to generate a heme iron-bound peroxyhemiacetal-like intermediate. It is known that the 1-β-hydrogen is stereospecifically removed in the formation of the C-1, C-10 double bond.[146] A concerted cyclic rearrangement of the peroxyhemiacetal intermediate is shown in Figure 21A to give the olefin product, formic acid, and the ferric resting state of P450. The peroxyhemiacetal intermediate could also break down by nonconcerted rearrangement or sequential β-scission (radical) mechanisms. This type of oxidative deformylation concomitant with introduction of a double bond has been shown to occur by several researchers. Cole and Robinson[147] have demonstrated that a 2,4-dien-3-ol analog of the 19-aldehyde intermediate (Figure 21A) nonenzymatically reacts with H_2O_2 to produce the corresponding estrogen derivative. Vaz, Coon, and Roberts[148,149] have shown that liver microsomal P450-2B4 catalyzes oxidative deformylation of cyclohexanecarboxaldehyde to cyclohexene and formic acid as well as of several branched aldehyde compounds (such as isobutylaldehyde and trimethylacetaldehyde) to the corresponding olefin products and formic acid. The same group[150] has also shown that P450-2B4 will convert 3-oxodecalin-4-ene-10-carboxaldehyde, a bicyclic analog (having the ring AB) of 19-oxoandrostenedione (see Figure 21A), to an aromatic analog of estrone, thus mimicing the oxida-

tive deformylation reaction of aromatase. The P450-2B4-catalyzed reactions can be supported by dioxygen and NADPH or by hydrogen peroxide but not by other peroxide shunt oxygen donors.[148−150]

Although these results seem to argue persuasively for the key involvement of P450 state **6a** in the deformylation step, alternative mechanisms in which the postulated ferryl−oxo porphyrin cation species of P450 **7** *does* participate in this step have been proposed earlier by Korzekwa and co-workers[151] and more recently by Ahmed and Davis.[152] In an iron−porphyrin model study, however, Watanabe et al.[153] have reported that the ferryl−oxo porphyrin cation species exclusively oxidize aldehyde compounds to carboxylic acids (Figure 3, reaction l.ii), rather than to deformylated compounds. Furthermore, Valentine and co-workers[154] have recently shown that the ferric porphyrin−peroxide species can directly epoxidize electron-poor olefins having a carbonyl group such as cyclohexenone. Clearly, additional experimental work will be needed to further resolve the mechanism of oxidative deformylation by aromatase.

(*iv*) *P450-14α-demethylase*. The reaction sequence for the 14α-demethylase is similar to that for aromatase as far as the first two hydroxylation steps to yield the 14α-formyl steroid derivative.[155−157] The proposed deformylation mechanism (Figure 21B) starts in the same way as with aromatase, via attack of the ferric−peroxide P450 intermediate to give a peroxyhemiacetal-type intermediate. The mechanism differs in how this intermediate breaks down to give the olefin product. In this case, it is thought to proceed via a Baeyer−Villiger rearrangement to the 14α-formyloxy derivative, an intermediate recently isolated by Fischer et al.[158] Deprotonation of the 15α-proton by an appropriately positioned base (shown as the Fe^{III}-OH group in Figure 21B) leads to elimination of the 14α-formyloxy group to give formic acid and the olefin product. Isolation of the 14α-formyloxy steroid derivative is the strongest piece of evidence in favor of the Baeyer−Villiger rearrangement mechanism. However, the same type of rearrangement has been shown by Akhtar and co-workers[144,145] not to be involved in aromatase-catalyzed reactions; the 19-formyloxy derivative of androstenedione, the Baeyer−Villiger rearrangement intermediate, is not converted to the expected aromatized product by microsomal human placental aromatase, but the 19-*β*-hydroxy derivative is formed instead. Thus, it remains to be clarified whether the two similar types of P450-catalyzed deformylation reactions carried out by aromatase and the 14α-demethylase proceed by two different mechanisms, and if so, what factors are the causes of the difference.

5. Nitric Oxide Synthesis

Nitric oxide synthase[159−162] has been found to be a thiolate-ligated heme-containing monooxygenase, like P450. The molecular structure of nitric oxide synthase is similar to that of P450-BM3 (*vide supra*) in that both enzymes are self-sufficient oxygenases having the heme and flavin (FAD and FMN) domains within one fused large molecule. However, the absence of amino acid sequence homology between heme domains of the two enzymes places nitric oxide synthase outside of a P450 family. It catalyzes the NADPH-dependent formation of NO and citrulline from L-arginine via a two-step process in which an atom of oxygen is incorporated from O_2 in each step. *N*-Hydroxy-L-arginine is an intermediate in the reaction. The enzyme is discussed in great detail by Marletta elsewhere in this volume.[163]

6. P450-Catalyzed Production of Carcinogens and Tissue-Damaging Metabolites

The majority of metabolites formed from xenobiotics and from endogenous P450 substrates (Figure 3) are physiologically essential or beneficial. However, a few P450 enzymes that are inducible by chemicals such as aromatic hydrocarbons, phenobarbital, isosasfranole, and ethanol convert otherwise unreactive xenobiotics to highly reactive, electrophilic metabolites which readily react with nucleophilic biological macromolecules such as DNA bases and lipoproteins.[31,164] This process has been shown to result in carcinogenesis or liver necrosis. The most notorious example is the activation of benzo[*a*]pyrene (the precarcinogen) by P450 to the diol epoxide (the carcinogen) followed by formation of an adduct with the guanine residue of DNA.[165,166] Similarly, epoxidized aflatoxin B_1[167] and anthrathenes,[165] and N-hydroxylated 2-(acetylamino)fluorene (upon further enzymic conversion to a strongly electrophilic sulfate ester),[166,167] also form an adduct with the DNA guanine residue. Other types of metabolic activation of substrates also occur; *N*-nitrosoalkylamines and polyhalogenated compounds (e.g., halothane) undergo respectively oxidative and reductive metabolism by P450 to generate alkyl radicals.[14,42] Valproic acid[169] and acetaminophen[77,164] are dehydrogenated by P450 (Figure 3m.ii) to form a terminal olefin (Δ^4-valproic acid) and a quinone imine (*N*-acetyl-*p*-benzoquinone imine), respectively. These metabolites subsequently cause liver necrosis by forming a covalent bond to lipoproteins.

III. Secondary Amine Monooxygenase (SAMO)

A. Background

Secondary amine monooxygenase, a soluble NADPH-dependent heme-containing oxygenase, was first identified by Large and co-workers[170−172] in extracts of *Pseudomonas aminovorans*. The enzyme has been shown to consist of three polypeptides with an overall $\alpha_2\beta_2\delta_2$ structure.[173] In addition to iron protoporphyrin IX, the enzyme contains FMN and Fe_2S_2 prosthetic groups which are presumed to participate in the delivery of electrons from NADPH to the heme iron center in the course of catalysis.[173]

Secondary amine monooxygenase catalyzes the oxidative dealkylation of secondary amines to aldehydes and primary amines with dimethylamine as its best substrate (eq 8). This reaction occurs early

$$(CH_3)_2NH + NADPH + O_2 + H^+ \rightarrow CH_3NH_2 + NADP^+ + HCHO + H_2O \quad (8)$$

in the metabolism of amines when *P. aminovorans* is grown on trimethylamine as its sole carbon source[172] (Figure 22). The fact that the enzyme is inhibited

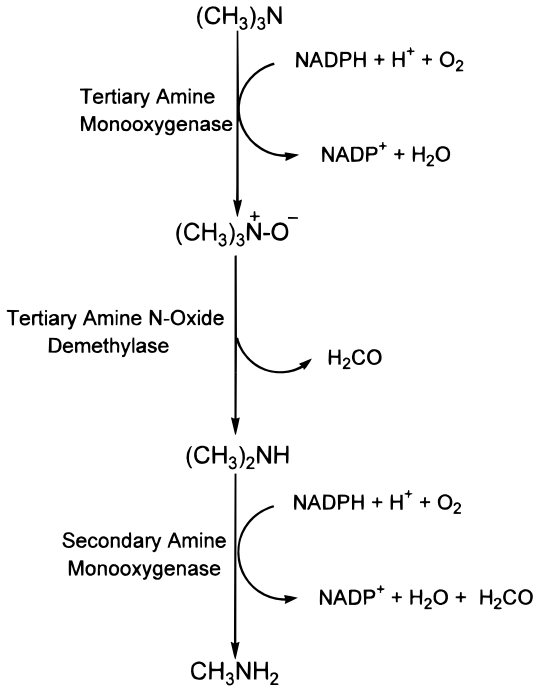

Figure 22. Metabolism of amines by *Pseudomonas aminovorans.*

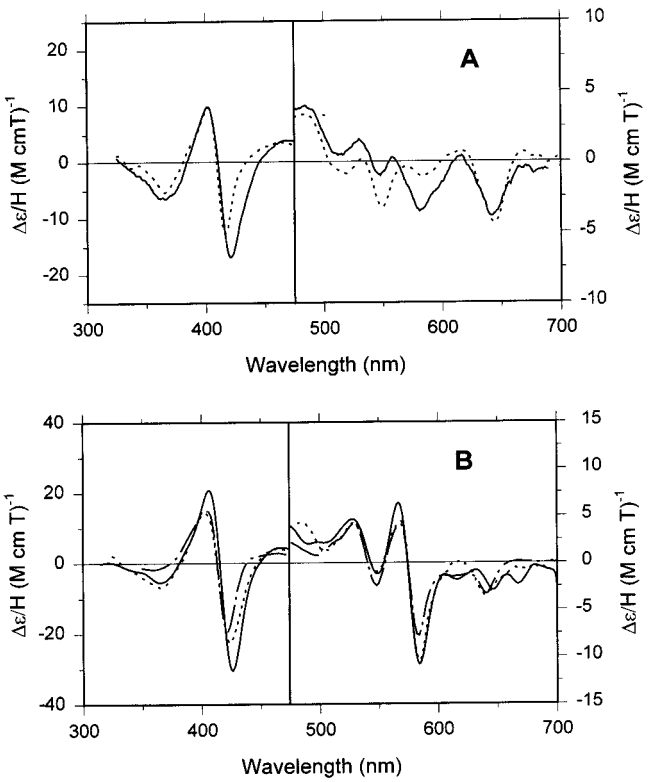

Figure 23. (A) Magnetic circular dichroism spectra of ferric secondary amine monooxygenase at pH 6.8 (solid) and myoglobin at pH 7.1 (dashed). (B) Magnetic circular dichroism spectra of ferric secondary amine monooxygenase at pH 9.0 (solid), myoglobin at pH 9.0 (dashed), and substrate-bound secondary amine monooxygenase at pH 6.8 (dot−dash). Adapted from ref 176.

by carbon monoxide[174] suggests that it is the heme and not the FMN that is the oxygen-activating prosthetic group. Catalysis of such oxidative dealkylations by P450s have been well established.[175] However, in 1975, Brook and Large[174] discovered that ferrous−CO secondary amine monooxygenase exhibits spectral properties similar to analogous preparations of myoglobin and distinct from the P450s. The interest in secondary amine monooxygenase thus stems from the unique relationship between its structure and function: It is a non-thiolate ligated heme enzyme that catalyzes a monooxygenation reaction. Structural and mechanistic studies of secondary amine monooxygenase have only begun to help clarify the requirements for oxygen activation by P450 type and non-thiolate type heme iron centers.

B. Active Site Structure

1. The Ferric State

Detailed spectroscopic studies of secondary amine monooxygenase including electronic absorption, MCD, and EPR spectroscopy were published by Dawson and co-workers in 1989.[176] The electronic absorption parameters of the ferric enzyme and ferric−ligand adducts have been found to match those of myoglobin[177] much more closely than those of P450-CAM.[178] MCD spectroscopy, being a much more sensitive probe of electronic structure,[179] was also used to characterize the ferric coordination sphere. MCD spectra of ferric secondary amine monooxygenase at neutral and alkaline pH (Figure 23A) closely parallel those of similar preparations of myoglobin and are distinct from P450-CAM.[9] The pH-dependent spectral change incurred in myoglobin is due to the conversion from high to low spin caused by deprotonation of the bound water molecule *trans* to the proximal histidine.[176] The similarities between the MCD spectra of ferric myoglobin and secondary amine monooxygenase as a function of pH led to the suggestion that the latter also contains a water (or hydroxide) distal ligand *trans* to histidine. Interestingly, the MCD spectrum of the dimethylamine adduct of ferric secondary amine monooxygenase at neutral pH (Figure 23B) matches the MCD spectrum of alkaline ferric secondary amine monooxygenase (Figure 23A), suggesting that dimethylamine itself is acting as a base in the deprotonation event.[176] The mechanistic function (if any) of the deprotonation of the bound water is not known.

Addition of exogenous ligands to heme proteins is a common strategy used in the determination of the identity of the proximal ligand donated by the protein. MCD spectra of the cyanide (Figure 24A) and azide (Figure 24B) adducts of secondary amine monooxygenase[176] are overplotted with the corresponding adducts of myoglobin[176] to highlight the similarities of the electronic properties between the heme coordination spheres of the two proteins. The MCD spectra of the analogous adducts of ferric P450-CAM are very different.[9] These results go beyond the initial report of Brook and Large[174] in providing specific evidence that the non-thiolate proximal ligand in ferric secondary amine monooxygenase is histidine.

EPR spectra of aquo−ferric secondary amine monooxygenase[176] are also indicative of a histidine-ligated heme iron with predominately axial high-spin g values (5.99, 2.04).[176] Unlike myoglobin,[180] however, aquo−ferric secondary amine monooxygenase exhibits a small percentage of low-spin character with g values at 2.82, 2.29, and 1.64.[176] The EPR

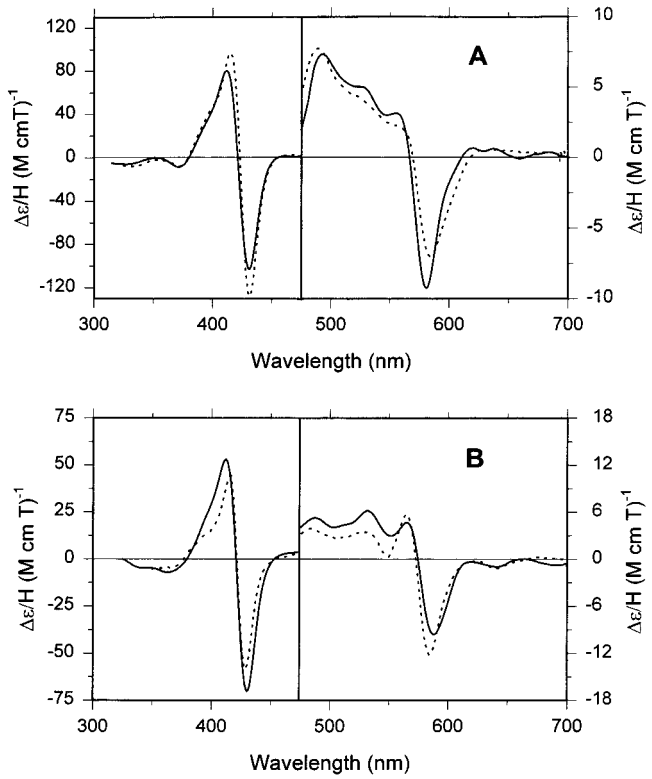

Figure 24. (A) Magnetic circular dichroism spectra of the ferric−cyanide adducts of secondary amine monooxygenase at pH 6.8 (solid) and myoglobin at pH 7.1 (dashed). (B) Magnetic circular dichroism spectra of the ferrric−azide adducts of secondary amine monooxygenase at pH 6.8 (solid) and myoglobin at pH 7.1 (dashed). Adapted from ref 176.

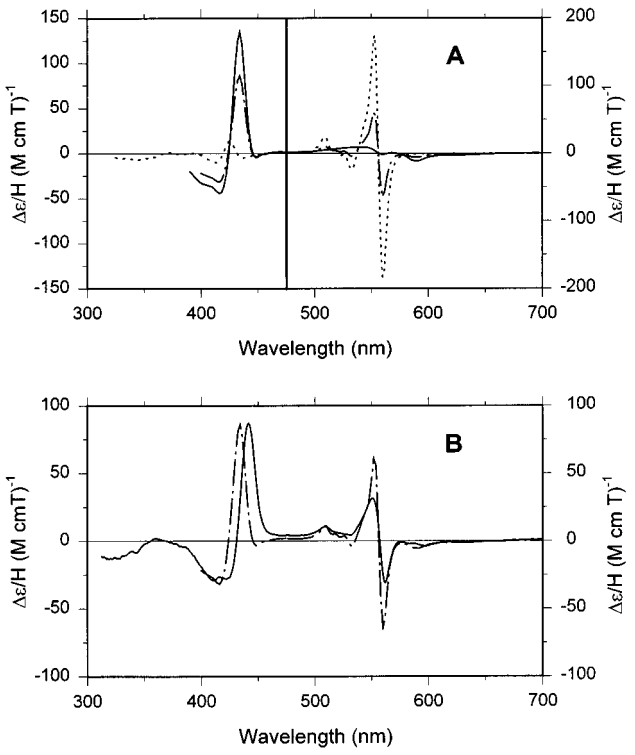

Figure 25. (A) Magnetic circular dichroism spectra of deoxyferrous myoglobin at pH 7.1 (solid), cytochrome b_5 at pH 7.0 (dashed), and a computer-generated model spectrum consisting of 65% five-coordinate high-spin (deoxyferrous myoglobin) and 35% six-coordinate low-spin (deoxyferrous cytochrome b_5) (dot−dash). (B), Magnetic circular dichroism spectra of deoxyferrous secondary amine monooxygenase (solid) and the model spectrum (dot−dash). Note the *y*-axis scale change from (A). Adapted from refs 176 and 193.

spectra of the ferric−azide adduct of secondary amine monooxygenase[176] are distinct from P450-CAM[46] and are indicative of a completely low-spin histidine-ligated heme iron such as myoglobin.[181] In addition, rhombicity and tetragonality terms[182−184] calculated from the *g* values of the azide adduct of secondary amine monooxygenase[185] were found to be within 10% of those determined for azide-ligated ferric myoglobin.[186,187] These spectroscopic studies provide convincing evidence for the assignment of histidine as the proximal ligand in ferric secondary amine monooxygenase.

2. The Ferrous State

Deoxyferrous secondary amine monooxygenase exhibits electronic absorption[176] and MCD (Figure 25A)[176] spectra that are distinct from those of both myoglobin[177] and P450-CAM[178] and are instead somewhat similar to those of cytochrome b_5, a bis(histidine)-ligated heme protein.[188,189] The MCD spectrum of ferrous cytochrome b_5 (Figure 25A) is dominated by an intense derivative-shaped feature centered at 555 nm which is indicative of a six-coordinate low-spin state. This feature is present in the spectrum of deoxyferrous secondary amine monooxygenase but is much less intense (Figure 25A). Meanwhile, the Soret region of the MCD spectrum of deoxyferrous secondary amine monooxygenase resembles that of deoxyferrous myoglobin (Figure 25A), again except for intensity. These observations led to the proposal that the heme iron of deoxyferrous secondary amine monooxygenase is a mixture of five-coordinate high-spin histidine-bound and six-coordinate low-spin bis(histidine)-ligated.[176,185] In support of this hypothesis, a computer-generated MCD spectrum formed by combining the spectrum of ferrous b_5 (65%) and deoxyferrous myoglobin (35%) has been prepared and closely matches the spectrum of deoxyferrous secondary amine monooxygenase (Figure 25B).

The partially bound sixth ligand is displaced upon addition of O_2 or CO to form the O_2 or CO ferrous adducts (a reaction that does not occur with b_5). These results suggest that there is a histidine residue on the distal side of the heme which binds weakly to the ferrous heme iron in the absence of oxygen or other exogenous ligands. The mechanistic implications of the presence of a distal histidine will be discussed in the next section. The absorption and MCD spectra (not shown) of the oxyferrous and ferrous−CO adducts of secondary amine monooxygenase are each similar to the corrresponding myoglobin derivatives, as expected if both have proximal histidine ligation.

C. Mechanism

As described in section IIJ, mechanisms of N-dealkylations of alkylamines catalyzed by cytochrome P450 are of particular interest. The secondary amine monooxygenase system was a natural choice to further examine oxidative N-dealkylation because of its “bridging position” between the histidine-ligated heme peroxidases and the thiolate-ligated P450s. A kinetic deuterium isotope effect study of secondary amine monooxygenase was published by Hawkins

and Dawson in 1992.[190] Because the net intermolecular and intramolecular isotope effects were apparently masked by a high forward commitment to catalysis, a common problem in isotope effect studies, the isotope effect was determined through an intrasubstituent isotope effect experiment in which (1,1,1′,1′-d_4)dimethylamine was used as a substrate to unmask the isotope effect. This experiment yielded an isotope effect of 1.76, and the result (on the basis of the premise that low isotope effects (1−3) rule out the hydrogen atom abstraction[191]) was interpreted as an indication that the mechanism proceeds through the electron transfer/deprotonation mechanism (Figure 19: **24** → **25** → **26** → **28**). However, as described in section IIJ, the validity of ruling out N-dealkylation reaction pathways on the basis of the magnitude of the isotope effect obtained from only one deuterated and nondeuterated substrate combination has been called into question.[119] Thus, it has not been unequivocally established for secondary amine monooxygenase *or* the P450s that only one mechanism can exclusively describe oxidative N-dealkylkation reactions. It is unlikely, however, that the reaction catalyzed by secondary amine monooxygenase occurs through the peroxidase electron transfer/deprotonation pathway where electron transfer occurs at the edge of the heme and a suitable proton acceptor is absent (Figure 19: **24** → **25** → **27** → **28**). Such a reaction mechanism has been shown to exhibit large isotope effects (8.72−10.1) without masking for N-dealkylations of *N*-methyl-*N*-(trideuteriomethyl)aniline by hemoglobin, myoglobin, and various histidine-ligated peroxidases.[191] The P450s exhibit small isotope effects (1.61−3.05)[191] and also do not follow the peroxidase electron transfer/deprotonation mechanism.[113] Because it shows an isotope effect of only 1.76,[190] secondary amine monooxygenase appears to be distinct from the peroxidases in this mechanistic respect even though it is histidine-ligated. More work will be required to distinguish which of the two remaining mechanistic pathways (Figure 19: **24** → **25** → **26** → **28 or 24** → **26** → **28**) best describes the mechanism of N-dealkylation catalyzed by secondary amine monooxygenase.

Though structural and mechanistic studies of secondary amine monooxygenase to date have been limited to only those studies described in this review, they have enabled us to make predictions regarding the overall catalytic mechanism. Secondary amine monooxygenase has all the tools required for activation of molecular oxygen. The redox centers required to bridge the electrochemical gap between NADPH and the reduction of ferric to ferrous heme and oxyferrous to ferric peroxide heme are present in the enzyme. Furthermore, if the distal side of the heme active site has a histidine, it could function in a mechanism similar to that seen in the peroxidases, where heterolytic cleavage to form compound I is assisted by a distal histidine.[10] This would compensate for the lack of electron-releasing character or "push" provided by a proximal thiolate ligand as seen in P450.[10]

The stability of the oxyferrous adduct[173,176] argues against it playing a direct role in substrate oxygenation. Consumption of 1 equiv of NADPH per equivalent of substrate oxidized[173] indicates that two electrons are consumed in the reaction which together with the binding of O_2 would form a heme ferric−peroxide adduct. The question now remaining is whether the ferric−peroxide adduct or compound I is the active oxygen catalytic species. The involvement of ferric−peroxide as an active oxygen intermediate has only recently been implicated in oxygen insertion reactions catalyzed by P450 aromatase,[144,145] nitric oxide synthase,[163] and heme oxygenase.[192] In the P450 aromatase and nitric oxide synthase cases, the distal oxygen of the ferric−peroxide adduct is proposed to act as a nucleophile and attack electrophilic sites on the substrate.[144,145,163] This type of mechanism can be ruled out for lack of such a suitable electrophilic carbon in dimethylamine. In the heme oxygenase-catalyzed conversion of heme to α-hydroxyheme[192] (section IV), the ferric−peroxide adduct is the subject of electrophilic addition of the terminal peroxide oxygen to the α-heme edge to form α-hydroxyheme. If dimethylamine were to function as a nucleophile and attack the distal oxygen, the product would be *N*-hydroxydimethylamine. Breakdown of this relatively stable compound to yield methylamine and formaldehyde is highly unlikely. We can therefore conclude that a ferric−peroxide intermediate is an unlikely candidate for the active oxygen intermediate in the N-dealkylation of dimethylamine. This leaves an oxo−ferryl porphyrin cation radical, compound I-type, intermediate as the most likely species responsible for the oxygen insertion reaction. Preliminary studies indicate[193] that a complex resembling horseradish peroxidase compound II is formed upon addition of H_2O_2 to ferric secondary amine monooxygenase. Such an observation does not rule out the possibility of compound I formation followed by rapid oxidation of a nearby amino acid as in the case of cytochrome *c* peroxidase where the radical rests on a tryptophan residue.[194] Detection of such a protein radical in secondary amine monooxygenase has yet to be attempted. It should be noted that the spectroscopic similarities between secondary amine monooxygenase and myoglobin do not necessarily extend to the state of ionization or hydrogen bonding of the proximal histidine. We expect however, that there must be some degree of ionization or hydrogen bonding to assist in efficient cleavage of the O−O bond to form compound I from the ferric−peroxide species. It is hoped that future resonance Raman and EPR investigations will reveal the electron-donating properties of the proximal histidine.

In summary, the following mechanism for the oxidative demethylation of dimethylamine is proposed based on the current understanding of the structure of secondary amine monooxygenase and requirements for oxygen activation (Figure 26). One-electron reduction of the aquo−ferric resting state**, 30,** results in loss of H_2O and is accompanied by binding of the substrate. This state is partially six-coordinate low spin, **31b**, and partially five-coordinate high spin, **31a**. Addition of O_2 yields the stable oxyferrous complex, **32**. Addition of the second electron forms the ferric−peroxide adduct, **33**. Diprotonation of the distal peroxide oxygen followed by heterolytic cleavage of the O−O bond yields compound I, the oxo−ferryl porphyrin cation radical, **34**.

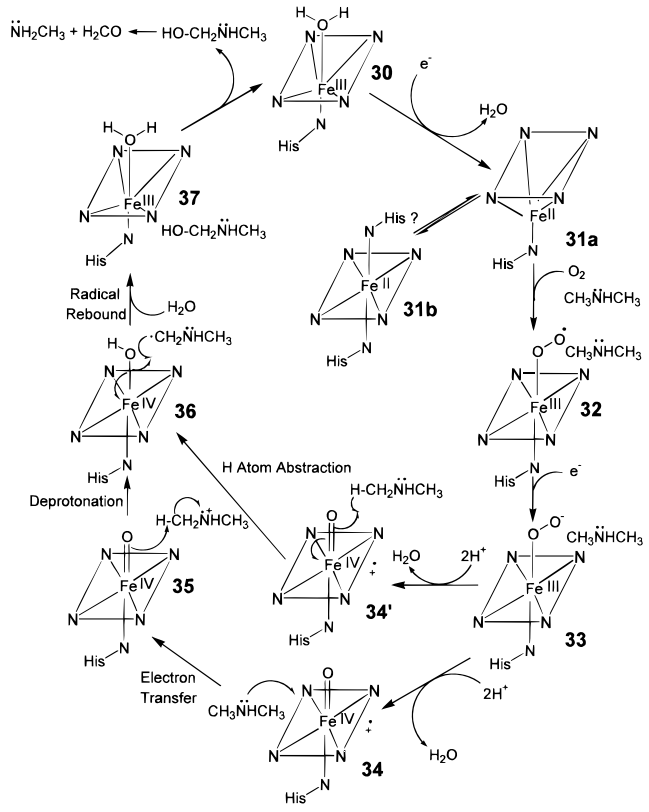

Figure 26. Proposed reaction mechanism for the secondary amine monooxygenase catalyzed N-demethylation of dimethylamine.

The two posssible pathways at this point are (i) one-electron transfer from dimethylamine to compound I to yield compound II and a dimethylamine cation radical, **35**, which is then deprotonated to give an iron-bound hydroxyl radical and dimethylamine radical, **36** (**34** → **35** → **36**) or (ii) hydrogen atom abstraction by compound I, **34′**, to give the dimethylamine radical and the iron-bound hydroxyl radical, **36** (**34′** → **36**). At this point, radical rebound yields the carbinolamine **37**, which undergoes loss of formaldehyde to give methylamine and addition of H_2O regenerates the high-spin ferric−aquo resting state, **30**. Again, this is the best working hypothesis for the mechanism based on available information and currrent knowledge of heme monooxygenase chemistry. Further study of this system will undoubtedly lead to a more complete understanding of the requirements for heme-catalyzed oxygen activation.

IV. Heme Oxygenase (HO)

A. Background

Heme oxygenase, first characterized by Schmid and co-workers,[195,196] is a microsomal enzyme which catalyzes the first key step in heme catabolism, the oxidative degradation of heme (iron−protoporphyrin IX) to biliverdin and carbon monoxide[197−199] (Figure 27). The overall reaction is quite complex and involves two well-characterized intermediates: α-mesohydroxyheme and verdoheme (Figure 27). The enzyme can be purified from several different organ sources including liver,[200,201] spleen,[202,203] brain,[204] and testis.[204] Though it has two known isoforms, referred to as HO-1 (33 kDa) and HO-2 (36 kDa),[204−206] it is generally assumed that they have similar active

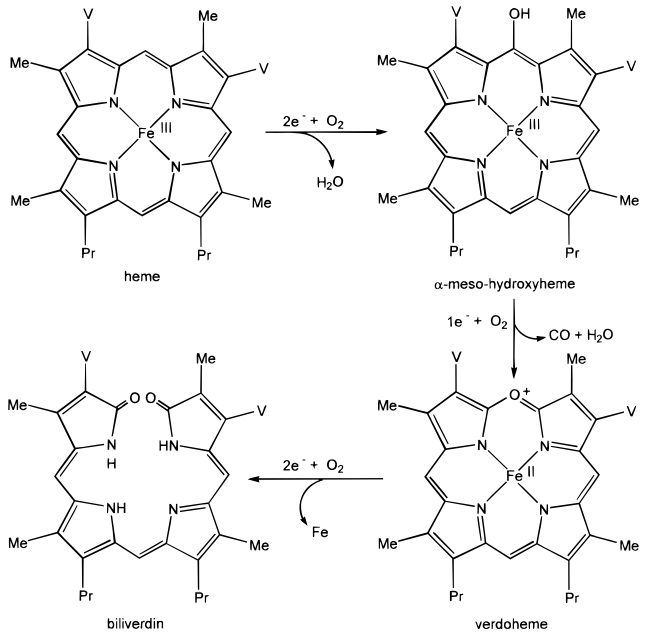

Figure 27. Probable reaction sequence of intermediates in the heme oxygenase-catalyzed conversion of heme to biliverdin. Adapted from ref 211 (copyright 1993, American Chemical Society).

sites and share a similar mechanism of action. HO-1 is inducible and is highly expressed in the spleen and liver. HO-2 is constitutive and found primarily in the brain. Recent studies suggesting that the CO liberated from heme by heme oxygenase may act as a physiological messenger[207,208] have heightened interest in the heme oxygenase system.

Heme oxygenase by itself contains no prosthetic groups. Thus, unlike the other oxygen-activating enzymes discussed in this review, it is not a heme protein per se. It binds heme in a 1:1 ratio[200] and constrains it to an environment suitable for a site-specific, O_2-dependent heme self-oxidation. It is therefore best described as a transient heme protein and is the only system currently known to utilize heme simultaneously as both a prosthetic group and substrate.[203] For the purpose of this discussion, the term "heme oxygenase" refers to the heme−heme oxygenase complex unless otherwise specified.

Like the P450s and secondary amine monooxygenase, heme oxygenase requires a flavin redox center for electron transfer from NADPH via NADPH-cytochrome P450 reductase.[199] Because of this relationship to P450, heme oxygenase was originally thought to involve P450 as a terminal oxidase.[195,196] However, Yoshida, Kikuchi, and co-workers[200,203,209] have established that in terms of electronic absorption, heme oxygenase is spectrally distinct from P450 and similar to myoglobin and suggested that the binding of heme could occur through a coordination linkage with an amino acid residue as a ligand.[198] As with secondary amine monooxygenase, the implications of a heme-containing enzyme having a non-thiolate heme iron center while retaining the ability to carry out oxygen insertion reactions is of obvious interest. Studies of heme oxygenase have only recently become greatly facilitated by overexpression of truncated forms of the rat liver HO-1 isozyme where the hydrophobic membrane-spanning domain has been removed.[210,211] One of these truncated-

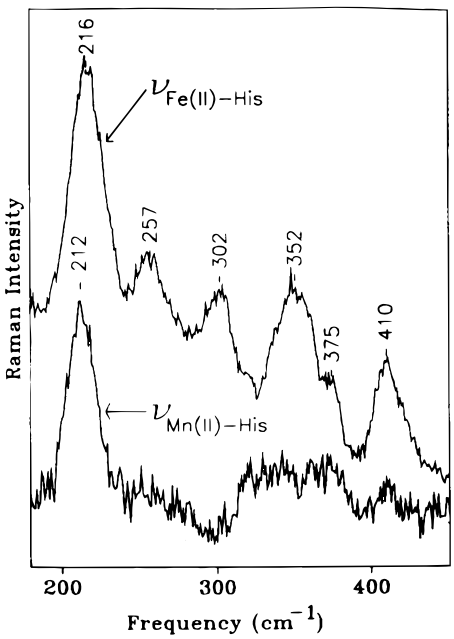

Figure 28. Resonance Raman spectra of Fe^{II}-protoporphyrin IX−heme oxygenase complex (upper trace) and Mn^{II}-protoporphyrin IX−heme oxygenase complex (lower trace) in the low-frequency region. (Reproduced with permission from ref 214. Copyright 1993 American Chemical Society.)

overexpressed systems has been fused with NADPH-dependent cytochrome P450 reductase to create a catalytically self-sufficient single protein system,[212] thereby improving the efficiency with which mechanistic studies could be pursued.

B. Active Site Structure

1. Ligation States

The electronic absorption spectra of heme oxygenase resemble those of myoglobin.[200,203,209] This was a preliminary indication that histidine might serve as a proximal ligand. His-25, which is present within the highly conserved 24-amino acid domain in the rat HO-1 isozyme, was thought to be a logical candidate,[210,213] and mutagenesis of this conserved residue to alanine was found to abolish all enzymatic activity.[212,213] Though this result provides strong support for the hypothesis, additional spectroscopic studies have been carried out to unequivocally establish the identity of the axial ligands. Resonance Raman spectroscopy has been particularly useful in this regard. Independent studies by Ortiz de Montellano, Loehr, and co-workers[214] and by Rousseau, Yoshida, Ikeda-Saito, and co-workers[215] provided direct evidence for histidine ligation to the heme iron of heme oxygenase. The Raman stretching frequencies for the porphyrin skeletal modes of deoxyferrous and ferric heme oxygenase were found to be similar to those of several five-coordinate high-spin deoxyferrous and six-coordinate high-spin ferric histidine-ligated heme proteins (data not shown). In addition, a Raman band at 216−218 cm^{-1} in the low-frequency resonance Raman spectrum of deoxyferrous heme oxygenase was assigned to a Fe−His mode[214,215] (Figure 28). The low value of this mode (relative to other histidine-ligated heme proteins) is attributed to the lack of strong hydrogen bonding or ionization of the

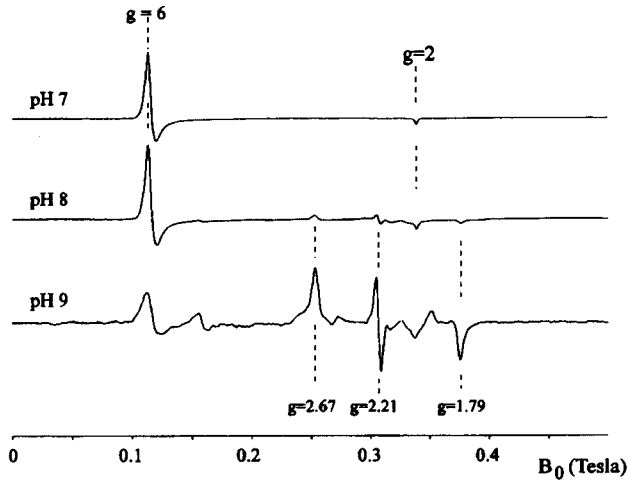

Figure 29. EPR spectra of ferric heme−heme oxygenase complex measured at 6 K. Reproduced with permission from ref 215 (copyright 1994, Journal of Biological Chemistry).

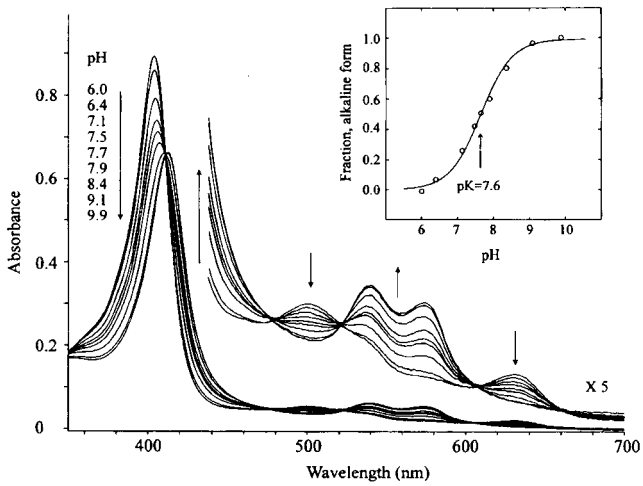

Figure 30. Electronic absorption spectra of the ferric heme−heme oxygenase complex between pH 6 and 10 at 20 °C. Reproduced with permission from ref 215 (copyright 1994, Journal of Biological Chemistry).

ligated histidine, which typically results in Fe−His stretches in a range from 233 to 246 cm^{-1}.[216,217] That the same mode is found at 212 cm^{-1} for Mn^{II}-protoporphyrin IX−heme oxygenase, (Figure 28)[214] provides additional evidence for the assignment.

The EPR spectrum of ferric heme oxygenase (Figure 29) exhibits *g* values at approximately 6 and 2 in agreement with those of myoglobin and indicative of a high-spin ferric complex.[214,215] Upon raising the pH, a new set of signals appears with *g* values at 2.67, 2.21, and 1.79 (Figure 29) which are representative of a histidine-ligated heme protein undergoing a high- to low-spin conversion.[215] This conversion is thought to be due to deprotonation of a water molecule bound in the sixth position[214,215] and is also seen in electronic absorption[214,215,218] (Figure 30) and MCD spectra.[218] The pK_a calculated from a pH titration is 7.6.[214] The hyperfine structure seen in the EPR spectra of ferrous−NO heme oxygenase (Figure 31) gives additional evidence for the assignment of histidine as the proximal ligand,[214,215] and furthermore, the hyperfine coupling constant of 0.74 mT is similar to that observed for myoglobin rather than that of the peroxidase ferrous−NO complexes.[219] This provides support for neutral histidine ligation

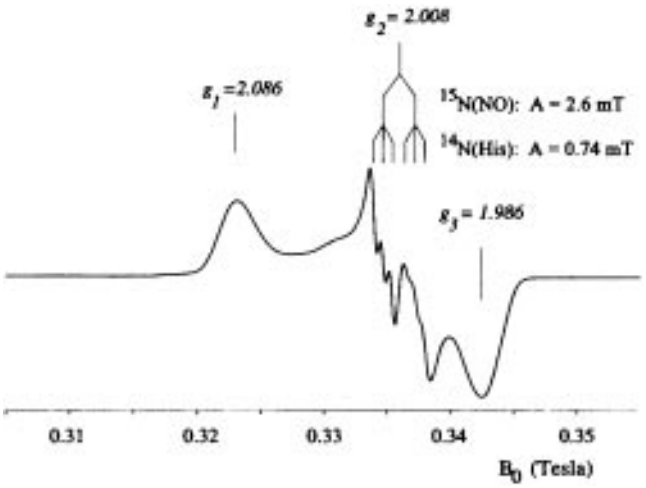

Figure 31. EPR spectrum of the ferrous heme−heme oxygenase ^{15}NO complex measured at 30 K. Reproduced with permission from ref 214 (copyright 1993, American Chemical Society).

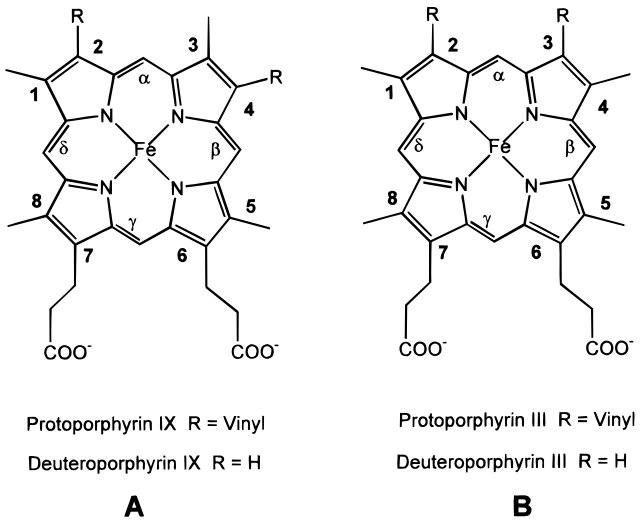

Figure 32. Structures of type IX (A) and type III (B) iron porphyrins. Adapted from ref 225.

as opposed to ligation by an ionized or strongly hydrogen-bonded histidine.[215] Additional resonance Raman studies[220] of ferric heme oxygenase have corroborated the above conclusion that ferric heme oxygenase is ligated by water at neutral pH and hydroxide at alkaline pH. On a Fe−CO stretching frequency vs C−O stretching frequency correlation diagram, the ferrous−CO adduct of heme oxygenase falls in the same range as myoglobins, hemoglobins, and imidazole-ligated porphyrin derivatives and far from the range including partially ionized, imidazole-ligated heme proteins such as the peroxidases.[220] The MCD spectra of several derivatives of ferric and ferrous heme oxygenase also match those of parallel myoglobin complexes.[218] Recent EXAFS[218] studies indicate that the Fe to proximal histidine bond distance is 2.08 Å and the Fe to distal ligand bond distance is 1.93 Å, values that are very close to those of myoglobin and different from those of typical peroxidases.[218,221] These studies all provide very convincing evidence that a neutral histidine serves as the proximal ligand in heme oxygenase. Mutation of His-25 to alanine in rat liver heme oxygenase[222,223] not only brings about a loss of catalytic activity,[213,223] as discussed above, but also results in loss of the Raman Fe−His stretching mode[222] and the hyperfine splitting in the ferrous−NO EPR spectrum.[223] When exogenous imidazoles are added to the His-25Ala mutant, they enter the heme proximal pocket, ligate to the heme iron (as proven by the appearance of a Fe−imidazole stretching mode in the resonance Raman spectrum), and restore catalytic activity.[224] These studies have established unequivocally that His-25 of heme oxygenase from rat liver serves as the proximal ligand and proves the utility of combining various spectroscopic methods with mutagenesis in the determination of axial coordination in hemeproteins.

2. Active Site Environment

A proton NMR study of cyanoferric heme oxygenase published by La Mar and co-workers in 1994[225] drew some important conclusions regarding substrate binding, heme electronic structure, and steric influences on a bound ligand. Binding of iron protoporphyrin IX or iron deuteroporphyrin IX (Figure 32A) to substrate-free heme oxygenase yields heterogeneous ^{1}H NMR spectra. The analogous spectra obtained from iron protoporphyrin III or iron deuteroporphyrin III which have a 2-fold axis (Figure 32B) are much better resolved, indicating that isomeric binding of substrate iron porphyrin occurs in two orientations with an approximate ratio of 1:1 and that the orientational disorder occurs about the α,γ-meso axis. The best evidence for the heme orientational disorder was obtained in 2D ^{1}H NMR spectra of iron protoporphyrin IX which showed that the 3-methyl group of one isomer experiences the same environment as the 2-vinyl of the other isomer (interaction with an aromatic residue). Once the contributing resonances of the two isomers were resolved using the cyanoferric iron protoporphyrin IX−heme oxygenase complexes, the researchers were able to re-examine the multiplicity of the peaks in the high-spin ferric ^{1}H NMR spectra and conclude that similar orientational disorder is present in the non-cyanide-inhibited functional heme-bound heme oxygenase as well. This result is not discouraging from a mechanistic point of view because it indicates that the α-meso carbon is held in the same position in space relative to the protein environment in both isomers, which is what one would expect on the basis of the regioselectivity of the reaction for the α-meso heme edge.

In the same study,[225] an unusual pattern of spin density on the heme periphery of cyanoferric heme oxygenase has been elucidated using isotope labeling and 2D NMR. The results indicate that spin density is localized primarily to the pyrrole carbons adjacent to the α,γ axis. This is attributed to a direct electronic effect of the protein on the heme as could occur through a perturbation of the α-meso carbon by a nearby anionic side chain. This was thought to be a reasonable mechanism of perturbation because the pattern attributed to the specific spin delocalization is lost at acidic pH. The authors have suggested that this type of perturbation would activate the α-meso carbon for an electrophilic aromatic substitution reaction rather than make it an enhanced site for nucleophilic attack.[225]

In addition, the pattern of dipolar shifts for cyanoferric heme oxygenase was shown to be different for each of the two possible heme orientations. This is indicative of steric influences on the orientation of the bound cyanide ligand and suggests that, during catalysis, the two different heme orientations might have different reaction kinetics while sharing reaction regiospecificity. It is thought[225] that this differential steric constraint imposed by noncoordinating active site residues on the bound ligand is responsible for the wide variation in heme oxygenase activity exhibited in reactions with various synthetic iron porphyrins.[226]

Evidence for a highly bent structure of coordinated dioxygen in oxyferrous rat liver heme oxygenase was presented by Rousseau and co-workers in 1995.[227] Oxygen isotope shift resonance Raman experiments revealed that the frequency of 565 cm^{-1} for the Fe−O_2 stretch is the lowest of all oxyferrous neutral histidine-ligated heme proteins.[227] Furthermore, the isotope shift pattern is independent of pH, temperature, and D_2O exchange, thus confirming that the low frequency is not due to protonation of the distal oxygen. Calculation of a theoretical curve for the correlation of the normalized isotope shift vs the bending angle (determined from Raman and crystallographic data of hemoglobin and myoglobin) enabled the researchers to assign a Fe−O−O bending angle of 110°, an angle that could bring the distal oxygen atom into van der Waals contact with a meso-edge carbon. This small angle is expected to be the result of strong steric interactions of bound O_2 with residues in the distal pocket.[227] This result is in agreement with the results of the NMR study previously described[225] and is, again, encouraging from a mechanistic standpoint in that the bound dioxygen appears to be constrained to promote a regiospecific oxidation.

The role of His-132 at this time is the subject of some controversy. Ortiz de Montellano, Loehr, and co-workers have examined various mutants of His-132 of heme oxygenase and proposed a role for His-132 as the distal histidine.[228] On the other hand, Ikeda-Saito and co-workers suggested that similar His-132 mutations have no effect on activity.[223]

C. Mechanism

1. Conversion of Heme to α-Mesohydroxyheme

It has been established that reduction of heme oxygenase by NADPH-dependent cytochrome P450 reductase results in a ferrous species that readily binds O_2 or CO and that, like P450, a second reduction is required for the formation of an active-oxygen species which carries out the α-meso hydroxylation of bound heme to form α-mesohydroxyheme.[200] (Figure 27). Wilks and Ortiz de Montellano[211] were the first to attempt to identify the active heme−oxygen intermediate responsible for this first oxidation step. Model studies have indicated that metalloporphyrins will react with H_2O_2 under certain conditions to yield meso-hydroxylated products,[229] so a similar strategy was used. It was found that H_2O_2 does support the formation of α-mesohydroxyheme and, in the presence of O_2, the additional step to verdoheme.[211] This experiment suggested the possibility of involvement of an oxo−ferryl complex

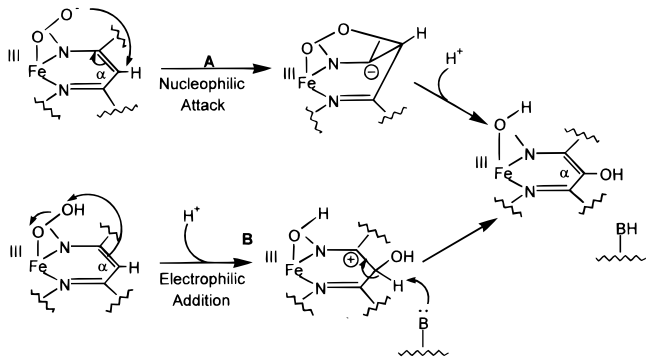

Figure 33. Two possible mechanisms of reaction of a ferric−hydroperoxide active oxygen intermediate to yield α-mesohydroxyheme. (A) nucleophilic attack of iron-bound peroxide; (B) electrophilic aromatic substitution. Adapted from ref 211.

generated by heterolytic cleavage of the O−O bond such as that observed or postulated with iron porphyrins,[230] peroxidases,[59] globins,[231,232] catalases,[233] and monooxygenases.[14] To further examine this possibility, the reaction was repeated using *m*-chloroperbenzoate in place of H_2O_2. This leads to formation of a compound II-type oxo−ferryl species which is only one oxidation equivalent above the ferric resting state.[211] Transient observance of an EPR signal with $g = 2.006$ indicates that a compound I-type oxo−ferryl porphyrin cation radical had formed which subsequently underwent one-electron reduction through protein oxidation. The lack of verdoheme formation demonstrates that the oxo−ferryl could not be the catalytic species. These authors also argued against free hydroxyl radical (generated through homolytic breakdown of ferric−hydroperoxide) as a viable intermediate as it would be less regioselective.[211]

The remaining mechanistic alternatives at this time, were therefore limited to the potential reactivity of a ferric−peroxide or ferric−hydroperoxide active heme−oxygen intermediate. The two possibilities envisioned here (Figure 33) were nucleophilic attack of the unprotonated terminal oxygen of a ferric−peroxide intermediate on the α-meso carbon (Figure 33A) or an electrophilic addition of the terminal protonated oxygen of a ferric−hydroperoxide intermediate onto the α-meso carbon (Figure 33B).[211]

The authors have suggested[211] that the compound II oxo−ferryl species that formed through addition of *m*-chloroperbenzoate was a result of heterolysis of the iron-ligated *m*-chloroperbenzoate O−O bond and that this occurrence could have been influenced by steric interactions of distal residues with the bulky aryl hydroperoxyacid. It was expected that, if this was the mechanism of heterolysis, it could be avoided through the use of an alkyl hydroperoxide with less steric bulk.[192] When ethyl hydroperoxide was added to ferric heme oxygenase, two products were obtained: compound II, which is a result of some O−O homolytic cleavage, and α-mesoethoxyheme,[192] which is a result of electrophilic aromatic addition of ethoxide from the ferric−ethyl hydroperoxide adduct to the α-meso carbon (Figure 34). It was this experiment which distinguished the mechanism of the first oxidation of heme as electrophilic addition (Figure 33B). The nucleophilic attack mechanism (Figure

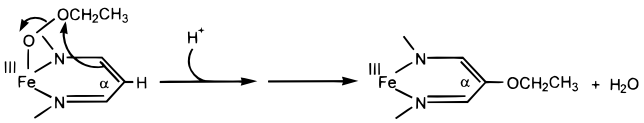

Figure 34. Electrophilic α-meso ethoxidation reaction.

33A) could be ruled out because a terminal alkylated oxygen atom is not nucleophilic.[192]

This mechanism (**38** → **42a** in Figure 35) is consistent with all the known structural features of the active site of heme oxygenase. Apparently, the neutral proximal histidine stabilizes the ferric−hydroperoxide adduct, **41**, until the terminal oxygen is specifically oriented, through the steric influence of distal pocket residues, to come into contact with the α-meso carbon. Electrophilic addition of the terminal oxygen to the π electrons of the double bond involving α-meso carbon leads to hydroxyl substitution at the α-meso carbon (Figure 33B). The resulting sp^3 α-meso carbon intermediate is then deprotonated by a nearby base, possibly the anionic functional group responsible for the electronic perturbation at the α-meso edge[225] as discussed above. The remaining ferric-bound oxo is protonated twice and lost as H_2O (evidence has been presented[234] that the ferric α-mesohydroxyheme−heme oxygenase complex is five-coordinate; see below).

2. Conversion of α-Mesohydroxyheme to Verdoheme

Recent work by Ikeda-Saito,[234] Ortiz de Montellano,[235] and their co-workers has significantly clarified the mechanism of conversion of α-mesohydroxyheme to ferrous verdoheme. The coordination structure of ferric α-mesohydroxyheme was established by Ikeda-Saito[234] through comparisons of electronic absorption and EPR spectra of α-mesohydroxyheme-bound heme oxygenase with α-mesohydroxyheme reconstituted into both myoglobin and His64Ile myoglobin, the latter of which cannot bind H_2O in the distal position due to the absence of its distal His-64.[236,237] The similarities between the spectra of these three proteins indicate that the α-mesohydroxyheme−heme oxygenase complex as well as the analagous native myoglobin reconstituted with α-mesohydroxyheme are also five-coordinate complexes.[234] Thus, it appears as though ferric α-mesohydroxyheme with neutral histidine as a fifth ligand is incapable of binding a sixth ligand to its heme iron. This is an indication that the altered electronic structure of the porphyrin has changed the iron coordination chemistry.[234] The resonance Raman spectrum of ferric α-mesohydroxyheme-bound heme oxygenase is unusual and is also unaffected by D_2O. This led the researchers to propose a ferric oxophlorin structure (**42b** in Figure 35) as the dominant resonance structure for this species.[236] This structure is one of the three resonance forms of ferric α-mesohydroxyheme

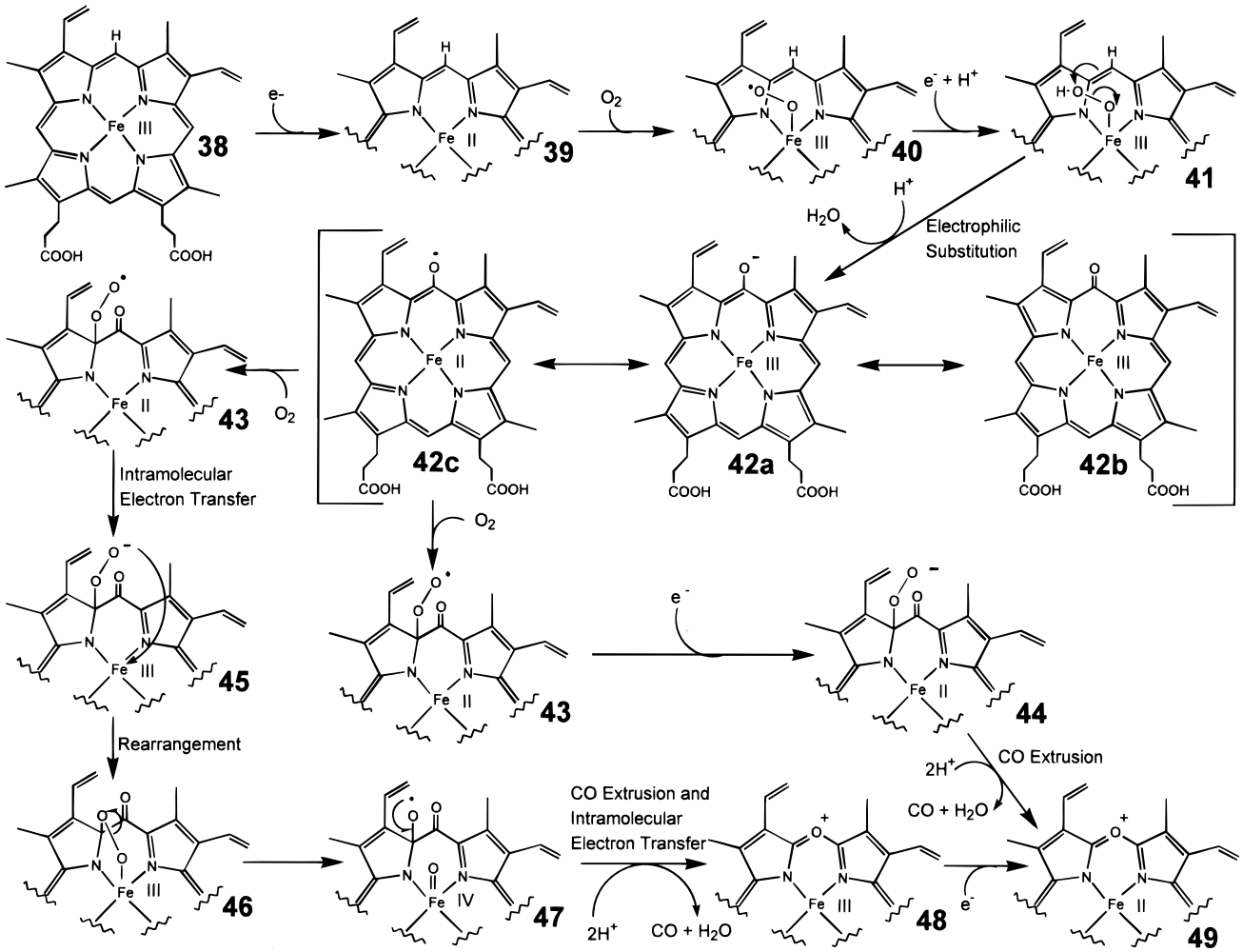

Figure 35. Proposed mechanisms of heme oxygenase-catalyzed conversion of heme to verdoheme. Adapted from refs 234 and 235.

proposed by Morishima and co-workers.[238,239] The other two forms proposed are α-mesohydroxylate, **42a**, and a ferrous neutral radical form, **42c**.

Reduction of the ferric oxophlorin, **42b**, by dithionite yields a species with electronic absorption and resonance Raman spectra characteristic of five-coordinate high-spin ferrous histidine-ligated heme proteins.[234] This indicates that, upon reduction, the porphyrin regains the symmetry that was initially lost upon formation of the ferric oxophlorin structure. In addition, the resonance Raman spectrum of this new species shows a D_2O effect. This observation led the authors to conclude that the proton-bearing α-hydroxy form is the structure of this reduced species. Thus, one-electron reduction of α-mesohydroxyheme is accompanied by a keto−enol transition.[234]

Ikeda-Saito and co-workers[234] have proposed that the conversion of ferric α-mesohydroxyheme to verdoheme could proceed in two parallel pathways: (i) oxygenation of the ferrous neutral radical, **42c**, followed by one-electron reduction (Figure 35) or (ii) by reduction of **42c** followed by oxygenation (not shown).[234]

The experiments reported by Ikeda-Saito[234] were carried out under a CO atmosphere because the stable ferrous−CO adduct of verdoheme provides a means for spectrophotometric quantitation of verdoheme product. Addition of O_2 to ferric α-mesohydroxyheme-bound heme oxygenase leads to conversion of the rhombic ferric high-spin EPR signal to a radical-type signal at $g = 2.004$ which is indicative of an unpaired electron residing at a location distant from the heme iron.[234] A very similar radical EPR signal also occurs when O_2 is added to ferric myoglobin reconstituted with α-mesohydroxyheme and has been proposed to arise from a peroxy radical species,[234,240] **43**. One-electron reduction of this species results in the rapid formation of ferrous verdoheme, **49**, presumably via a ferrous−peroxy species **44**.[234] The inability of CO to inhibit the conversion of α-mesohydroxyheme to ferrous verdoheme provides evidence that the peroxy radical species **43** is most likely formed by addition of unactivated O_2 to the heme-edge radical site.[234] This type of novel reaction of oxygen at a porphyrin edge has also been recently reported for phagocytic cytochrome b_{558}[241] and is an excellent example of the reactive versatility of iron porphyrins. These results prove that the heme oxygenase-catalyzed conversion of α-mesohydroxyheme to ferrous verdoheme requires oxygen and one reducing equivalent.[234]

Ortiz de Montellano has even more recently examined the conversion of α-mesohydroxyheme to verdoheme and found that it is possible to form ferric verdoheme by addition of O_2 to **42c** in the absence of CO.[235] As with the Ikeda-Saito mechanism,[234] O_2 is proposed to attack at the heme edge to give **43**. However, in the absence of a reducing agent (and CO), Ortiz de Montellano[235] proposed an internal electron transfer to yield a ferric complex with edge-bound peroxy anion, **45**, which rearranges to a bridging peroxy species **46**. Homolytic cleavage of the O−O bond leads to **47** followed by CO extrusion and intramolecular electron transfer to yield ferric verdoheme, **48**. Ferrous verdoheme can then be formed by one-electron reduction. Further, Ortiz de Montellano[235] suggested that the radical species **43** observed by Ikeda-Saito[234] is a CO adduct, **43**·CO, and that this species is unable to undergo the internal electron transfer required to form ferric verdoheme. Nonetheless, in both mechanisms, O_2 and one electron are required to form ferrous verdoheme from ferric α-mesohydroxyheme.

In summary, Figure 35 illustrates the possible mechanisms of verdoheme formation starting from the normal heme substrate and includes all of the mechanistic details known to date. One-electron reduction of heme, **38,** yields deoxyferrous heme, **39,** which then binds O_2 to give oxyferrous heme, **40**. Addition of a second electron and a proton creates the ferric−hydroperoxide species, **41**. Heterolytic O−O bond cleavage via an electrophilic addition reaction to the α-meso edge yields α-mesohydroxyheme, which consists of three major resonance structures: a ferric oxophlorin structure **42b**, a ferric phenolate structure, **42a**, and a ferrous neutral radical species, **42c**.

In the presence of CO, the mechanism of ferrous verdoheme formation is as follows: Dioxygen binds to a pyrrole carbon adjacent to the α-meso carbon to give the proposed ferrous peroxy radical species, **43**. Addition of one electron results in the peroxy species **44**, which is presumed to be the active oxygen intermediate.[234,235] This then reacts rapidly to extrude CO and form ferrous verdoheme, **49**. The pathway summary for the case when CO is present is **42c** → **43** → **44** → **49**.[234]

In the absence of CO, ferric verdoheme can be formed as follows: Dioxygen binds to **42c** as above to form **43**. An intramolecular electron transfer from the ferrous iron to the bound superoxide yields **45**. Ligation of the anionic terminal peroxide oxygen to the ferric iron generates the ferric peroxo-bridged complex, **46**. Homolytic cleavage of the O−O bond results in **47**, which is set up for extrusion of CO and intramolecular electron transfer to give ferric verdoheme, **48**. One-electron reduction of ferric verdoheme yields the ferrous complex, **49**. The pathway summary is **42c** → **43** → **46** → **47** → **48** → **49.**[235]

It is interesting to note that both of the oxidations of heme catalyzed by heme oxygenase discussed herein (Figure 27) utilize peroxy-type active oxygen intermediates instead of the compound I-type oxo−ferryl intermediate which is thought to be the catalytic species in P450 oxidations.[10,14] In the formation of α-mesohydroxyheme, it appears as though neutral histidine proximal ligation, which is an unusual feature for a heme-containing monooxygenase, provides the essential fine tuning of the heme coordination sphere to stabilize the peroxy species with respect to O−O bond cleavage until the bound peroxide adopts an orientation suitable for each regiospecific oxidation. The distal site heme pocket structure might also significantly contribute to the stabilization of the ferric peroxy species. The proposed mechanisms for generation of ferrous verdoheme are unusual in that O_2 appears to add directly to a radical at the heme edge. The steric interactions responsible for the two regiospecific oxidations are also of obvious importance. These studies of heme oxygenase highlight the reactive

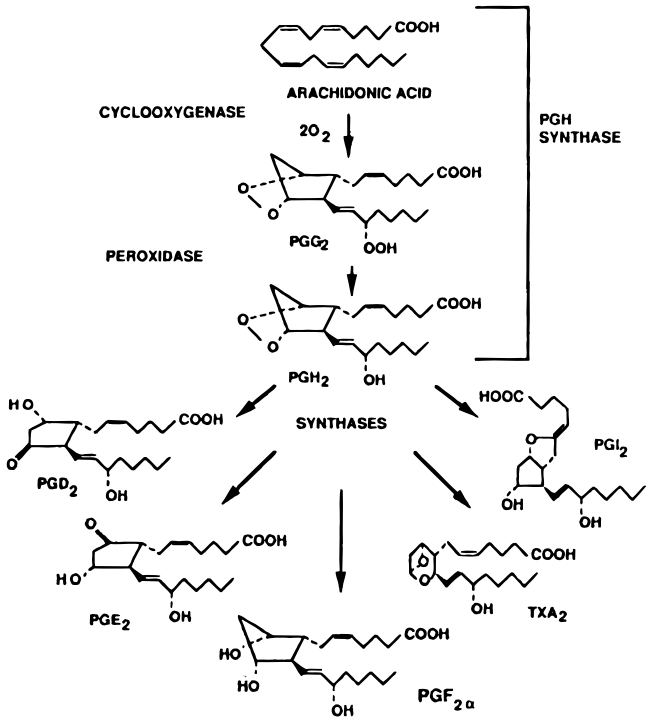

Figure 36. Common biosynthetic pathway for the conversion of arachidonic acid to a variety of prostanoids (PG, prostaglandin; TX, thromboxane). Cyclooxygenase and peroxidase reactions of PGHS are included. Adapted from ref 242.

versatility of iron porphyrins and provide even more support for the consensus that the identity of the proximal ligand and the nature of the heme active site environment play crucial roles in various mechanisms of heme-catalyzed oxygen activation reactions.[9b,15]

V. Prostaglandin H Synthase (PGHS)

A. Background

PGHS is a bifunctional, heme-containing enzyme that catalyzes the conversion of arachidonic acid to prostaglandin H_2,[242−244] a major precursor of prostaglandins, prostacyclins, and thromboxanes (Figure 36; see also section IIK.3). The two activities associated with PGHS are as follows: (i) cyclooxygenase activity, incorporation of two molecules of O_2 into the polyunsaturated fatty acid substrate, arachidonic acid, coupled with serial cyclization to the endoperoxide, hydroperoxide, prostaglandin G_2 (PGG_2); and (ii) peroxidase activity, a net two-electron reduction of the hydroperoxide moiety of PGG_2 to the corresponding alcohol, PGH_2. Two isozymes, PGHS-1 (constitutively expressed form) and PGHS-2 (inducible form), have been identified.[242] PGHS-1 and PGHS-2 exhibit ~60% sequence homology to one another and have been shown to possess similar catalytic activities. The majority of PGHS mechanistic studies have employed isozyme PGHS-1 and will therefore be the primary focus of this review.

As discussed previously (section I), dioxygen possesses a triplet ground state which is relatively unreactive toward the singlet ground state of most organic molecules. Traditionally, oxygenases have utilized a variety of prosthetic groups to overcome this problem.[245] For incorporation of both oxygen atoms of O_2 into a single organic substrate, intramolecular dioxygenase activity (see section I) by heme-containing enzymes (see section VI) requires formation of a complex between O_2 and ferrous high-spin heme. No ferrous or oxyferrous species have been observed during catalytic turnover of PGHS, nor is enzyme activity affected by carbon monoxide,[246] a potent inhibitor of heme systems that employ ferrous intermediates. Clearly, if PGHS does not activate O_2 in a heme-dependent manner, it must employ an alternative mechanism of substrate oxygenation. Nonetheless, both cyclooxygenase and peroxidase activities of PGHS have been shown to be heme-dependent,[247−249] although the protein contains only one heme prosthetic group per subunit.[250]

B. Active Site Structure

As isolated, the heme prosthetic group has been spectroscopically characterized to be ferric high-spin, exhibiting an electronic absorption spectrum which is typical of other ferric high-spin peroxidase enzymes with a Soret peak at 410−412 nm and a band at 630 nm.[251] Detailed spectroscopic studies by Ruf and co-workers[252] and by Tsai, Palmer and co-workers[253] provided considerable insight into the heme coordination structure of PGHS. The EPR spectrum of the ferric enzyme was consistent with a mixture of two types of high-spin [g = 6.6, 5.4, 2.0 (rhombic, five coordinate) and g = 6.0, 2.0 (axial, six coordinate)] and a single low-spin (g = 2.98, 2.19, 1.56) heme species.[252,253a] MCD spectra of the fluoride, azide, cyanide, and imidazole derivatives of PGHS closely resemble the corresponding derivatives of metmyoglobin, indicating similarities in the heme coordination structure of PGHS and myoglobin.[253b] MCD spectroscopy has also been used to determine the overall contribution of low-spin character to be 20% at ambient temperature, increasing to 50% at 167 K, suggesting that an equilibrium exists between five- and six- [(bishistidine)] coordinate heme.[253a] Resonance Raman studies failed to identify a five-coordinate high-spin species as suggested above, but instead inferred that a mixture of six-coordinate high- and low-spin heme is present.[253b] From these observations, these authors concluded that two histidine residues are the axial heme ligands in PGHS, with the distal histidine being only weakly associated. A recent crystal structure determination of PGHS-1 from sheep seminal vesicles by Garavito and co-workers[254] has identified two adjacent, yet clearly distinct active sites. The heme group is located at the peroxidase site with the iron coordinated to the protein via His-388. As is commonly the case in peroxidase enzymes, a distal histidine residue has been identified at position 207 (Figure 37).

C. Cyclooxygenase Activity

Cyclooxygenase activity is hydroperoxide-dependent. Hydroperoxides, such as PGG_2 have been proposed to cause oxidation of the heme to ultimately produce a protein-based radical.[255] Early experiments by Hamberg and Samuelsson[256] showed that the *pro-S* hydrogen atom was abstracted from C-13 (circled in Figure 38) with high stereoselectivity during incubation of [13_D-^{3}H,3-^{14}C]- and [13_L-^{3}H,3-^{14}C]-8,11,14-eicostrienoic acid with crude PGHS-

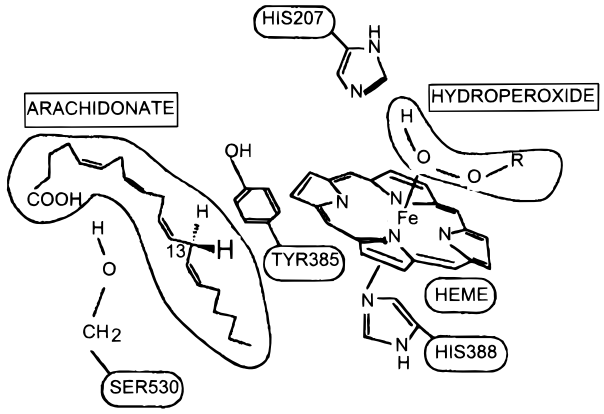

Figure 37. Model of the cyclooxygenase (left) and peroxidase (right) active sites of prostaglandin H synthase (PGHS-1) in the presence of substrates, arachidonate and hydroperoxide respectively. Reproduced with permission from ref 242 (copyright 1991, Elsevier).

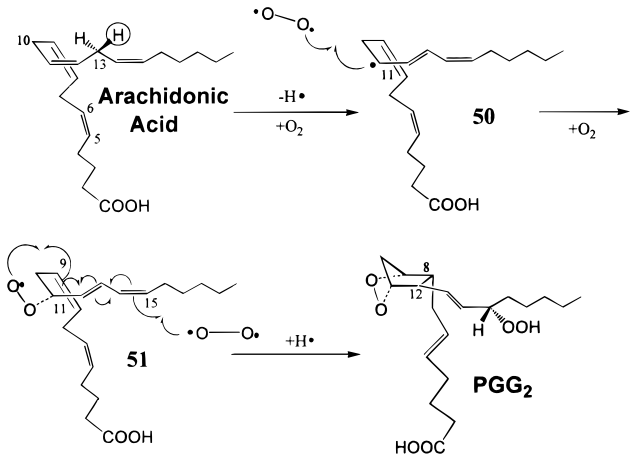

Figure 38. Schematic representation of the cyclooxygenase reaction of prostaglandin H synthase. The 13-*pro-S* hydrogen atom is circled. Adapted from ref 242.

containing homogenates of sheep vesicular glands. This abstraction results in a resonance-stabilized substrate radical which can react directly with O_2. Through allylic resonance (Figure 38, **50**), attack by O_2 occurs at C-11 to produce the 11-peroxyl radical, **51**. Cyclization to the bicyclic 9,11-endoperoxide is then coupled to bond formation between C-8 and C-12, isomerization of the C-12 double bond into the C-13 position, and reaction at C-15 with a second molecule of O_2. This gives the 15-peroxyl radical (not shown) which abstracts a hydrogen atom to form PGG_2 (Figure 38). The main function of the cyclooxygenase active site may be to position the substrate in a suitable orientation to ensure correct activation. The cyclooxygenase active site has been shown to consist of a long narrow channel, lined almost entirely with hydrophobic amino acids.[254] Examination of the crystal structure in the presence of a cyclooxygenase inhibitor, (*S*)-flurbiprofen, has indicated that Arg-120 may facilitate precise substrate binding by interacting with the carboxylate moiety of arachidonic acid.[254] Replacement of Arg-120 with Glu resulted in a 20-fold decrease in the specific activity of PGHS and a 100-fold increase in the apparent K_m for substrate.[257]

The cyclooxygenase activity of PGHS has been the focus of much attention as the site of anti-inflammatory drug inhibition. Both aspirin and ibuprofen compete with arachidonic acid for binding at the cyclooxygenase active site,[258] although the former results in a time-dependent, irreversible inhibition of cyclooxygenase activity through acetylation of the nearby Ser-530 residue; see Figure 37.[259] While both agents affect cyclooxygenase activity, they exhibit little or no effect on peroxidase activity.

D. Peroxidase Activity

The peroxidase activity of PGHS has been assigned two functions: (i) It has been implicated in the generation of a protein radical that ultimately initiates the cyclooxygenase activity (see below) and (ii) in the reduction of PGG_2 to PGH_2. In comparison to the cyclooxygenase active site, peroxidase activity has been shown to occur in a relatively shallow cleft in which the heme group is considerably exposed to solvent,[254] presumably to accommodate large fatty acid-based hydroperoxides and to facilitate peroxidase reactivity, which has been proposed to occur at the heme edge.[65]

Hydroperoxides such as PGG_2 interact directly with the ferric heme. Incubation of PGHS in the presence of high concentrations of cyanide (250 mM) results in inhibition of cyclooxygenase activity that is characteristic of peroxide deficiency.[246] Addition of exogenous hydroperoxide or accumulation of peroxide product was observed to lower the sensitivity toward cyanide, leading Helmer and Lands[246] to conclude that competition for binding to the ferriheme must exist between cyanide and hydroperoxide. In addition, the disappearance of both ferric high- and low-spin EPR signals upon addition of hydroperoxides to PGHS provides further evidence for a direct hydroperoxide−heme interaction.[253b] Heterolytic O−O bond cleavage, facilitated by the distal histidine and the polar nature of the amino acids at the active site, results in the generation of a species formally two oxidation equivalents above the ferric resting state and release of PGH_2 (eq 9). This species

$$[Fe^{III}(Porph)] + PGG_2 \rightarrow [O{=}Fe^{IV}(Porph^{\bullet+})] + PGH_2 \quad (9)$$

is known as compound I in peroxidase systems and consists of low spin ferryl iron with a porphyrin π-radical cation, $[O{=}Fe^{IV}(Porph^{\bullet+})]$, in which both oxidizing equivalents remain at the heme. The peroxidase cycle ferric state must be regenerated by interaction with a reducing cosubstrate. This can occur either by two successive one-electron reductions[260] in which another oxoferryl intermediate, compound II, $[O{=}Fe^{IV}(Porph)]$, formally one oxidation equivalent above the ferric state is formed first (eq 10). It is then reduced back to the ferric state by a

$$[O{=}Fe^{IV}(Porph^{\bullet+})] + \text{substrate} \rightarrow [O{=}Fe^{IV}(Porph)] + \text{oxidized substrate} \quad (10)$$

$$[O{=}Fe^{IV}(Porph)] + \text{substrate} \rightarrow [Fe^{III}(Porph)] + \text{oxidized substrate} \quad (11)$$

second molecule of reducing substrate (eq 11). Alternatively, direct transfer of the oxo moiety from compound I,[261] a process analogous to the oxygen-

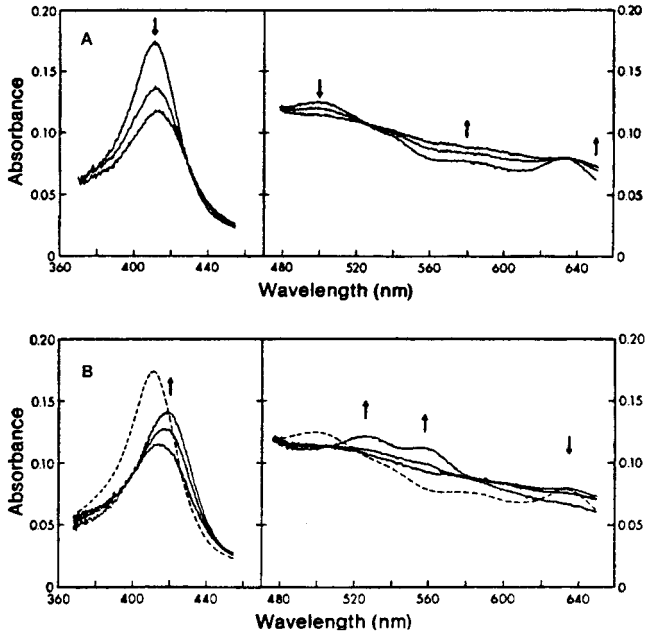

Figure 39. Rapid scan electronic absorption spectra. (A) Reaction between prostaglandin H synthase (PGHS) and 5-phenylpent-4-enyl 1-hydroperoxide (PPHP) to form compound I. (B) Reaction between PGHS and PPHP to form compound II. The arrows indicate the direction of the absorbance change with increasing time for both (A) and (B). All spectra were collected at 5 °C. Reproduced with permission from ref 251 (copyright 1985, Journal of Biological Chemistry).

ation reaction of the P450s (see section II), will regenerate the ferric state in one step.

With PGHS, two short-lived intermediates resembling compounds I and II of the classical heme-containing peroxidase, horseradish peroxidase,[262] have been observed independently in two laboratories.[251,263] Intermediate I was assigned as PGHS compound I based on the considerable decrease in Soret peak intensity and the "featureless" visible region, Figure 39A, which is characteristic of compound I-like species. The second intermediate, Figure 39B, was assigned to either compound II- or compound II-type heme with a protein-derived radical, [O=Fe^{IV}(Porph)]protein•, analogous to the ES complex of cytochrome *c* peroxidase.[264,265] These latter two formulations are difficult to differentiate spectroscopically as both hemes possess identical electronic structures.

E. Interdependence of Peroxidase and Cyclooxygenase Activities

Clearly, an interdependence exists between the cyclooxygenase and peroxidase activities of PGHS, suggesting the existence of a species common to both activities. Compound I[260] and compound II[266] have each been proposed as the common connection between the pathways. Much of the evidence accumulated has implicated a protein radical, [O=Fe^{IV}-(Porph)]Tyr•. This species is presumably derived from electron transfer from a tyrosine residue to compound I, followed by deprotonation. Initial evidence indicating participation of a protein radical came from the observation that in the reaction of PGHS with PGG_2 under anaerobic conditions, the ferric high-spin-derived EPR signal was converted to

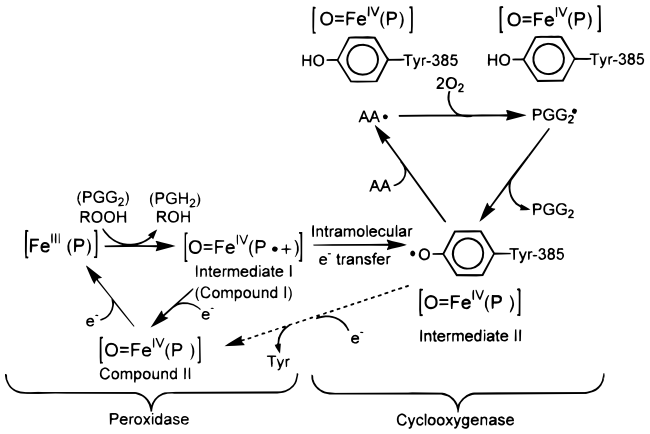

Figure 40. Model for the peroxide-dependent activation of prostaglandin H synthase cyclooxygenase activity. (P) represents the porphyrin macrocycle; AA, arachidonate; PGG_2, prostaglandin G_2. Adapted from ref 263.

a new doublet signal at $g = 2.005$.[255] Comparison of the EPR spectral shape and hyperfine coupling parameters to the well-characterized tyrosyl radical of ribonucleotide reductase,[267−269] strongly suggested the participation of a similar species for PGHS. This new intermediate corresponds to that observed in Figure 39B and was assigned to [O=Fe^{IV}(Porph)]-protein•. Subsequently, at least three distinct tyrosyl radicals of different spatial orientations have been detected by EPR.[270−272] Tsai and co-workers have employed isotope replacement and site-directed mutagenesis techniques to locate and identify these radicals.[273] Replacement of Tyr-385 with perdeuterated tyrosine resulted in no change in enzymatic activity or radical formation but caused a significant narrowing of the EPR signal relative to that normally observed for reaction with hydroperoxides. This provided strong support for the proposed intermediacy of a tyrosyl radical. Cyclooxygenase activity was abolished when Tyr-385 was mutated to Phe or was chemically modified (nitrated) by incubation with tetranitromethane. These findings were further corroborated by the crystal structure,[254] which places Tyr-385 in close proximity to both the heme-edge and protein-bound arachidonate; *i.e.*, Tyr-385 could interact with the heme to become a radical which in turn could directly abstract a hydrogen atom from the substrate.

Ruf has proposed a model[255,263] describing the involvement of higher heme oxidation states and a tyrosyl radical in the initiation of cyclooxygenase activity (Figure 40). Ferric heme is oxidized to intermediate I (compound I) by direct reaction with hydroperoxides (physiologically with PGG_2). Intramolecular electron transfer coupled with deprotonation from Tyr-385 to intermediate I results in the generation of intermediate II, a high-valent iron−oxo species analogous to compound II, and the Tyr-385 radical. This radical abstracts a hydrogen atom from arachidonic acid (AA), which undergoes the cyclooxygenase reaction to produce a PGG_2 radical (right side of Figure 40). Subsequent regeneration of the tyrosyl radical enables cycloxygenase catalysis to continue without further involvement of intermediate I of the peroxidase cycle. Ruf's model, often referred to as the "branched-chain" mechanism, adequately explains the dependence on hydroperox-

ides to initiate cyclooxygenase activity, the requirement for only one heme per protein subunit and the retention of cyclooxygenase activity in preparations (those incubated in the presence of high concentrations of cyanide or Mn^{III}-protoporphyrin IX−reconstituted protein) that exhibit little or no peroxidase activity. Alternatively, Backovic and Dunford have described a "tightly coupled" mechanism that implicates compound I of the peroxidase cycle as the primary oxidant in cyclooxygenase catalysis.[274] In an attempt to distinguish between the "branched-chain" and "tightly coupled" mechanisms, Tsai and co-workers have examined the arachidonate metabolites formed in the reaction of PGHS with arachidonate and reducing cosubstrate.[275] The absence of direct coupling between PGG_2 formed during the cyclooxygenase activity and PGG_2 reduction during the peroxidase cycle in the branched-chain mechanism, would be expected to result in an accumulation of PGG_2. In a tightly coupled system, compound I must be regenerated by additional PGG_2 molecules, hence not allowing PGG_2 build up. Tsai et al. observed accumulation of micromolar concentrations of PGG_2, providing strong support in favor of the branched-chain mechanism. In addition, the stoichiometry of reducing cosubtrate oxidized to fatty acid oxygenated was determined to be less than 1.3. This is inconsistent with a tightly coupled system, which would require 2 equiv of reducing cosubstrate for every mole of arachidonate oxidized.

Bakovic and Dunford have recently shown that, in the absence of reducing cosubstrates and arachidonate, hydroperoxides react directly with compound I to form a transient complex, $[O{=}Fe^{IV}(Porph^{\bullet+})]{-}PGG_2$.[276] They have concluded that this enzyme−substrate complex forms prior to the reduction of compound I by hydroperoxides (by overall hydrogen atom transfer), resulting in formation of compound II and a peroxyl radical, not the compound II−tyrosyl radical species. Tyrosyl radical formation must therefore occur at some later stage, possibly by reaction between compound II and the peroxyl radical (eq 12). The authors do however emphasize that the

$$\begin{aligned}[O{=}Fe^{IV}(Porph^{\bullet+})] + PGG_2 &\rightleftarrows \\ [Fe{=}O^{IV}(Porph^{\bullet+})]{-}PGG_2 &\rightarrow \\ [O{=}Fe^{IV}(Porph)] + PGG_2^{\bullet} &\rightarrow \\ [O{=}Fe^{IV}(Porph)]protein^{\bullet} + PGG_2 \quad (12)\end{aligned}$$

reaction of PGG_2 with compound I may be irrelevant under physiological conditions where reducing substrates are present that rapidly reduce compound I, resulting in increased concentrations of compound II.

Assignment of a specific role for tyrosyl radicals in PGHS catalysis has proven controversial. A detailed study of reaction kinetics by Kulmacz and co-workers have provided a unified mechanistic model[277] that accurately predicts the kinetic behavior of PGHS under a variety of reaction conditions, yet failed to attribute a direct function to a tyrosyl radical. In a low-temperature EPR study of Fe^{III}- and Mn^{III}-protoporphyrin IX−reconstituted PGHS, Eling, Mason, Marnett, and co-workers observed that the protein-derived radicals formed upon addition of arachidonate appeared at a considerably slower rate than eicosanoid products were formed. This led to the conclusion that the protein radical observed is not catalytically competent species in the cyclooxygenase pathway.[278a] In addition, the radical produced upon reaction of Mn^{III}-reconstituted PGHS with arachidonate did not resemble a tyrosyl radical.[278a] Previously Hayaishi and co-workers had shown that while Mn^{III}-reconstituted PGHS exhibited little or no peroxidase activity, it still sustained cyclooxygenase activity.[278b] In this respect, Mn^{III}-reconstituted horseradish peroxidase has been shown to be readily oxidized by peroxides or peracids to the Mn^{IV} state[278c,d] and a protein radical.[278d] But the the peroxidase activity of Mn^{III}-reconstituted horseradish peroxidase is very low.[278c] These observations, although somewhat contradictory to the involvement of tyrosyl radicals in the cyclooxygenase pathway, do lend support to Ruf's branched-chain mechanism, which requires only initial formation of compound I to generate the active protein radical. The cyclooxygenase pathway is then self-dependent, regenerating the protein radical as a part of the mechanism.

Previously, it had been observed that an arachidonic acid radical was formed during anaerobic incubation with PGHS.[279a,b] Recently, EPR has been employed to study the interactions between tyrosyl radicals formed during reaction with hydroperoxides and fatty acid substrates (Figure 41). In this study, Tsai and co-workers have provided the first direct evidence implicating tyrosyl radical formation in cyclooxygenase activity.[280] The reaction of PGHS with ethyl hydroperoxide under anaerobic conditions produced a wide doublet EPR signal characteristic of a tyrosyl radical (Figure 41, Ia). The signal intensity of this species decreased upon incubation in the presence of O_2, Ia′. Addition of arachidonate resulted in the formation of a new isotropic signal with $g = 2.004$, Ib, which was distinct from the wide doublet tyrosyl radical signal. This new signal persisted with time, although its intensity did decrease, Ic. Introduction of O_2 following the addition of arachidonate regenerates the tyrosyl radical signal, Ib′ and Ic′, which is consistent with Ruf's model of a catalytic cycle (Figure 40). To confirm the assignment of this new species as a substrate-based radical, Tsai et al.[280] examined the reaction of selectively deuterated arachidonate with PGHS (Figure 41, II). Reaction of PGHS with hydroperoxide once again produced the wide doublet signal, IIa, which upon aerobic incubation showed a decrease in signal intensity, IIa′. Addition of deuterated substrate produced a radical species, IIb and IIc, for which the EPR signals were clearly different from those of nondeuterated substrate. Aerobic incubation of these samples once again regenerated the original tyrosyl radical species, IIb′ and IIc′. These results provide the strongest evidence to date that initiation of cyclooxygenase activity by substrate radical formation occurs in a tyrosyl radical-dependent manner.

Major advances have been made in our understanding of PGHS catalysis. Nonetheless, many aspects of its reactivity remain both controversial and unclear. Although the mechanisms of the individual activities of PGHS (cyclooxygenase and peroxidase) are commonly accepted, inconsistencies arise in the nature of their interdependence due in part to the

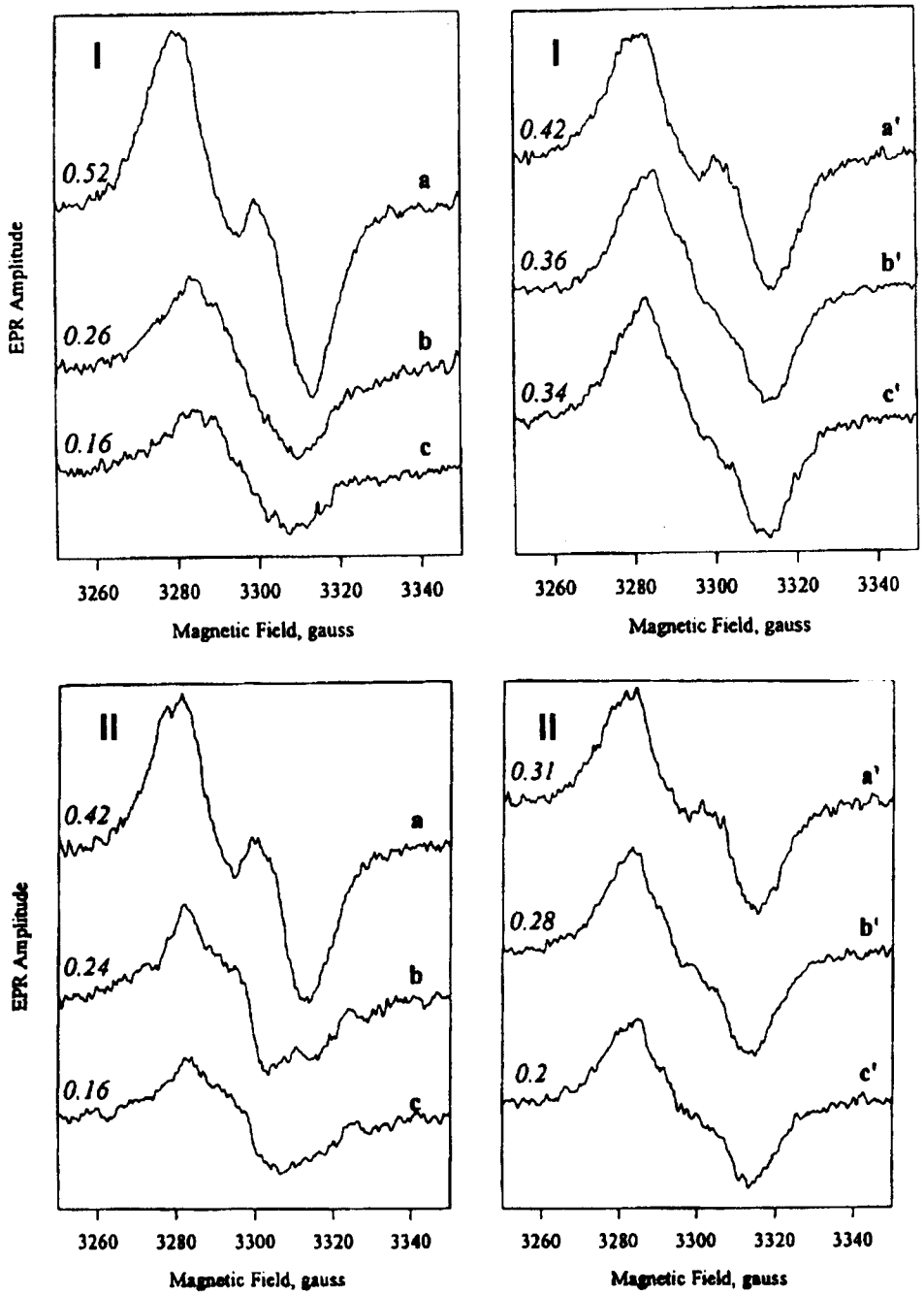

Figure 41. EPR spectra during the following reaction. (I) Prostaglandin H synthase (PGHS-1) radical (wide doublet) and arachidonate. Samples were incubated under anaerobic conditions: 1.5 equiv of ethyl hydroperoxide (EtOOH) for 20 s before addition of arachidonate. EPR spectra were obtained for samples 12 s after addition of EtOOH (Ia) and 12 (Ib) or 60 s (Ic) after subsequent addition of arachidonate (1.5 equiv). Spectra Ia′−Ic′ were obtained for the same three samples (Ia−Ic) after thawing and aerobic incubation for 20 s. (II) PGHS-1 radical (wide doublet) with deuterated arachidonate. Samples were incubated under anaerobic conditions with 1.5 equiv of EtOOH for 20 s before addition of (d_8)aracidonate (1.5 equiv). EPR spectra were obtained for samples taken 13 s after addition of EtOOH (IIa), and 14 (IIb) or 56 s (IIc) after the subsequent addition of (d_8)arachidonate. Spectra IIa′−IIc′ were obtained for the same three samples (IIa−IIc) after thawing and aerobic incubation for 20 s. The value at the left side of each spectrum is the signal intensity (in spins/heme). Reproduced with permission from ref 280 (copyright 1995, Journal of Biological Chemistry).

complexity of the system. Although protein radicals are not uncommon in biological systems, especially tyrosyl radicals, it has proved challenging to directly implicate any such species in PGHS activity. PGHS provides an effective alternative to iron protoheme-based dioxygen activation described elsewhere in this review. Clearly, a system of such intriguing biochemical properties and physiological importance will remain the subject of intense research for many years.

VI. Indoleamine 2,3-Dioxygenase (IDO) and Tryptophan 2,3-Dioxygenase (TDO)

A. Similarities and Distinctions between the Two Dioxygenases

Both IDO and TDO are cytosolic (soluble) heme proteins that catalyze the conversion of L-Trp to *N*-formylkynurenine, the first and rate-determining step of the kynurenine pathway of L-Trp metabolism,

Table 1. Comparison of Indoleamine Dioxygenase (IDO) and Tryptophan Dioxygenase (TDO)

properties	IDO[281,282]	TDO[283]
mol wt	45 000[287,288]	191 000 (liver),[289] 122 000 (*Pseudomonas*)
subunits	1	4 (α_4[289] or $\alpha_2\beta_2$)
carbohydrate	4.8%	none
prosthetic group	protoheme IX (1)	protoheme IX (2)[290]
oxygen source	O_2 (and $O_2^{\bullet-}$)	O_2
substrates	L- and D-Trp, 5-hydroxy-L- and D-Trp, tryptamine, serotonin	L-Trp (and D-Trp)[291]
turnover no. for L-Trp (s^{-1})	2	7 (liver), 17 (*Pseudomonas*)[292]
distribution		
mammals	ubiquitous (except liver)	liver
bacteria	none	*Pseudomonas acidovorans*
inducers	influenza virus, lipopolysuccharide, interferon γ	tryptophan, kynurenine, hydrocortisone

by oxidatively cleaving the tryptophan pyrrole ring between its 2- and 3-positions upon incorporation of both oxygen atoms of O_2 (eq 13).[281−283] Thus, TDO

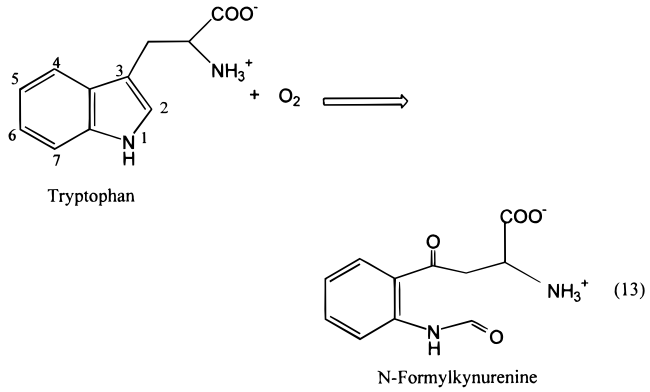

(13)

was first called "tryptophan pyrrolase" when initially isolated by Kotake and Masayama in the mid-1930s,[284] and later "tryptophan 2,3-dioxygenase" by Hayaishi. It is sometimes also called "tryptophan oxygenase".[283] In mammals, TDO is located exclusively in the liver.[283] The enzyme has also been isolated from *Pseudomonas acidovorans*. IDO was isolated initially as a D-Trp-cleaving enzyme from rabbit small intestine in the late 1960s by Hayaishi and co-workers.[285] Subsequently the enzyme was shown to be a heme-containing glycoprotein, ubiquitously distributed in mammals (except the liver), which is able to utilize both enantiomers of Trp as substrates.[281] It can also oxygenate several other Trp derivatives including 5-hydroxy-tryptophan, tryptamine and serotonin (5-hydroxytryptamine).[281,286,287] Since substrates for this dioxygenase must have the α-amino group of Trp, it was designated "indoleamine 2,3-dioxygenase" by Hayaishi.[286] Although both dioxygenases catalyze the same reaction (eq 13), they are otherwise distinct (Table 1). Copper, once thought to be one of the cofactors for TDO, is not required for catalysis.[290] L- and D-Trp are comparable substrates for IDO in terms of turnover number (V_{max}), but the former has 10−50 times smaller K_m values (pH-dependent) than the latter.[293] In terms of V_{max} and specificity constant (V_{max}/K_m), the other tryptophan derivatives are much poorer substrates than L-Trp, exhibiting less than 2.5 and 1.5% of the values for L-Trp, respectively.[287]

The amino acid sequence of rat liver TDO has recently been determined from its cDNA, and its molecular structure has been revealed to be that of a homotetramer.[289] IDO has been purified also from human placenta[294] and mouse epididymis,[295] and the amino acid sequences have been determined for the enzymes from these sources.[288,296,297] The catalytic properties and substrate specificity of IDO from these sources are similar.[287,294,295]

In contrast to a relatively simple Trp-metabolizing role of hepatic TDO which initiates the kynurenine pathway leading to the formation of pyridine nucleotide coenzyme (NAD),[283] several possible physiological roles for IDO have been suggested. Most significantly, it is associated with the antiviral and antiproliferative activities of interferon γ.[282,298,299] Alternatively it has been shown that local synthesis of the neurotoxin quinolic acid, an L-Trp metabolite of the kynurenine pathway, in the central nervous system follows the induction of IDO in macrophage.[300] Thus, IDO is implicated to be of neuropathological significance. As a third possibility, IDO has been suggested to be related to an antioxidant defense in mononuclear phagocytes since increased amounts of aminophenolic antioxidants, which are metabolites of tryptophan, are found in the cells following the induction of IDO.[301]

B. Roles of Superoxide ($O_2^{\bullet-}$) as an Activator and Oxygen Source for IDO

One of the unique features of IDO is that the ferric enzyme (Figure 42, **52**) readily reacts with $O_2^{\bullet-}$ to yield the oxygenated enzyme ($Fe^{2+}O_2$) (**53**)[302] ($k_{O_2^{\bullet-}} = 7 \times 10^6\ M^{-1}\ s^{-1}$ at pH 7),[303,304] (eq 14), which can also

$$Fe^{3+} + O_2^{\bullet-} \rightarrow Fe^{2+}O_2 \qquad (14)$$

$$Fe^{2+} + O_2^{\bullet-} \rightarrow Fe^{2+}O_2 \qquad (15)$$

be generated by addition of O_2 to the ferrous enzyme (Fe^{2+}) (**54**) [$k_{O_2} = (6.3\text{-}7.4) \times 10^6\ M^{-1}\ s^{-1}$ at pH 7][303] (eq 15). The oxygenated enzyme can be presented also as $Fe^{3+}O_2^{\bullet-}$ (see section IC). This $O_2^{\bullet-}$-binding property of IDO is similar to those of horseradish peroxidase and catalase ($k_{O_2^{\bullet-}}$ at pH 7 = $\sim 1.6 \times 10^6$ and $2.1 \times 10^6\ M^{-1}\ s^{-1}$, respectively,[305] but clearly different from those of hemoglobin, myoglobin, cytochrome P450, or TDO, which have very low reactivities with $O_2^{\bullet-}$.[306−308] Addition of Trp to oxygenated IDO, **53**, produces *N*-formylkynurenine[302] via the ternary $Fe^{2+}O_2$−Trp complex, **55**.

Possible utilization of superoxide by IDO *in vivo* was examined by Hayaishi and co-workers by using the dispersed cell suspensions of the rabbit small intestine.[309] When superoxide dismutase activity was suppressed by adding the inhibitor diethyldithiocarbamate, the intracellular IDO activity was mark-

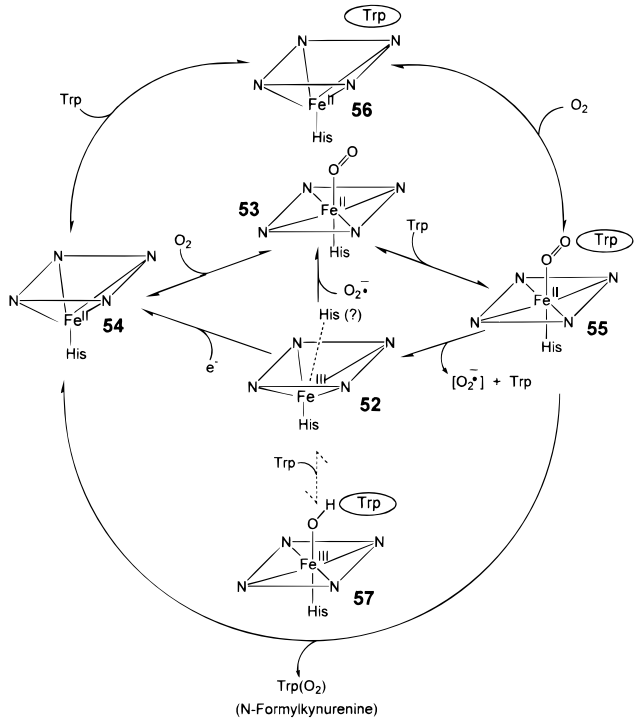

Figure 42. Proposed catalytic reaction cycle(s) for indoleamine 2, 3-dioxygenase (IDO) and tryptophan 2, 3-dioxygenase (TDO). The porphyrin macrocycle is abbreviated as a parallelogram with nitrogens at the corners. The outer cycle is a most likely common reaction cycle for the both enzymes. However, since IDO is distinct from TDO in that (i) its tryptophan (Trp)−enzyme−O_2 ternary complex (**55**) is considerably autoxidizable and (ii) its Trp-free enzyme−O_2 complex (**53**) is relatively stable, the Trp-free forms of the enzyme−O_2 complex (**55**) and ferric enzyme (**52**) may be involved as a major (the former) and minor (the latter) intermediates during the steady state. Formation of the ferric enzyme−L-Trp complex (**57**) appears to be the cause of the substrate inhibition observed for IDO but not TDO. Adapted from ref 315.

edly accelerated. Furthermore, addition of substrates (purines) of xanthine oxidase *in the presence of methylene blue* also enhanced the IDO activity in the cells. The researchers interpreted these results to be indicative of intracellular utilization of $O_2^{\bullet-}$ by IDO.[282,309]

Sono has investigated on the roles of (a) superoxide, generated using xanthine oxidase−hypoxanthine in the presence and absence of methylene blue, and of (b) ascorbic acid−methylene blue in the reductive activation of ferric IDO and reached the following conclusions:[310] Methylene blue acts as an electron mediator from these donors (reduced xanthine oxidase and ascorbic acid) to the ferric dioxygenase. With the increase in the amount of xanthine oxidase, the IDO activity is enhanced to an apparent maximal level either in the absence or presence of methylene blue when L-Trp is used as substrate. In the absence of methylene blue, superoxide dismutase effectively inhibits the IDO activity, indicating that $O_2^{\bullet-}$ is the major reductant (activator) of IDO under these conditions. The apparent maximum catalytic activity (turnover, $\sim 2\ s^{-1}$) can be obtained with steady state $O_2^{\bullet-}$ concentrations of $\geq 2 \times 10^{-6}$ M. Under normal physiological conditions, however, steady-state concentrations of $O_2^{\bullet-}$ are kept very low (e.g., $\sim 1 \times 10^{-11}$ M in mitochondria)[311,312] since superoxide dismutase effectively removes intracellular $O_2^{\bullet-}$. On the other hand, *in the presence of methylene blue*, the IDO activity at its near-maximum level is no longer inhibited by superoxide dismutase, indicating that IDO is predominantly activated by reduced xanthine oxidase via the electron mediator methylene blue *without* requiring $O_2^{\bullet-}$.

The findings in the above two studies are consistent with each other. Furthermore, a pulse radiolysis kinetic study of the reaction of ferric IDO with $O_2^{\bullet-}$ has revealed that L-Trp effectively inhibits this reaction, e.g., $\sim 50\ \mu$M L-Trp caused 50% inhibition at pH 7.[304] All these results suggest that, under physiological conditions, utilization of $O_2^{\bullet-}$ by IDO seems insignificant because of the ubiquitous presence of superoxide dismutase in cells. The only exceptions to this would be the cases of burst production of $O_2^{\bullet-}$ either by NADPH oxidase in phagocytic cells (e.g., neutrophils)[313,314] or by xanthine oxidase in other cells during reperfusion following ischemia.[312] However, no particular connections between these extraordinary physiological conditions and the IDO activity have been demonstrated. This leads to a speculation that in order for IDO to be active in tissues, a certain, yet to be identified, natural electron carrier (which would take the place of methylene blue) must exist.[295]

C. Catalytic Cycle

The proposed catalytic cycle of IDO is schematically illustrated in Figure 42. Under physiological steady-state conditions, the majority of the enzyme is likely to be in the active, ferrous form. However, *in vitro* catalysis starts from the inactive ferric form, **52**. Formation of the Trp−ferric enzyme adduct, **57** ($K_d = 50-200\ K_m$)[293,315] appears to be catalytically unfavorable and the likely cause of the substrate inhibition which is exclusively observed with the L-isomer of Trp (and 5-hydroxy-Trp) for IDO[285,315] but not for TDO. Thus, for IDO, the Trp-free ferric enzyme is either reduced to the ferrous state**, 54,** which then binds Trp and O_2 to form the ternary complex (Trp−Fe^{2+}−O_2) **55** or, if $O_2^{\bullet-}$ is available, binds $O_2^{\bullet-}$ to generate the oxygenated enzyme ($Fe^{2+}O_2$) **53** followed by Trp binding. An equilibrium analysis of Trp binding to the deoxyferrous and the oxygenated enzyme suggests that Trp binds more readily to the ferrous enzyme, followed by O_2 (**54** → **56** → **55**).[315] The reverse binding order of these two substrates (**54** → **53** → **55**), however, has not been excluded. Once formed, the ternary complex decomposes to the ferrous enzyme and product. For TDO, the outer circle in Figure 42 is the principal catalytic cycle that was unambiguously established for this dioxygenase; ferrous TDO does not readily bind O_2 in the absence of L-Trp.[316] Note that, in the principal catalytic cycle, no redox changes of the enzyme heme iron are involved for either dioxygenase.

The turnover number for rabbit intestinal IDO is $\sim 2\ s^{-1}$ [287,293] (cf. 17 s^{-1} for rat liver TDO).[292] However, in contrast to TDO, the O_2 complex of ferrous IDO is readily autoxidizable in the presence of substrate (autoxidation rates 2.8×10^{-2} and $4.7 \times 10^{-4}\ s^{-1}$ at pH 7.0 and 25 °C in the presence and absence of Trp, respectively).[302,303] Thus, during the turnover, the enzyme autoxidizes at a rate of 0.028 s^{-1} (eq 16). The ferric enzyme generated needs to be reactivated.

$$Trp-Fe^{2+}-O_2 \rightarrow Fe^{3+} + Trp + [O_2^{\bullet -}] \quad (16)$$

Based on the relative rates of turnover/autoxidation reactions, it can be estimated that, *if* $O_2^{\bullet -}$ *is the only activator of the enzyme in vivo (and if the presence of superoxide dismutase can be ignored),* IDO may utilize O_2 and $O_2^{\bullet -}$ as the oxygen sources in a ratio of ~70:1 (= ~2:0.028) when L-Trp is used as substrate.[303]

D. Heme Iron Coordination Structures

All the enzyme intermediates shown in Figure 42 have been isolated and characterized with several spectroscopic techniques (including electronic absorption, natural and magnetic circular dichroism, EPR, and NMR spectroscopy)[287,317−321] for both IDO and TDO (except for its Trp-free oxygenated form). The endogenous axial ligand coordinated to the heme prosthetic group has been shown to be histidine for both dioxygenases.[287,317−319] However, in the native ferric form, IDO and TDO differ somewhat in that IDO is six coordinate, apparently having a nitrogen donor as the sixth ligand *trans* to the proximal histidine (**52**), yet is predominantly high spin,[318] while water is a likely sixth ligand for ferric high-spin TDO as it is for ferric myoglobin.[317] These spectroscopic and spin-state properties of native ferric IDO can be simulated by coordination of benzimidazole, a sterically hindered and electron-deficient (i.e., less basic) nitrogen donor, to ferric myoglobin.[318] This suggests that histidine constrained to coordinate in its 1-H tautomer rather than the more normally found 3-H tautomer could be the cause of the observed spectral properties of IDO. Upon addition of L-Trp to the ferric IDO, **52**, and TDO, a spin-state change occurs, especially in alkaline pH (pH >7.5) resulting in a predominantly (~70% for IDO)[318] (**57**) or partially (30-50% for TDO)[320] low-spin state. These spin-state changes are accompanied by coordination of hydroxide as a sixth ligand for both enzymes.[317,318,320] However, the L-Trp-induced formation of the low-spin complex, **57**, appears to be related to the substrate inhibition for IDO[315] as mentioned above. The ferrous enzyme and its complexes with O_2 as well as CO and NO exhibit spectral properties that are very similar to those of the analogous myoglobin derivatives. An addition of L-Trp to these dioxygenase derivatives causes slight spectral blue shifts in the Soret region.[315,322,323] The L-Trp·ferrous enzyme$-O_2$ ternary complex, **55**, was successfully generated and stabilized as a transient state for both dioxygenases at ~5 °C for TDO[316] and below −20 °C in cryogenic mixed solvents for IDO.[323]

E. Tryptophan Analogs and Substituted Tryptophans as Mechanistic Probes

Cady and Sono have demonstrated that methylation or substitutions of the indole nitrogen with oxygen or sulfur (to form the oxygen or sulfur analog of Trp) converts the substrate Trp to competitive inhibitors for IDO.[324] These results strongly suggest that (i) the free form of the indole NH group is an important requirement for substrate and (ii) the electronic property of the indole nitrogen is also important since its replacement by a more electron-inductive sulfur or oxygen atom eliminates the substrate nature of Trp. In addition, the inability of 1-methyl-Trp, which readily reacts with singlet oxygen,[325] to serve as a substrate for the dioxygenase suggests that singlet oxygen is not involved in the enzymic dioxygenation of Trp. Furthermore, the effects of substitutions of hydrogen atom(s) on the indole benzene ring of Trp with a methyl or methoxy group or with fluorine atom(s) on the catalytic activity of IDO have been examined by the same researchers.[325,326] It has been found that both the L and D forms of 4-, 5-, and 6-fluoro-Trp, 5- and 6-methyl-Trp, and 5-methoxy-Trp are relatively good substrates (in terms of V_{max}) as compared with unsubstituted L- and D-Trp. Curiously, however, 7-fluoro- (and 4,7- and 5,7-difluoro-Trp) and 7-methyl-Trp no longer serve as substrates but instead are inhibitors.[327] The 7-fluoro-Trp's are competitive inhibitors, while the inhibition mode (competitive or noncompetitive) for 7-methyl-Trp is ambiguous.[326] A series of competitive inhibitors (with their K_i values) is depicted in Figure 43.

Detailed examination of the catalytic data for these substituted Trp substrates has revealed a general correlation in which the presence of an electron-withdrawing fluorine substituent led to low V_{max} values, while the electron-donating methyl substitution led to high V_{max} values. The exceptionally low V_{max} value for 6-methyl-L-Trp (Figure 44, top) was attributed, at least in part, to "improper" binding to the enzyme as judged from the somewhat unusual electronic absorption spectrum of its complex with IDO in comparison with those for the other substrate-type substituted Trp's.[326,327] 6-Methyl-D-Trp exhibited an expected V_{max} value similar to that of 5-methyl-D-Trp and higher than that of unsubstituted D-Trp. With respect to the K_m values (Figure 44, bottom), substituted L-Trp's having bulkier methyl and methoxy groups have noticeably larger K_m values (i.e., weaker binding affinity for the enzyme) than those having smaller fluorine or hydrogen atoms as expected. The extremely low V_{max} values for 5-hydroxy-L-Trp (Figure 44, top) as well as 5-hydroxy-D-Trp (not shown) may be attributed to a considerably higher pK_a value (i.e, basicity) of their indole NH group (pK_a = 19.2) than those for the other substituted Trp's (pK_a = 16.3−16.9).[328]

Analogous studies have been carried out by Wiseman and co-workers[329] with rat liver TDO by using such fluoro- and methyl-substituted Trp's as those used for the IDO activity study described above. These researchers have obtained only relative V_{max}/K_m values for the substituted Trp's vs unsubstituted L-Trp in competition experiments. Although some similarities exist in the results of the two studies with certain substituted Trp's (e.g., the very low V_{max}/K_m value for 7-fluoro-Trp), their major findings for TDO are significantly different from those obtained for IDO. For example, 6-fluoro-L-Trp (as well as 6-fluoro-DL-Trp) has been shown to be the best substrate for TDO (having the highest V_{max}/K_m value, being 1.64-fold higher than that of L-Trp) among all the substituted Trp's used. This is not the case for IDO (Figure 44); 6-fluoro-L-Trp has the second best V_{max}/K_m value (4.4), which is less than half of the value (9.4) of L-Trp. It is not clear whether the different results

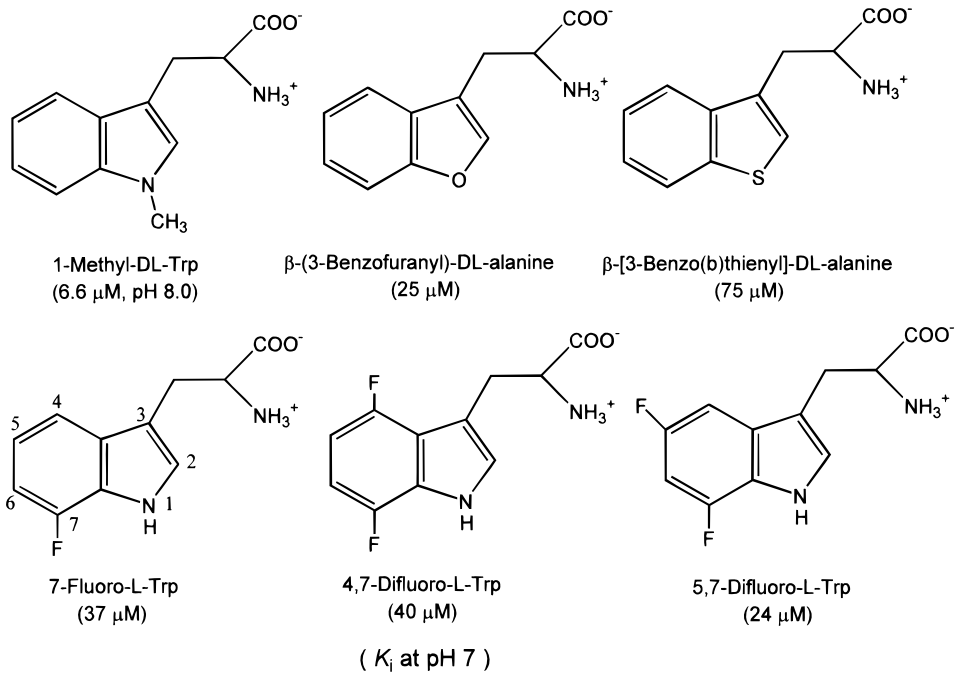

Figure 43. Trp analogs and substituted Trp's that have been discovered as competitive inhibitors for indoleamine 2, 3-dioxygenase. The K_i values at pH 7 (except for the value at pH 8 for 1-methyl-DL-Trp) are indicated in parentheses.

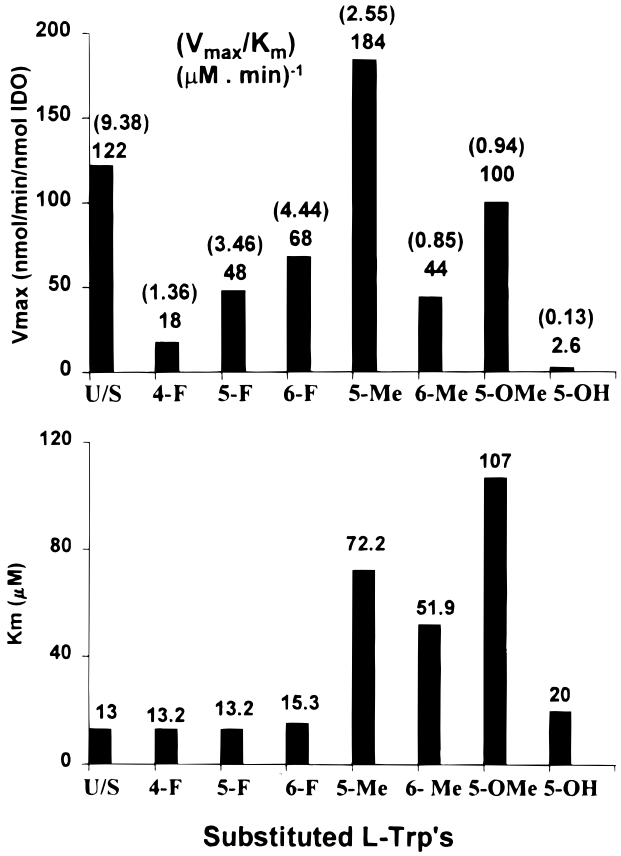

Figure 44. The V_{max}, K_m, and V_{max}/K_m values at pH 7.0 for substituted and unsubstituted (U/S) L-Trp's, which serve as substrates for indoleamine 2, 3-dioxygenase.

in the two studies with the substituted Trp's are due to the use of two different enzymes or due to the different analysis methods.

F. Plausible Reaction Mechanism

Both IDO and TDO cleave an aromatic ring having an NH group attached directly to the bond cleaved. This is similar to the phenol ring cleavage catalyzed by non-heme iron dioxygenases such as catechol 3,4-dioxygenases[330a] and protocatechuate 4,5-dioxygenase[330b] or by the copper-containing protein quercetinase,[331] for which an OH group is attached to the substrate aromatic ring.[2] Thus, in contrast to heme iron and non-heme iron-containing monooxygenases such as P450 and methane monooxygenase,[332] respectively, which are able to oxygenate completely unactivated alkanes, IDO and TDO require a functionalized double bond for the substrate to help oxygen incorporation.[2] In this respect, even singlet O_2, a considerably reactive oxygen species, cannot react with alkanes or unactivated aromatic compounds. Based on the results obtained from the studies with the Trp analogs and substituted Trp's as described in the previous section, and other available experimental evidence, plausible reaction mechanisms are presented below for both IDO and TDO.

1. Ionic Mechanism

A proposed ionic reaction mechanism[333] for the IDO- and TDO-catalyzed conversion of Trp to *N*-formylkynurenine is displayed in Figure 45. The heme iron-bound O_2 is not singlet O_2 but mimics the reaction by singlet O_2 in this particular case. In the enzyme active site, **58**, O_2 coordinates to the ferrous heme iron to form the heme$-O_2$ complex (formulated as $Fe^{II}-O_2$) **59**, which can now react by an ionic mechanism. Next, deprotonation of the indole NH by an active site base (B̈) stimulates the nucleophilic attack by the relatively electron-rich indole carbon 3 on the distal oxygen atom of the bound O_2. The result of this concerted electron rearrangement is intermediate **60**, the 3-indolenylperoxy$-$Fe(II) complex. Because the basicity of the indole nitrogen significantly influences the rate of the oxygenation (Trp vs 5-hydroxy-Trp, Figure 44) and because the availability of the free indole NH group is essential for the oxygenation (Figure 43), the enzyme base-

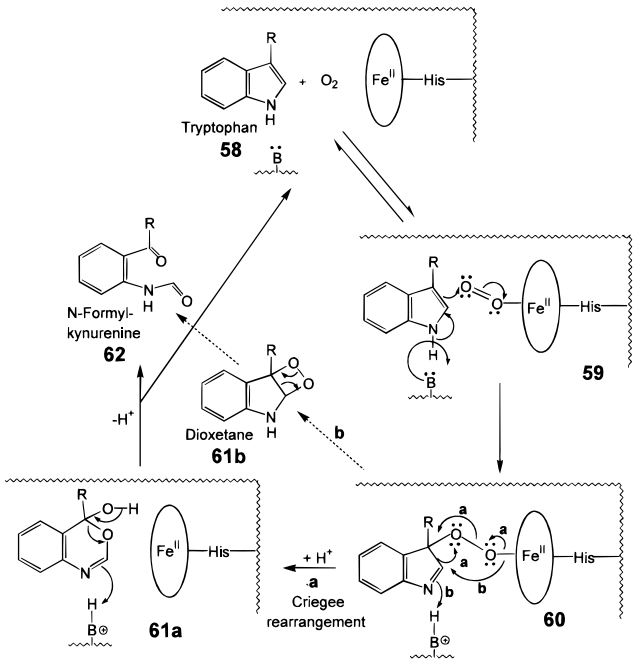

Figure 45. Proposed ionic reaction mechanism for conversion of tryptophan to *N*-formylkynurenine catalyzed by indoleamine 2,3-dioxygenase and tryptophan 2,3-dioxygenase. The reaction sequence at the enzyme active site is schematically illustrated. The ellipse circling Fe^{II} represents the porphyrin ring and B is a specific base involved in catalysis. Note that the enzyme heme$-O_2$ complex (**59** is formulated as $Fe^{II}-O_2$ to account for the ionic mechanism. Following the formation of the 3-indolenylperoxy$-Fe^{II}$ intermediate (**60**), two alternative mechanisms for its conversion to the product are shown: (a) Criegee-type rearrangement and (b) dioxetane pathways. Adapted from ref 333.

assisted deprotonation of the indole NH group can be considered as "activation" of substrate by the enzyme. The above mechanism is also consistent with the opposite effects of electron-withdrawing (fluorine atom) and -donating (methyl group) substituents on the indole benzene ring on the V_{max} value as described in a previous section for substituted Trp's. Interestingly, Makino, Ishimura, and coworkers have found from their heme substitution study of bacterial TDO that the stronger the electron-withdrawing nature of the porphyrin 2,4-substituents (diacetyl > divinyl > diethyl groups) the greater the V_{max} value for L-Trp.[292] Since the heme iron becomes more electron-deficient when the porphyrin side chains are more electron-withdrawing, this effect will decrease the electron density of the heme iron-coordinated dioxygen. This in turn will enhance its electrophilicity in favor of a nucleophilic attack by the indole 3-carbon on the distal oxygen atom to form the 3-indolenylperoxy$-$Fe(II) complex.

Two pathways have been proposed to convert intermediate **60** into product (Figure 45). Pathway a involves a Criegee-type rearrangement to intermediate **61a**, which further rearranges to form the product *N*-formylkynurenine.[2,333] A variation to the Criegee rearrangement has been proposed by Nakagawa (not shown), in which the α-amino group (in R) of Trp in **60** undergoes intramolecular addition to the indole carbon at the 2-position to form the tricyclic compound 3a-hydroperoxyhexahydropyrroloindole (not shown) as an intermediate.[333] Fraser and Hamilton[335] have suggested that a specific

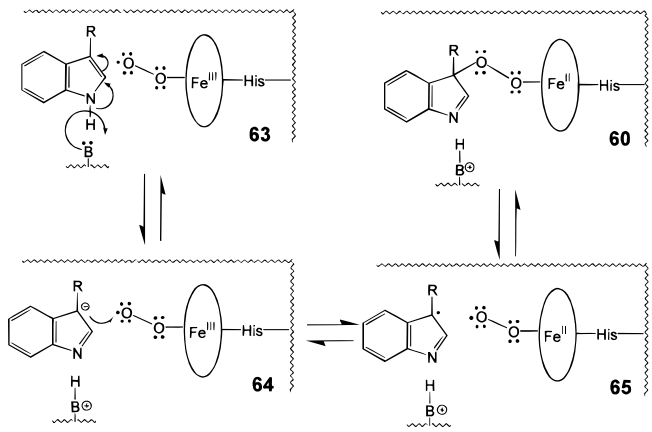

Figure 46. Proposed radical mechanism for the formation of the 3-indolenylperoxy$-Fe^{II}$ intermediate (**60**) catalyzed by tryptophan (and indoleamine) 2,3-dioxygenase(s). Note that the enzyme$-O_2$ complex is represented as $Fe^{III}-O_2^{\bullet-}$ in this mechanism. See the text for detailed description. Adapted from ref 329.

nucleophilic group of the enzyme rather than the α-amino group of the substrate Trp might add to the C-2 position prior to the Criegee rearrangement. The nucleophilic group is subsequently detached from the substrate upon the formation of the final product. Pathway b for the conversion of **60** to **62** involves a dioxetane intermediate **61b**. Once formed, the dioxetane rearranges to give *N*-formylkynurenine (**62**). However, Hamilton[2,333] initially suggested that the dioxetane mechanism is unfavorable because of (i) the excess endothermicity (for an enzyme reaction) involved in forming the dioxetane from **60** and (ii) the extreme exothermicity for the decomposition of **61b** to **62**. In the enzymic reaction, no light emission (chemiluminescence) has been detected which would be expected to accompany the decomposition of the dioxetane.[2] Mechanistic studies by Muto and Bruice[336] and Fraser and Hamilton[335] on nonenzymic conversion of 2-phenyl-3-methyl-3-hydroperoxyindolenine to *o*-benzamidoacetophenone (by the former) and 2,3-dimethyl-3-hydroperoxyindolenine to *o*-acetamidoacetophenone (by the latter) have suggested that, although both the dioxetane and Criegee rearrangement mechanisms may be feasible in enzymic reactions, the rearrangement pathway appears to predominate.

2. Radical Mechanism

An alternative radical mechanism has been proposed for the formation of 3-indolenylperoxy$-$Fe(II) complex (Figure 45, **59** → **60**) by Wiseman and coworkers[329] as depicted in Figure 46. According to the proposed mechanism, enzyme base-catalyzed deprotonation of the indole NH group generates Trp anion (**64**), which is reversibly one-electron oxidized by the heme$-O_2$ complex (which is formulated as $Fe^{III}-O_2^{\bullet-}$) to form Trp radical (Trp$^{\bullet}$) and $Fe^{II}-O_2^{\bullet-}$ (**65**). These two radical species rapidly and reversibly combine to yield the 3-indolenylperoxy$-Fe^{II}$ complex, **60**. For the subsequent conversion of this intermediate to the product *N*-formylkynurenine, these researchers have proposed the dioxetane pathway. The IDO activity data obtained by using various substituted Trp's and the TDO activity data obtained by heme substitution as described above are consistent not only with the

ionic but also with the radical mechanism. However, for the radical mechanism, even though thermodynamic and kinetic energy barriers for each and overall reaction processes have been considered by the researchers, the feasibility of one-electron oxidation of Trp ($E^{\circ\prime}$ = 1.05 V vs NHE, i.e., 0.81 V vs SCE)[337] by the heme−O_2 complex ($E^{\circ\prime}$ = -0.36 V vs SCE in dimethyl sulfoxide)[338] has remained to be proven, as this is a thermodynamically unfavorable reaction.

G. Metal–Chelate Model Studies for the Two Dioxygenases

Metal−chelators such as Co(salen),[339] Mn−phthalocyanine,[340] and Co−, Mn−, and Fe−tetraphenylporphyrins[341−344] have been shown to serve as models for IDO and TDO as catalysts for dioxygenation of Trp derivatives. The involvement of the ternary complex of O_2, substrate, and Mn−phthalocyanine as a catalytic intermediate has been demonstrated.[340] However, mechanistic details of the reaction catalyzed by these models, particularly, which redox states of the metals are involved in catalysis, and whether the reaction proceeds by an ionic or radical mechanism,[343,344] have not yet been established.

VII. Summary

The activation of molecular oxygen for insertion into organic molecules is a problem of fundamental importance to aerobic life. The reactivity of dioxygen with organic substrates is inherently low because of high kinetic energy barriers associated with the triplet (biradical) ground state of dioxygen. The enzymes that overcome this difficulty and carry out these reactions are known as oxygenases, and the heme-containing oxygenases are the most thoroughly understood examples of such enzymes. This review has summarized our current understanding of the active site structures and mechanisms of action and dioxygen activation of six heme-containing oxygenases: cytochrome P450, secondary amine monooxygenase, heme oxygenase, prostaglandin H synthase, indoleamine 2,3-dioxygenase, and tryptophan 2,3 dioxygenase. The structures of postulated reactive oxygen species for these oxygenases (except for prostaglandin H synthase) vary from ferryl−oxo porphyrin π-cation radical to ferric−peroxide (or hydroperoxide) to ferrous−dioxygen complex (A, B, and C, respectively, in Figure 47). The P450 enzymes contain a cysteine proximal heme ligand while the rest are histidine-ligated. The active site structures of four P450 isoforms and prostaglandin H synthase have been established by X-ray crystallography. The special role of cysteine as an electron-releasing factor in the activation of dioxygen to generate the oxo−iron high-valent reactive oxygen intermediate in the P450 enzymes has been discussed. Much less is known about the mechanism of oxygen activation by secondary amine monooxygenase while heme oxygenase has been proposed to incorporate oxygen in the first step of heme catabolism via a mechanism involving the nucleophilic porphyrin meso carbon and the electrophilic distal oxygen of a ferric−hydroperoxide intermediate. The deprotonated form (ferric−peroxide) of such an intermediate has also been

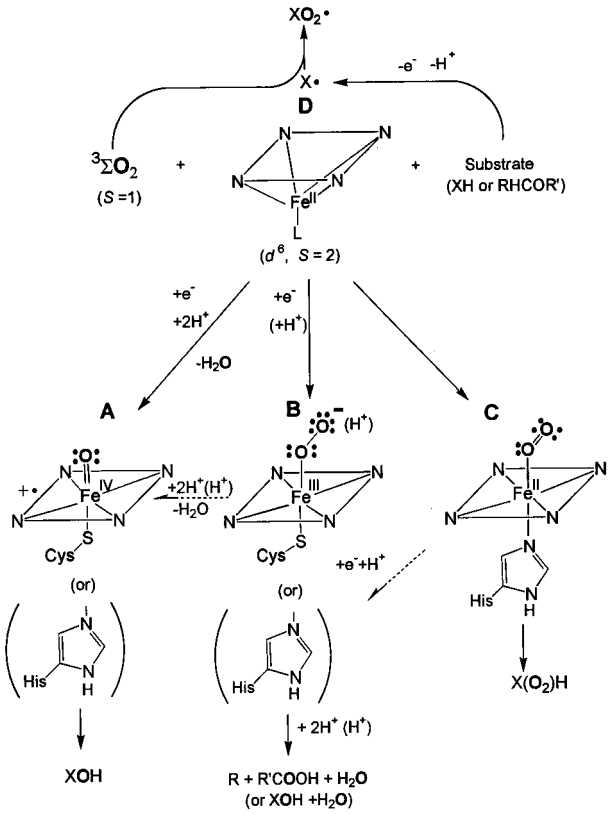

Figure 47. Schematic summary of the postulated structures of heme iron-coordinated active oxygen species (A, B, C) resulting from dioxygen activation by various oxygenases discussed in this review. These active oxygen species (A, B) are generated by ligation of ground-state dioxygen ($^3\Sigma O_2$) (diradical) to deoxyferrous heme (d^6, S = 2) to form the ferrous−dioxygen complex (C), followed by its one-electron reduction. Heterolytic cleavage of the O−O bond of the ferric−hydroperoxide (B with H^+) accompanied with proton uptake leads to the ferryl−oxo porphyrin π-cation radical species (A). The oxygen atom(s) of the dioxygen incorporated into the substrate (XH or RH_2COR') or water is (are) shown by bold-faced circles. Shown at the top (D) is the case where substrate is one-electron oxidized by the enzyme (e.g., PGHS) to a radical ($X^\bullet$), which nonenzymatically combines with the ground-state dioxygen (a diradical) to form a dioxygenated substrate−peroxy radical ($XO_2^\bullet$).

proposed as the active nucleophilic oxygen form in three C−C bond-cleaving P450 lyases. Prostaglandin H synthase, on the other hand, does not even form a metal−dioxygen complex and instead activates the substrate (one-electron oxidizes to it radical form, D in Figure 47) for oxygen addition. Finally, the reactive oxygen form of indoleamine and tryptophan dioxygenases is considered to be the ferrous−dioxygen adduct which can directly incorporate both dioxygen atoms by an ionic mechanism in forming oxygenated products.

The various mechanisms through which these enzymes accomplish their oxygenation reactions are testament to the reactive versatility of the heme prosthetic group. The ubiquitous involvement of dioxygen in the biosynthesis or transformation of steroids, prostaglandins, amino acids, and other biomolecules and in the metabolism and breakdown of drugs and other xenobiotics adds significance to understanding how heme-containing oxygenase enzymes function and how the structures of their active sites relate to their functions as detailed herein.

VIII. Abbreviations

EPR	electron paramagnetic resonance
EXAFS	extended X-ray absorption fine structure
Heme	iron protoporphyrin IX (heme *b*)
HO	heme oxygenase
IDO	indoleamine 2,3-dioxygenase
MCD	magnetic circular dichroism
NHE	normal hydrogen electrode
NMR	nuclear magnetic resonance
P450	cytochrome P450
P450-2B1	rat liver microsomal cytochrome P450
P450-2B4	rabbit liver microsomal cytochrome P450
P450-2C11	rat liver microsomal P450
P450-BM3	fatty acid-hydroxylating P450 from *Bacillus megaterium*
P450-CAM	camphor-hydroxylating P450 from *Pseudomonas putida*
P450-eyrf	macrolide-hydroxylating P450 from *Saccaropolyspora erythraea*
P450-NOR	nitric oxide-reducing P450 from *Fusarium oxysporum*
P450-SCC	cholesterol side chain-cleaving P450
P450-TERP	α-terpineol-oxidizing P450 from *Pseudomonas spheroides*
PGG_2	prostaglandin G_2
PGH_2	prostaglandin H_2
PGHS	prostaglandin H synthase
PGI_2	prostacyclin
SAMO	secondary amine monooxygenase
SCE	standard calomel electrode
TDO	tryptophan 2,3-diooxygenase
Trp	tryptophan
TXA_2	thromboxane A_2

IX. Acknowledgments

We thank Professors Masao Ikeda-Saito and Paul Ortiz de Montellano for helpful discussions concerning heme oxygenase and for conveying results from their laboratories prior to publication. Research on heme-containing oxygenases in the Dawson laboratory have been supported through grants from the NIH and NSF. M.S. also thanks Professor Osamu Hayaishi for the initial opportunity to work on indoleamine 2,3-dioxygenase, Professor Robert S. Phillips for the substituted tryptophans, Dr. Susan G. Cady for her contribution to the dioxygenase studies, and the NIH for financial support for the major portion of the studies on the dioxygenase cited in this review. J.H.D. expresses his great appreciation to Professor Harry Gray for the warm hospitality extended to him during a sabbatical leave spent at CalTech while this review was written. Finally, we thank the other members of the Dawson research group for their assistance in the preparation of this review: Zanna Beharry, Jennifer Cheek, Issa Isaac, Bill Kemnitzer, Mary Lamcyzk, Amy Ledbetter, and Alycen Pond.

References

(1) (a) Ingraham, L. L.; Meyer, D. L. *Biochemistry of Dioxygen*; Plenum: New York, 1985. (b) Traylor, T. G.; Traylor, P. S. In *Active Oxygen in Biochemistry*; Valentine, J. S., Foote, C. S., Liebman, J., Greenberg, A., Eds.; Blackie, Academic & Professional: Glasgow, U.K., 1995; pp 84-187. (c) Valentine, J. S. In *Bioinorganic Chemistry*; Bertini, I., Gray, H. B., Lippard, S. J., Valentine, J. S., Eds.; University Science Books: Mill Valley, CA, 1994; pp 253−313. (d) Wood, P. M. *Trends Biochem. Sci.* **1987**, *12*, 250.
(2) Hamilton, G. A. In *Molecular Mechanisms of Oxygen Activation*; Hayaishi, O., Ed.; Academic: New York, 1974; Chapter 10, pp 405−451.
(3) Halliwell, B.; Gutteridge, J. M. C. *Biochem. J.* **1984**, *219*, 1.
(4) Kemal, C.; Chan, T. W.; Bruice, T. C. *J. Am. Chem. Soc.* **1977**, *99*, 7272.
(5) Mason, H. S.; Fawlks, W.; Peterson, J. *J. Am. Chem. Soc.* **1955**, *77*, 2914.
(6) Hayaishi, O.; Katagiri, M.; Rothberg, S. *J. Am. Chem. Soc.* **1955**, *77*, 5450.
(7) Hayaishi, O. In: ref 2, Chapter 1, pp 1−28.
(8) (a) Jones, R. D.; Summerville, D. A.; Basolo, F. *Chem. Rev.* **1979**, *79*, 139. (b) Summerville, D. A.; Jones, R. D.; Hoffman, B. M.; Basolo, F. *J. Chem. Educ.* **1979**, *56*, 157. (c) Drago, R. S.; Cordon, B. B. *Acc. Chem. Res.* **1980**, *13*, 353. (d) Momenteau, M.; Reed, C. A. *Chem. Rev.* **1994**, *94*, 659.
(9) (a) Dawson, J. H.; Sono, M. *Chem. Rev.* **1987**, *87*, 1255. (b) Dawson, J. H. *Science* **1988**, *240*, 433.
(10) Nebert, D. W.; Gonzalez, F. J. *Annu. Rev. Biochem.* **1987**, *56*, 945.
(11) (a) Guengerich, F. P.; Macdonald, T. L. *FASEB J.* **1990**, *4*, 2453. (b) Guengerich, F. P.; Macdonald, T. L. *Adv. Electron Transfer Chem.* **1993**, *3*, 191.
(12) Porter, T. D.; Coon, M. J. *J. Biol. Chem.* **1991**, *266*, 13469.
(13) White, R. E. *Pharmacol. Ther.* **1991**, *49*, 21.
(14) Watanabe, Y.; Groves, J. T. *Enzymes* **1992**, *20*, 405.
(15) *Cytochrome P450: Structure, Mechanism, and Biochemistry*, 2nd ed.; Ortiz de Montellano, P. R., Ed.; Plenum: New York, 1995.
(16) Groves, J. T.; Han, Y.-Z. In: ref 15, Chapter 1, pp 3-48.
(17) Marnett, L. J.; Kennedy, T. A. In: ref 15, Chapter 2, pp 49−80.
(18) Mueller, E. J.; Loida, P. J.; Sligar, S. G. In: ref 15, Chapter 3, pp 83−124.
(19) Poulos, T. L.; Cupp-Vickery, J.; Li, H. In: ref 15, Chapter 4, pp 125−150.
(20) Peterson, J. A.; Graham-Lorence, S. E. In: ref 15, Chapter 5, pp 151−180.
(21) Ortiz de Montellano, P. R. In: ref 15, Chapter 8, pp 245−303.
(22) Capedvila, J. H.; Zeldin, D.; Makita, K.; Karara, A.; Falck, J. R. In: ref 15, Chapter 13, pp 443−472.
(23) Guengerich, F. P. In: ref 15, Chapter 14, pp 473−536.
(24) Mansuy, D.; Renaud, J-P. In: ref 15, Chapter 15, pp 537−574.
(25) Garfinkel, D. *Arch. Biochem. Biophys.* **1958**, *77*, 493.
(26) Klingenberg, *Arch. Biochem. Biophys.* **1958**, *75*, 376.
(27) Omura, T.; Sato, R. *J. Biol. Chem.* **1964**, *239*, 2370.
(28) Mason, H, S.; North, J. C.; Vanneste, M. *Fed. Proc., Fed. Am. Soc. Exp. Biol.* **1965**, 1172.
(29) Estabrook, R. W.; Cooper, D. Y.; Rosenthal, O. *Biochem. Z.* **1963**, *338*, 741.
(30) (a) Nelson, D. R. In: ref 15, Chapter 16, pp 575−606. (b) Nebert, D. W.; Nelson, D. R.; Adesnik, M.; Coon, M. J.; Estabrook, R. W.; Gonzalez, F. J.; Guengerich, F. P.; Gunsalus, I. C.; Johnson, E. F.; Kemper, B.; Levin, W.; Phillips, I. R.; Sato, R.; Waterman, M. R. *DNA* **1989**, *8*, 1.
(31) Guengerich, F. P. *Cancer Res.* **1988**, *48*, 2946.
(32) White, R. E.; Coon, M. J. *Annu. Rev. Biochem.* **1980**, *49*, 315.
(33) Gunsalus, I. C.; Meeks, J. R.; Lipscomb, J. D.; Debrunner, P.; Münck, E. In: ref 2, Chapter 14, pp 559−613.
(34) (a) Poulos, T. L.; Finzel, B. C.; Howard, A. J. *J. Mol. Biol.* **1987**, *195*, 687. (b) Poulos, T. L. *Adv. Inorg. Biochem.* **1988**, *7*, 1. (c) Poulos, T. L. *Curr. Opinion Struct. Biol.* **1995**, *5*, 767. (d) Poulos, T. L.; Finzel, B. C.; Gunsalus, I. C.; Wagner, G. C.; Kraut, J. *J. Biol. Chem.* **1985**, *260*, 16122.
(35) Fulco, A. J. *Annu. Rev. Pharmacol. Toxicol.* **1991**, *31*, 177.
(36) Ravichandran, K. G.; Boddupalli, S. S.; Haserman, C. A.; Peterson, J. A.; Deisenhofer, J. *Science* **1993**, *261*, 731.
(37) Haseman, C. A.; Ravichandran, K. G.; Peterson, J. A.; Deisenhofer, J. *J. Mol. Biol.* **1994**, *236*, 1169.
(38) Cupp-Vickery, J.; Poulos, T. L. *Nat. Struct. Biol.* **1995**, *2*, 144.
(39) (a) Brewer, C. B.; Peterson, J. A. *J. Biol. Chem.* **1988**, *263*, 791. (b) Pederson, T. C.;Austin, R. H.; Gunsalus, I. C. In *Microsomes and Drug Oxidations*; Ullrich, V., Roots, I., Hildebrandt, A., Estabrook, R. W., Conney, A. H., Eds.; Pergamon Press: Oxford, England, 1977; pp 275−283.
(40) Loida, P. J.; Sligar, S. G. *Biochemistry* **1993**, *32*, 11530.
(41) Kadkhodayan, S.; Coulter, E. D.; Maryniak, D. M.; Bryson, T. A.; Dawson, J. H. *J. Biol. Chem.* **1995**, *270*, 28042.
(42) Ullrich, V. *Top. Curr. Chem.* **1979**, *83*, 67.
(43) Raag, R.; Poulos, T. L. In *Frontiers in Biotransformation*; Ruckpaul, K., Rein, H., Eds.; Akademie Verlag: Berlin, 1992; Chapter 1, pp 1−43.
(44) Dawson, J. H.; Holm, R. H.; Trudell, J. R.; Barth, G.; Linder, R. E.; Bunnenberg, E.; Djerassi, C.; Tang, S. C. *J. Am. Chem. Soc.* **1976**, *98*, 3707.
(45) Sono, M.; Andersson, L. A.; Dawson, J. H. *J. Biol. Chem.* **1982**, *257*, 8308.
(46) Sono, M.; Dawson, J. H. *J. Biol. Chem.* **1982**, *257*, 5496.
(47) Liu, H. I.; Sono, M.; Kadkhodayan, S.; Hager, L. P.; Hedman, B.; Hodgson, K. O.; Dawson, J. H. *J. Biol. Chem.* **1995**, *270*, 10544.
(48) (a) Adachi, S.; Nagano, S.; Ishimori, K.; Watanabe, Y.; Morishima, I.; Egawa, T.; Kitagawa, T.; Makino, R. *Biochemistry* **1993**, *32*, 241. (b) Higuchi, T.; Shimada, K.; Maruyama, N.; Hirobe, M. *J. Am. Chem. Soc.* **1993**, *115*, 7551.

(49) (a) Gerber, N. C.; Sligar, S. G. *J. Am. Chem. Soc.* **1992**, *114*, 8742. (b) Gerber, N, C.; Sligar, S. G. *J. Biol. Chem.* **1994**, *269*, 4260.

(50) (a) Imai, M.; Shimada, H.; Watanabe, Y.; Matsushima-Hibiya, Y.; Makino, R.; Koga, H.; Horiguchi, T.; Ishimura, Y. *Proc. Natl. Acad. Sci. U.S.A.* **1989**, *86*, 7823. (b) Martinis, S. A.; Atkins, W. M.; Stayton, P. S.; Sligar, S. G. *J. Am. Chem. Soc.* **1989**, *111*, 9252.

(51) Yoem, H.; Sligar, S. G.; Li, H.; Poulos, T. L.; Fulco, A. J. *Biochemistry* **1995**, *34*, 14733.

(52) (a) Kimata, Y.; Shimada, H.; Hirose, T.; Ishimura, Y. *Biochem. Biophys. Res. Commum.* **1995**, *208*,96. (b) Shimada, H.; Kimata, Y.; Hirose, T.; Kanamori, Y.; Toba, Y.; Ishimura, Y. *Abstracts of Papers*, 9th International Conference on Cytochrome P450 Biochemistry, Biophysics and Molecular Biology, Zurich, Switzerland, 1995; Pmec-16.

(53) For mammalian P450 enzymes, mutation of the corresponding Thr residue to Ala yielded various results depending on the isoforms; an increased turnover number and decreased uncoupling [Thr319 in rat $P450_d$(1A2): Ishigooka, M.; Shimizu, T.; Hiroya, K.; Hatano, M. *Biochemistry* **1992**, *31*, 1528] or changes in substrate recognition [Thr301 in rabbit $P450_{3a}$(2E1): Fukuda, T.; Imai, Y.; Komori, M.; Nakamura, M.; Kusunose, E.; Satouchi, K.; Kusunose, M. *FEBS Lett.* **1992**, *312*, 252.].

(54) (a) Shimada, H.; Makino, R.; Imai, M.; Horiuchi, T.; Ishimura, Y. In *International Symposium on Oxygenases and Oxygen Activation*; Nozaki, M., Yamamoto, S., Ishimura, Y., Eds.; Yamada Science Foundation: Tokyo, 1990; pp 133−136. (b) Shimada, H.; Makino, R.; Unno, M.; Horiuchi, T.; Ishimura, Y. In *Cytochrome P450. The 8th International Conference*; Lechner, M. C., Ed.; John Libbey Eurotext: Paris, 1994; pp 299−306.

(55) (a) Groves, J. T.; Haushalter, R. C.; Nakamura, M.; Nemo, T. E.; Evans, B. J. *J. Am. Chem. Soc.* **1981**, *103*, 2884. (b) Groves, J. T. *J. Chem. Educ.* **1985**, *62*, 928.

(56) Guengerich, F. P.; Ballou, D. P.; Coon, M. J. *Biochem. Biophys. Res. Commun.* **1976**, *70*, 951

(57) (a) Blake, R. C.; Coon, M. J. *J. Biol. Chem.* **1980**, *255*, 4100. (b) Blake, R. C.; Coon, M. J. *J. Biol. Chem.* **1981**, *256*, 5755.

(58) (a) Kobayashi, K.; Amano, M.; Kanbara, Y.; Hayashi, K. *J. Biol. Chem.* **1987**, *262*, 5445. (b) Kobayashi, K.; Iwamoto, T.; Honda, K. *Biochem. Biophys. Res. Commun.* **1994**, *201*, 1348. (c) Davydov, R.; Kappl, R.; Hütterman, J.; Peterson, J. A. *FEBS Lett.* **1991**, *295*, 113.

(59) Tajima, K.; Edo, T.; Isuzu, K.; Imaoka, S.; Funae, Y.; Oka, S.; Sakurai, H. *Biochem. Biophys. Res. Commun.* **1993**, *191*, 157.

(60) Egawa, T.; Shimada, H.; Ishimura, Y. *Biochem. Biophys. Res. Commun.* **1994**, *201*, 1464.

(61) Wagner, G. C.; Palcic, M. M.; Dunford, H. B. *FEBS Lett.* **1983**, *156*, 244.

(62) Palcic, M. M.; Rutter, R.; Araiso, T.; Hager, L. P.; Dunford, H. B. *Biochem. Biophys. Res. Commun.* **1980**, *94*, 1123.

(63) Hager, L. P.; Hollenberg, P. F.; Rand-Meir, T.; Chaing, R.; Doubek, D. *Ann. N.Y. Acad. Sci.* **1975**, *244*, 80.

(64) Sundaramoorthy, M.; Terner, J.; Poulos, T. L. *Structure* **1995**, *3*, 1367.

(65) Ortiz de Montellano, P. R. *Annu. Rev. Pharmacol. Toxicol.* **1992**, *32*, 89.

(66) McCarthy, M. B.; White, R. E. *J. Biol. Chem.* **1983**, *258*, 9153.

(67) Loew, G. H.; Kert, C. J.; Hjelmeland, L. M.; Kirchner, R. F. *J. Am. Chem. Soc.* **1977**, *99*, 3534.

(68) (a) McMahon, R. E.; Sullivan, H. R.; Craig, J. C.; Pereira, W. E. *Arch. Biochem. Biophys.* **1969**, *132*, 575. (b) Hamberg, M.; Bjorkhem, I. *J. Biol. Chem.* **1971**, *246*, 7411. (c) Shapiro, S.; Piper, J. U.; Caspi, E. *J. Am. Chem. Soc.* **1982**, *104*, 2301.

(69) Daly, J. *Handb. Exp. Pharmacol.* **1971**, *28*, 285.

(70) Hjelmeland, L. M.; Aronow, L.; Trudell, J. R.; *Biochem. Biophys. Res. Commun.* **1977**, *76*, 541.

(71) Groves, J. T.; McClusky, G. A.; White, R. E.; Coon, M. J. *Biochem. Biophys. Res. Commun.* **1978**, *81*, 154.

(72) Dawson, J. H.; Eble, K. S. *Adv. Inorg. Bioinorg. Mech.* **1986**, *4*, 1.

(73) Gelb, M. H.; Heimbrook, D. C.; Mälkönen, P.; Sligar, S. G. *Biochemistry* **1982**, *21*, 370.

(74) Groves, J. T.; Subramanian, D. V. *J. Am. Chem. Soc.* **1984**, *106*, 2177.

(75) White, R. E.; Miller, J. P.; Favreau, L. V.; Bhattacharyya, A. *J. Am. Chem. Soc.* **1986**, *108*, 6024.

(76) Miwa, G. T.; Walsh, J. S.; Lu, A. Y. *J. Biol. Chem.* **1984**, *259*, 3000.

(77) White, R. E.; Groves, J. T.; McClusky, G. A. *Acta Biol. Med. Ger.* **1979**, *38*, 475.

(78) (a) Ortiz de Montellano, P. R.; Stearns, R. A. *J. Am. Chem. Soc.* **1987**, *109*, 3415. (b) Ortiz de Montellano, P. R. *Trends Pharmacol. Sci.* **1989**, *10*, 354.

(79) Bowry, V. W.; Lusztyk, J.; Ingold, K. U. *J. Am. Chem. Soc.* **1991**, *113*, 5687.

(80) (a) Griller, D.; Ingold, K. U. *Acc. Chem. Res.* **1980**, *13*, 317. (b) Newcomb, M. *Tetrahedron* **1993**, *49*, 1151.

(81) Atkinson, J. K.; Ingold, K. U. *Biochemistry* **1993**, *32*, 9209.

(82) Atkinson, J. K.; Hollenberg, P. F.; Ingold, K. U.; Johnson, C. C.; Tadic, M.-H. L.; Newcomb, M.; Putt, D. A. *Biochemistry* **1994**, *33*, 10630.

(83) Newcomb, M.; Le-Tadic, M.-H.; Putt, D. A.; Hollenberg, P. F. *J. Am. Chem. Soc.* **1995**, *117*, 3312.

(84) Newcomb, M.; Le-Tadic-Biadatti, M.-H.; Chestney, D. L.; Roberts, E. S.; Hollenberg, P. F. *J. Am. Chem. Soc.* **1995**, *117*, 12085.

(85) Wiberg, K. B.; Shobe, D.; Nelson, G. L. *J. Am. Chem. Soc.* **1993**, *115*, 10645.

(86) Bach, R. D.; Mintcheva, I.; Estévez, C. M.; Schlegel, H. B. *J. Am. Chem. Soc.* **1995**, *117*, 10121.

(87) In a strict sense, the k_{OH} value should probably be calculated without including the cation-derived product (**22**, Figure 13), to be $\sim 1.3 \times 10^{13}$ s and the lifetime ($t_{1/2}$) of the radical **15** should be calculated by $t_{1/2} = \ln 2/k_{OH}$ ($= 0.693/k_{OH}$) to be 53 fs rather than by $1/k_{OH}$. However, the contribution of the cation-derived product to the calculated k_{OH} value and of the small calculation error (ln 2 vs 1) to the $t_{1/2}$ value are quite small. Thus, the theoretical interpretations of the results by Newcomb et al.[84] for the radical mechanism are not significantly affected.

(88) Watabe, T.; Akamatsu, K. *Biochem. Pharmacol.* **1974**, *23*, 1079.

(89) Ortiz de Montellano, P. R.; Mangold, B. L. K.; Wheeler, C.; Kunze, K. L.; Reich, N. O. *J. Biol. Chem.* **1983**, *258*, 4202.

(90) Ostovic, D.; Bruice, T. C. *Acc. Chem. Res.* **1992**, *25*, 314.

(91) Ortiz de Montellano, P. R.; Correia, M. A. In: ref 15, Chapter 9, pp 305−364.

(92) Henschler, D.; Hoos, W. R.; Retz, H.; Dallmeier, E.; Metzler, M. *Biochem. Pharmacol.* **1979**, *28*, 543.

(93) Miller, R. E.; Guengerich, F. P. *Biochemistry* **1982**, *21*, 1090.

(94) Liebler, D. C.; Guengerich, F. P. *Biochemistry* **1983**, *22*, 5482.

(95) Miller, V. P.; Fruetel, J. A.; Ortiz de Montellano, P. R. *Arch. Biochem. Biophys.* **1992**, *298*, 697.

(96) Bruice, T. C.; Castellino, A. J. *J. Am. Chem. Soc.* **1988**, *110*, 7512.

(97) MacDonald, T. L.; Gutheim, W. G.; Martin, R. B.; Guengerich, F. P. *Biochemistry* **1989**, *28*, 2071.

(98) Groves. J. T.; Avaria-Neisser, G. E.; Fish, K. M.; Imachi, M.; Kuczkowski, R. L. *J. Am. Chem. Soc.* **1986**, *108*, 3837.

(99) Gross, Z.; Nimri, S. *J. Am. Chem. Soc.* **1995**, *117*, 8021.

(100) Jerina, D. M.; Daly, J. W. *Science* **1974**, *185*, 573.

(101) Cavalieri, E. L.; Rogan, E. G. *Pharmacol. Ther.* **1992**, *55*, 183.

(102) Cavalieri, E. L.; Rogan, E. G.; Devanesan, P. D.; Cremonesi, P.; Cerny, R. L.; Gross, M. L.; Bodell, W. J. *Biochemistry* **1990**, *29*, 4820.

(103) Rogan, E. G.; Devanesan, P. D.; RamaKrishna, N. V. S.; Higginbotham, S.; Padmavathi, N. S.; Chapman, K.; Cavalieri, E. L.; Jeong, H.; Jankowiak, R.; Small, G. J. *Chem. Res. Toxicol.* **1993**, *6*, 356.

(104) Burka, L. T.; Plucinski, T. M.; MacDonald, T. L. *Proc. Natl. Acad. Sci. U.S.A.* **1983**, *80*, 6680.

(105) Korzekwa, K. R.; Swinney, D. C.; Trager, W. F. *Biochemistry* **1989**, *28*, 9019.

(106) McMahon, R. E.; Culp, H. W.; Occolowiz, J. C. *J. Am. Chem. Soc.* **1969**, *91*, 3389.

(107) Parli, C. J.; Wang, N.; McMahon, R. E. *Biochem. Biophys. Res. Commun.* **1971**, *43*, 1204.

(108) McMahon, R. E.; Culp, H. W.; Craig, J. C. *J. Med. Chem.* **1979**, *22*, 1100.

(109) Kurebayashi, H. *Arch. Biochem. Biophys.* **1989**, *270*, 320.

(110) Shea, J. P.; Valentine, G. L.; Nelson, S. D. *Biochem. Biophys. Res. Commun.* **1982**, *109*, 231.

(111) Kedderis, G. L.; Dwyer, L. A.; Rickert, D. E.; Hollenberg, P. F. *Mol. Pharmacol.* **1983**, *758*, 760.

(112) Hollenberg, P. F. *FASEB J.* **1992**, *6*, 686.

(113) Guengerich, F. P.; Okazaki, O.; Seto, Y.; Macdonald, T. L. *Xenobiotica* **1995**, *7*, 689−709.

(114) Guengerich, F. P.; Müller-Enoch, D.; Blair, I. A. *Mol. Pharmacol.* **1986**, *261*, 5051.

(115) Seto, Y.; Guengerich, F. P. *J. Biol. Chem.* **1993**, *268*, 9986.

(116) (a) Watanabe, Y.; Iyanagi, T.; Oae, S. *Tetrahedron Lett.* **1982**, *23*, 533. (b) Watanabe, Y.; Oae, S.; Iyanagi, T. *Bull. Chem. Soc. Jpn.* **1982**, *55*, 188.

(117) Miwa, G. T.; Garland, W. A.; Hodshon, B. J.; Lu, A. Y. H.; Northrop, D. B. *J. Biol. Chem.* **1980**, *255*, 6049.

(118) Dinnocenzo, J. P.; Karki, S. B.; Jones, J. P. *J. Am. Chem. Soc.* **1993**, *115*, 7111.

(119) Karki, S. B.; Dinnocenzo, J. P.; Jones, J. P.; Korzekwa, K. R. *J. Am. Chem. Soc.* **1995**, *117*, 3657.

(120) Karki, S. B.; Dinnocenzo, J. P. *Xenobiotica* **1995**, *25*, 711.

(121) Griller, D.; Howard, J. A.; Marriott, P. R.; Scaiano, J. C. *J. Am. Chem. Soc.* **1981**, *103*, 619.

(122) Dinnocenzo, J. P.; Banach, T. E. *J. Am. Chem. Soc.* **1989**, *111*, 8646.

(123) Macdonald, T. L.; Zirvi, K.; Burka, L. T.; Peyman, P.; Guengerich, F. P. *J. Am. Chem. Soc.* **1982**, *104*, 2050.

(124) Hanzlik, R. P.; Tullman, R. H. *J. Am. Chem. Soc.* **1982**, *104*, 2048.

(125) (a) Ortiz de Montellano, P. R.; Beilan, H. S.; Kunze, K. L. *J. Biol. Chem.* **1981**, *256*, 6708. (b) Augusto, O.; Beilan, H. S.; Ortiz de Montellano, P. R. *J. Biol. Chem.* **1982**, *257*, 11288.

(126) Guengerich, F. P.; Martin, M. V.; Beaune, P. H.; Kremers, P.; Wolff, T.; Waxman, D. J. *J. Biol. Chem.* **1986**, *261*, 5051.

(127) Guengerich, F. P.; Böcker, R. H. *J. Biol. Chem.* **1988**, *263*, 8168.
(128) Lee, W. A.; Calderwood, T. S.; Bruice, T. C. *Proc. Natl. Acad. Sci. U.S.A.* **1985**, *82*, 4301.
(129) Groves, J. T.; Gilbert, J. A. *Inorg. Chem.* **1986**, *25*, 123.
(130) Hayashi, Y.; Yamazaki, I. *J. Biol. Chem.* **1979**, *254*, 9101.
(131) Vaz, A. D.; Coon, M. J. *Biochemistry* **1994**, *33*, 6442.
(132) (a) Watanabe, K.; Narimatsu, S.; Yamamoto, I.; Yoshimura, H. *J. Biol. Chem.* **1991**, *266*, 2709. (b) Watanabe, K.; Matsunaga, T.; Narimatsu, S.; Yamamoto, I.; Yoshimura, H. *Biochem. Biophys. Res. Commun.* **1992**, *188*, 114.
(133) Song, W. C.; Baertschi, S. W.; Boeglin, W. E.; Harris, T. M.; Brash, A. R. *J. Biol. Chem.* **1993**, *268*, 6293−6298.
(134) Vaz, A. D.; Roberts, E. S.; Coon, M. J. *Proc. Natl. Acad. Sci. U.S.A.* **1990**, *87*, 5499.
(135) Sugiura, M.; Iwasaki, K.; Kato, R. *Mol. Pharmacol.* **1976**, *12*, 322.
(136) (a) Kato, R.; Iwasaki, K.; Shiraga, T.; Noguchi, H. *Biochem. Biophys. Res. Commun.* **1976**, *70*, 681. (b) Yamazoe, Y.; Sugiura, M.; Kimataki, T.; Kato, R. *FEBS Lett.* **1978**, *88*, 337.
(137) Hernandez, P. H.; Mazel, P.; Gillette, J. R. *Biochem. Pharmacol.* **1967**, *16*, 1877.
(138) (a) Shoun, H.; Tanimoto, T. *J. Biol. Chem.* **1991**, *266*, 11078. (b) Nakahara, K.; Tanimoto, T.; Hatano, K.; Usuda, K.; Shoun, H. *J. Biol. Chem.* **1993**, *268*, 8350. (c) Shiro, Y.; Kato, M.; Iizuka, T.; Nakahara, K.; Shoun, H. *Biochemistry* **1994**, *33*, 11420. (d) Shiro, Y.; Fujii, M.; Isogai, Y.; Adachi, S.; Iizuka, T.; Obayashi, E.; Makino, R.; Nakahara, K.; Shoun, H. *Biochemistry* **1995**, *34*, 11420. (e) Shiro, Y.; Fujii, M.; Iizuka, T.; Adachi, S.; Tsukamoto, K.; Nakahara, K.; Shoun, H. *J. Biol. Chem.* **1995**, *270*, 1617.
(139) Nakahara, K.; Shoun, H.; Adachi, S.; Iizuka, T.; Shiro, Y. *J. Mol. Biol.* **1994**, *239*, 158.
(140) Hecker, M.; Ullrich, V. *J. Biol. Chem.* **1989**, *264*, 141.
(141) Byron, C.-Y.; Gut, M. *Biochem. Biophys. Res. Commun.* **1980**, *94*, 549.
(142) Burstein, S.; Middleditch, B. S.; Gut, M. *J. Biol. Chem.* **1975**, *250*, 9028.
(143) (a) Mak, A. Y.; Swinney, D. C. *J. Am. Chem. Soc.* **1992**, *114*, 8309. (b) Swinney, D. C.; Mak, A. Y. *Biochemistry* **1994**, *33*, 2185.
(144) Akhtar, M.; Corina, D. L.; Miller, S. L.; Shyadehi, A. Z.; Wright, J. N. *Biochemistry* **1994**, *33*, 4410.
(145) (a) Akhtar, M.; Calder, M. R.; Corina, D. L.; Wright, J. N. *Biochem. J.* **1982**, *201*, 569. (b) Akhtar, M.; Njar, V. C. O.; Wright, J. N. *J. Steroid Biochem. Mol. Biol.* **1993**, *44*, 375.
(146) (a) Townsley, J. D.; Broodie, H. J. *Biochemistry* **1968**, *7*, 33. (b) Fishman, J.; Guzik, H.; Dixon, D. *Biochemistry* **1969**, *8*, 4304. (c) Fishman, J.; Raju, M. S. *J. Biol. Chem.* **1981**, *256*, 4472.
(147) Cole, P. A.; Robinson, C. H. *J. Am. Chem. Soc.* **1988**, *110*, 1284.
(148) Vaz, A. D. N.; Roberts, E. S.; Coon, M. J. *J. Am. Chem. Soc.* **1991**, *113*, 5886.
(149) Roberts, E. S.; Vaz, A. D. N.; Coon, M. J. *Proc. Natl. Acad. Sci. U.S.A.* **1991**, *88*, 8963.
(150) Vaz, A. D. N.; Kessell, K. J.; Coon, M. J. *Biochemistry* **1994**, *33*, 13651.
(151) Korzekwa, K. R.; Trager, W. F.; Mancewicz, J.; Osawa, Y. *J. Steroid Biochem. Mol. Biol.* **1993**, *44*, 367.
(152) Ahmed. S.; Davis, P. J. *Bioorg. Med. Chem. Lett.* **1995**, *5*, 2789.
(153) Watanabe, Y.; Takehira, K.; Shimizu, M.; Harakawa, T.; Orita, H. *J. Chem. Soc. Chem. Commun.* **1990**, 927.
(154) Selke, M.; Sisemore, M. F.; Valentine, J. S. *J. Am. Chem. Soc.* **1996**, *118*, 2008.
(155) Gibbons, G. F.; Goad, L. J.; Goodwin, T. W. *J. Chem. Soc. Chem. Commun.* **1968**, 1458.
(156) Ramm. P. J.; Caspi, E. *J. Biol. Chem.* **1969**, *244*, 6064.
(157) Akhtar, M.; Rahimtula, A. D.; Watkinson, I. A.; Wilton, D. C.; Munday, K. A. *Eur. J. Biochem.* **1969**, *9*, 107.
(158) Fischer, R. T.; Trzaskos, J. M., Magollda, R. L.; Lo, S. S.; Brosz, C. S.; Larsen, B. *J. Biol. Chem.* **1991**, *266*, 6124.
(159) Marletta, M. A. *J. Biol. Chem.* **1993**, *268*, 12231.
(160) Bredt, D. S.; Snyder, S. H. *Annu. Rev. Biochem.* **1994**, *63*, 175.
(161) Masters, B. S. S. *Annu. Rev. Nutr.* **1994**, *14*, 131.
(162) Griffith, O. W.; Stuehr, D. J. *Annu. Rev. Physiol.* **1995**, *57*, 707.
(163) Reference deleted in proofs.
(164) Nelson, S. D.; Pearson, P. G. *Ann. Rev. Pharmacol. Toxicol.* **1990**, *30*, 169.
(165) Phillips, D. H. *Nature* **1983**, *303*, 468.
(166) Maugh, T. H. II. *Science* **1974**, *183*, 940.
(167) Essigmann, J. M.; Croy, R. G.; Nadzan, A. M.; Busby, W. F., Jr.; Reinhold, V, N.; Büchi, G.; Wogan, G. N. *Proc. Natl. Acad. Sci. U.S.A.* **1977**, *74*, 1870.
(168) Miller, E. C.; Miller, J. A. *Pharmacol. Rev.* **1966**, *18*, 805.
(169) Rettie, A. E.; Rettenmeier, A. W.; Howald, W. N.; Baillie, T. A. *Science* **1987**, *235*, 890.
(170) Eady, R. R.; Large, P. J. *Biochem. J.* **1969**, *111*, 37.
(171) Eady, R. R.; Jarman, T. R.; Large, P. J. *Biochem. J.* **1971**, *125*, 449.
(172) Jarman, T. R.; Large, P. J. *Biochem. Biophys. Res. Commun.* **1972**, *49*, 740.
(173) Alberta, J. A.; Dawson, J. H. *J. Biol. Chem.* **1987**, *262*, 11857.
(174) Brook, D. F.; Large, P. J. *Eur. J. Biochem.* **1975**, *55*, 601.
(175) Miwa, G. T.; Garland, W. A.; Hadson, B. J.; Lu, A. Y. H.; Northrup, D. B. *J. Biol. Chem.* **1980**, *255*, 6049.
(176) Alberta, J. A.; Andersson, L. A.; Dawson, J. H. *J. Biol. Chem.* **1989**, *264*, 20467.
(177) Antonini, E.; Brunori, M. *Hemoglobin and Myoglobin in their Reactions with Ligands*; North Holland: Amsterdam, 1971.
(178) Gunsalus, I. C.; Wagner, G. C. *Methods Enzymol.* **1978**, *52*, 166.
(179) Dawson, J. H.; Dooley, D. M. In *Iron Porphyrins Part 3*; Lever, A. B. P., Gray, H. B., Eds.; VCH: New York, 1989.
(180) Peisach, J.; Blumberg, W. E.; Ogawa, S.; Rachmilewitz, E. A.; Oltzik, R. J. *J. Biol. Chem.* **1971**, *246*, 3342.
(181) Helke, G. A.; Ingram, D. J. E.; Slade, E. F. *Proc. R. Soc. London B Biol. Sci.* **1968**, *169*, 275.
(182) Peisach, J.; Blumberg, W. E.; Adler, A. D. *Ann. N.Y. Acad. Sci.* **1970**, *206*, 310.
(183) Blumberg, W. E.; Peisach, J. *J. Adv. Chem. Ser.* **1971**, *No. 100*, 271.
(184) Walker, F. A.; Reis, D.; Balke, V. L. *J. Am Chem. Soc.* **1984**, *106*, 6888.
(185) Alberta, J. A. Purification and Characterization of Secondary Amine Monooxygenase. Ph.D. Thesis, University of South Carolina, Columbia, SC, 1986.
(186) Hollenberg, P. F.; Hager, L. P.; Blumberg, W. E.; Peisach, J. *J. Biol. Chem.* **1980**, *255*, 4801.
(187) Blumberg, W. E.; Peisach, J. In *Probes of Structure and Function of Macromolecules and Membranes*; Chance, B., Yonetani, T., Mildvan, A. S., Eds.; Academic: New York, 1971; Vol. 2, pp 215−229; as cited in ref 187.
(188) Svastis, E. W.; Dawson, J. H. *Inorg. Chim. Acta* **1986**, *123*, 83.
(189) Ozols, J.; Strittmatter, P. *J. Biol. Chem.* **1964**, *239*, 1018.
(190) Hawkins, B. K.; Dawson, J. H. *J. Am Chem. Soc.* **1992**, *114*, 3547.
(191) Miwa, G. T.; Walsh, J. S.; Kedderis, G. L.; Hollenberg, P. F. *J. Biol. Chem.* **1983**, *258*, 14445.
(192) Wilks, A.; Torpey, J.; Ortiz de Montellano, P. R. *J. Biol. Chem.* **1994**, *269*, 29553.
(193) Roach, M. P.; Dawson, J. H., unpublished data.
(194) Anni, H.; Yonetani, T. *Met. Ions Biol. Syst.* **1992**, *239*, 1018.
(195) Tenhunen, R.; Marver, H. S.; Schmid, R. *Proc. Natl. Acad. Sci. U.S.A.* **1968**, *61*, 748.
(196) Tenhunen, R.; Marver, H. S.; Schmid, R. *J. Biol. Chem.* **1969**, *244*, 6388.
(197) O'Carra, P. In *Porphyrins and Metalloporphyrins*; Smith, K. M., Ed.; Elsevier: Amsterdam, 1975; Chapter 4, p 123.
(198) Kikuchi, G.; Yoshida, T. *Mol. Cell Biol.* **1983**, *53*, 163.
(199) Maines, M. D. *FASEB J.* **1988**, *2*, 2557.
(200) Yoshida, T.; Kikuchi, G. *J. Biol. Chem.* **1979**, *254*, 4487.
(201) Bonkovsky, H. L.; Healy, J. F.; Pohl, J. *Eur. J. Biochem.* **1990**, *189*, 155.
(202) Yoshinaga, T.; Sassa, S.; Kappas, A. *J. Biol. Chem.* **1982**, *257*, 7778.
(203) Yoshida, T.; Kikuchi, G. *J. Biol. Chem.* **1978**, *253*, 4224.
(204) Maines, M. D.; Trakshel, G. M.; Kutty, R. K. *J. Biol. Chem.* **1986**, *261*, 411.
(205) Muller, R. M.; Taguchi, H.; Shibahara, S. *J. Biol. Chem.* **1987**, *262*, 6795.
(206) Cruse, I.; Maines, M. D. *J. Biol. Chem.* **1988**, *263*, 3348.
(207) Brune, B.; Ullrich, V. *Mol. Pharmacol.* **1987**, *32*, 497.
(208) Verma, A.; Hirsch,D. J.; Glatt, C. E.; Ronnett, G. V.; Snyder, S. H. *Science* **1993**, *259*, 381.
(209) Yoshida, T.; Noguchi, M.; Kikuchi, G. *J. Biol. Chem.* **1980**, *255*, 4418.
(210) Ishikawa, K.; Sato, M.; Ito, M.; Yoshida, T. *Biochem. Biophys. Res. Commun.* **1992**, 981.
(211) Wilks, A.; Ortiz de Montellano, P. R. *J. Biol. Chem.* **1993**, *268*, 22357.
(212) Wilks, A.; Black, S. M.; Miller, W. L.; Ortiz de Montellano, P. R. *Biochemistry* **1995**, *34*, 4421.
(213) McCoubrey,W. K.; Jr.; Maines, M. D. *Arch. Biochem. Biophys.* **1993**, *302*, 402.
(214) Sun, J.; Wilks, A.; Ortiz de Montellano, P. R.; Loehr, T. M. *Biochemistry* **1993**, *32*, 14151.
(215) Takahashi, S.; Wang, J.; Rousseau, D. L.; Ishikawa, K.; Yoshida, T.; Host, J.R.; Ikeda-Saito, M. *J. Biol. Chem.* **1994**, *269*, 1010.
(216) Teraoka, J.; Kitagawa, T. *J. Biol. Chem.* **1981**, *256*, 3969.
(217) Smulevich, G.; Mauro, J. M.; Fishel, L. A.; English, A. M.; Kraut, J.; Spiro, T. G. *Biochemistry* **1988**, *27*, 5477.
(218) Hawkins, B. K.; Wilks, A.; Powers, L. S.; Ortiz de Montellano, P. R.; Dawson, J. H. *Biochim. Biophys. Acta* **1996**, *1295*, 165.
(219) Yonetani, T.; Yamanoto, H.; Erman, J.; Leigh, J. S.; Reed, G. H. *J. Biol. Chem.* **1972**, *247*, 2447.
(220) Takahashi, S.; Wang, J.; Rousseau, D. L.; Ishikawa, K.; Yoshida, T.; Takeuchi, N.; Ikeda-Saito, M. *Biochemistry* **1994**, *33*, 5531.
(221) Powers, L.; Sinclair, R.; Chance, B.; Reddy, K. S.; Yamazaki, I. In *Synchrotron Radiation in the Biosciences;* Chance, B., Deisenhofer, J., Ebashi, S., Goodhead, D., Helliwell, J., Huxley, H., Iizuka, T., Kirz, J., Mitsui, T., Runbenstein, E., Sakabe, N., Sasaki, T., Schmahl, G., Stuhrmann, H., Wuthrich, K., Zaccai, G., Eds.; Oxford University: New York, 1994; p 247.
(222) Sun, J.; Loehr, T. M.; Wilks, A.; Ortiz de Montellano, P. R. *Biochemistry* **1994**, *33*, 13734.
(223) Ito-Maki, M.; Ishikawa, K.; Mansfield Matera, K.; Sato, M.; Ikeda-Saito, M.; Yoshida, T. *Arch. Biochem. Biophys.* **1995**, *317*, 253.

(224) Wilks, A.; Sun, J.; Loehr, T. M.; Ortiz de Montellano, P. R. *J. Am Chem. Soc.* **1995**, *117*, 2925.
(225) Hernández, G.; Wilks, A.; Paolesse, R.; Smith, K. M.; Ortiz de Montellano, P. R.; La Mar, G. N. *Biochemistry* **1994**, *33*, 6631.
(226) Frydman, R. B.; Frydman, B. *Acc. Chem. Res.* **1987**, *20*, 250.
(227) Takahashi, S.; Ishikawa, K.; Takeuchi, N.; Ikeda-Saito, M.; Yoshida, T.; Rousseau, D. L. *J. Am. Chem. Soc.* **1995**, *117*, 6002.
(228) Wilks, A.; Ortiz de Montellano, P. R.; Sun, J.; Loehr, T. M. *Biochemistry* **1996**, *35*, 930.
(229) Bonnett, R.; Dimsdale, M. J., *J. Chem. Soc. Perkin Trans.* **1972**, *I*, 2540.
(230) Meunier, B. *Chem Rev.* **1992**, *92*, 1411.
(231) King, N. K.; Winfield, M. E. *J. Biol. Chem.* **1963**, *238*, 1520.
(232) Yonetani, T.; Schleyer, H. *J. Biol. Chem.* **1967**, *242*, 1974.
(233) Hewson, W. D.; Hager, L. P. In *The Porphyrins*; Dolphin, D., Ed.; Academic Press: New York, 1979; Vol. 7, pp 295−332.
(234) Mansfield Matera, K.; Takahashi, S.; Fujii, H.; Hong, Z.; Ishikawa, K.; Yoshimura, T.; Rousseau, D. L.; Yoshida, T.; Ikeda-Saito, M. *J. Biol. Chem.* **1996**, *271*, 6618.
(235) Ortiz de Montellano, P. R., personal communication.
(236) Ikeda-Saito, M.; Hori, H.; Andersson, L. A.; Prince, R. C.; Pickering, I. J.; George, G. N.; Sanders, C. R., II; Lutz, L.; McKelvey, E. J.; Mattera, R. *J. Biol. Chem.* **1992**, *267*, 22843.
(237) Bogumil, R.; Maurus, R.; Hildebrand, D. P.; Brayer, G. D.; Mauk, G. *Biochemistry* **1995**, *34*, 10483.
(238) Fujii, H. Studies on the Electronic Structure and Reactivities of Catalytic Intermediates in Heme Enzymes Ph.D. Thesis, Kyoto University, Kyoto, Japan, 1990; as cited in ref 234.
(239) Morishima, I.; Fujii, H.; Shiro, Y.; Sano, S. *Inorg. Chem.* **1995**, *34*, 1528.
(240) Sano, S.; Sano, T.; Morishima, I.; Shiro, Y.; Maeda, Y. *Proc. Natl. Acad. Sci. U.S.A.*. **1986**, *83*, 531.
(241) Isogai, Y.; Iizuka, T.; Shiro, Y. *J. Biol. Chem.* **1995**, *270*, 7853.
(242) Smith, W. L.; Marnett, L. J.; DeWitt, D. L. *Pharmacol. Ther.* **1991**, *49*, 153.
(243) Marnett, L. J.; Maddipati, K. R. In *Peroxidases in Chemistry and Biology*; Everse, J., Everse, K. E., Grisham, M. B., Eds.; CRC Press: Boca Ranton, FL, 1991; Vol. 1, p 293.
(244) Smith, W. L.; Marnett, L. J. *Biochim. Biophys. Acta* **1991**, *1083*, 1.
(245) Sono, M.; Dawson, J. H. In *Encyclopedia of Inorganic Chemistry*; King, R. B., Ed.;Wiley: New York, 1994; Vol. 4, p 1661.
(246) Hemler, M. E.; Lands, W. E. M. *J. Biol. Chem.* **1980**, *255*, 6253.
(247) Miyamoto, T.; Ogino, N.; Yamamoto, S.; Hayashi, O. *J. Biol. Chem.* **1976**, *251*, 2626.
(248) Hemler, M.; Lands, W. E. M.; Smith, W. L. *J. Biol. Chem.* **1976**, *251*, 5575.
(249) Ruf, H. H.; Schuhn, D.; Nastainczyk, W. *FEBS Lett.* **1984**, *165*, 293.
(250) Kulmacz, R. J.; Lands, W. E. M. *J. Biol. Chem.* **1984**, *259*, 6358.
(251) Lambeir, A.-M.; Markey, C. M.; Dunford, H. B.; Marnett, L. J. *J. Biol. Chem.* **1985**, *260*, 14894.
(252) Karthein, R.; Nastainczyk, W.; Ruf, H. H. *Eur. J. Biochem.* **1987**, *166*, 173.
(253) (a) Kulmacz, R. J.; Tsai, A.-L.; Palmer, G. *J. Biol. Chem.* **1987**, *262*, 10524. (b) Tsai, A.-L.; Kulmacz, R. J.; Wang, J.-S.; Wang, Y.; Van Wart, H. E.; Palmer, G. *J. Biol. Chem.* **1993**, *268*, 8554.
(254) Picot, D.; Loll, P. J.; Garavito, M. *Nature* **1994**, *367*, 243.
(255) Karthein, R.; Dietz, R.; Nastainczyk, W.; Ruf, H. H. *Eur. J. Biochem.* **1988**, *171*, 313.
(256) Hamberg, M.; Samuelsson, B. *J. Biol. Chem.* **1967**, *242*, 5336.
(257) Mancini, J. A.; Riendeau, D.; Falgueyret, J.-P.; Vickers, P. J.; O'Neill, G. P. *J. Biol. Chem.* **1995**, *270*, 29372.
(258) Mizuno, K.; Yamamoto, S.; Lands, W. E. M. *Prostaglandins* **1982**, *23*, 743.
(259) DeWitt, D. L.; El-Harith, E. A.; Kraemer, S. A.; Andrews, M. J.; Yao, E. F.; Armstrong, R. L.; Smith, W. L. *J. Biol. Chem.* **1990**, *265*, 5192.
(260) Hsuanyu, Y.; Dunford, H. B. *J. Biol. Chem.* **1992**, *267*, 17649.
(261) Plè, P.; Marnett, L. J. *J. Biol. Chem.* **1989**, *264*, 13983.
(262) Dunford, H. B.; Stillman, J. S. *Coord. Chem. Rev.* **1976**, *19*, 187.
(263) Dietz, R.; Nastainczyk, W.; Ruf, H. H. *Eur. J. Biochem.* **1988**, *171*, 321.
(264) Bosshard, H. R.; Anni, H.; Yonetani, T. In *Peroxidases in Chemistry and Biology*; Everse, J., Everse, K. E., Grisham, M. B., Eds.; CRC Press: Boca Ranton, FL, 1991; Vol. 2, p 51.
(265) Sivaraja, M.; Goodin, D. B.; Smith, M.; Hoffmann, B. M. *Science* **1989**, *245*, 738.
(266) Pendleton, R. B.; Lands, W. E. M. In *Eicosanoids and Other Bioactive Lipids in Cancer and Radiation Injury*; Honn, K. V., Marnett, L. J., Nigam, S., Walden, T., Eds.; Kluwer Academic Publishing: Norwell, MA, 1991; p 209.
(267) Sjöberg, B.-M.; Reichard, P.; Grasland, A.; Ehrenberg, A. *J. Biol. Chem.* **1978**, *253*, 6863.
(268) Sjöberg, B.-M.; Reichard, P.; Grasland, A.; Ehrenberg, A. *J. Biol. Chem.* **1977**, *252*, 536.
(269) Graslund, A.; Sahlin, M.; Sjöberg, B.-M. *Environ. Health Perspect.* **1985**, *64*, 139.
(270) Smith, W. L.; Eling, T. E.; Kulmacz, R. J.; Marnett, L. J. Tsai, A.-L. *Biochemistry* **1992**, *31*, 3.
(271) Kulmacz, R. J.; Ren, Y.; Tsai, A. -L.; Palmer, G. *Biochemistry* **1990**, *29*, 8760.
(272) Tsai, A.-L; Palmer, G.; Kulmacz, R. J. *J. Biol. Chem.* **1992**, *267*, 17753.
(273) Tsai, A.-L.; Hsi, L. C.; Kulmacz, R. J.; Palmer, G.; Smith, W. L. *J. Biol. Chem.* **1994**, *269*, 3085.
(274) Bakovic, M.; Dunford, H. B. *Biochemistry* **1994**, *33*, 6475.
(275) Wei, C.; Kulmacz, R. J.; Tsai, A.-L. *Biochemistry* **1995**, *34*, 8499.
(276) Bakovic, M.; Dunford, H. B. *J. Biol. Chem.* **1996**, *271*, 2048.
(277) Kulmacz, R. J.; Pendleton, R. B.; Lands, W. E. M. *J. Biol. Chem.* **1994**, *269*, 5527.
(278) (a) Lassmann, G.; Odenwaller, R.; Curtis, J. F.; DeGray, J. A.; Mason, R. P.; Marnett, L. J.; Eling, T. E. *J. Biol. Chem.* **1991**, *266*, 20045. (b) Ogino, N.; Ohki, S.; Yamamoto, S.; Hayashi, O. *J. Biol. Chem.* **1978**, *253*, 5061. (c) Yonetani, T.; Asakura, T. *J. Biol. Chem.* **1969**, *244*, 4580. (d) Hori, H.; Ikeda-Saito, M.; Yonetani, T. *Biochim. Biophys. Acta* **1987,** *912*, 74. (e) Nick, R. J.; Ray, G. B.; Fish, K. M.; Spiro, T. G.; Groves, J. T. *J. Am. Chem. Soc.* **1991**, *113*, 1838.
(279) (a) Mason, R. P.; Kalyanaraman, B.; Tainer, B. E.; Eling, T. E. *J. Biol. Chem.* **1986**, *255*, 5019. (b) Schreiber, J.; Eling, T. E.; Mason, R. P. *Arch. Biochem. Biophys.* **1986**, *249*, 126.
(280) Tsai, A.-L.; Kulmacz, R. J.; Palmer. *J. Biol. Chem.* **1995**, *270*, 10503.
(281) Hayaishi, O. *J. Biochem. (Tokyo)* **1976**, *79*, 13.
(282) Hayaishi, O.; Takikawa, O.; Yoshida, R. *Prog. Inorg. Chem.* **1990**, *38*, 75.
(283) Feigelson, O.; Brady, F. O. In: ref 2, Chapter 3, pp 87−133.
(284) Kotake, Y.; Masayama, T. *Z. Physiol. Chem.* **1936**, *243*, 237.
(285) (a) Higuchi, K.; Kuno, S.; Hayaishi, O. *Arch. Biochem. Biophys.* **1967**, *120*, 397. (b) Yamamoto, S.; Hayaishi, O. *J. Biol. Chem.* **1967**, *242*, 5260.
(286) Hirata, F.; Hayaishi, O. *Biochem. Biophys. Res. Commun.* **1972**, *47*, 1112.
(287) Shimizu, T.; Nomiyama, S.; Hirata, F.; Hayaishi, O. *J. Biol. Chem.* **1978**, *253*, 4700.
(288) Tone, S.; Takikawa, O.; Habara-Ohkubo, A.; Kadoya, A.; Yoshida, R.; Kido, R. *Nucleic Acids Res.* **1990**, *18*, 367.
(289) Maezono, K.; Tashiro, K.; Nakamura, T. *Biochem. Biophys. Res. Commun.* **1990**, *170*, 176.
(290) Ishimura, Y.; Makino, R.; Ueno, R.; Sakaguchi, K.; Brady, F. O.; Feigelson, P.; Aisen, P.; Hayaishi, O. *J. Biol. Chem.* **1980**, *255*, 3835.
(291) Watababe, Y.; Fujiwara, M.; Yoshida, R.; Hayaishi, O. *Biochem. J.* **1980**, *189*, 393.
(292) Makino, R.; Iizuka, T.; Sakaguchi, K.; Ishimura, Y. In *Oxygenases and Oxygen Metabolism*; Nozaki, M., Yamamoto, S., Ishimura, Y., Coon, M. J., Ernster, L., Estabrook, R. W., Eds.; Academic Press: New York, 1980; pp 467−477.
(293) Sono, M. *Biochemistry* **1989**, *28*, 5400.
(294) Takikawa, O.; Kuroiwa, T.; Yamazaki, F.; Kido, R. *J. Biol. Chem.* **1988**, *263*, 2041.
(295) Ozaki, Y.; Nichol, C. A.; Duch, D. S. *Arch. Biochem. Biophys.* **1987**, *257*, 207.
(296) Dai, W.; Gupta, S. L. *Biochem. Biophys. Res. Commun.* **1990**, *168*, 1.
(297) Haraba-Ohkubo, A.; Takikawa, O.; Yoshida, R. *Gene* **1991**, *105*, 221.
(298) Pfefferkorn, E. R.; Rebhum, S.; Eckel, M. *J. Interferon Res.* **1986**, *6*, 267.
(299) Carlin, J. M.; Ozaki, Y.; Byrne, G. I.; Brown, R. R.; Borden, E. C. *Experientia* **1989**, *45*, 535.
(300) Heyes, M. P.; Saito, K.; Jacobowitz, D.; Markey, S. P.; Takikawa, O.; Vickers, J. H. *FASEB J.* **1992**, *6*, 2977.
(301) Christen, S.; Peterhans, E.; Stocker, R. *Proc. Natl. Acad. Sci. U.S.A.* **1978**, *75*, 3998.
(302) Hirata, F.; Ohnishi, T.; Hayaishi, O. *J. Biol. Chem.* **1977**, *252*, 4637.
(303) Taniguchi, T.; Sono, M.; Hirata, F.; Hayaishi, O.; Tamura, M.; Hayashi, K.; Iizuka, T.; Ishimura, Y. *J. Biol. Chem.* **1979**, *254*, 3288.
(304) Kobayashi, K.; Hayashi, K.; Sono, M. *J. Biol. Chem.* **1989**, *264*, 15280.
(305) (a) Shimizu, N.; Kobayashi, K.; Hayashi, K. *Biochim. Biophys. Acta* **1989**, *995*, 133. (b) Shimizu, N.; Kobayashi, K.; Hayashi, K. *J. Biol. Chem.* **1984**, *259*, 4414.
(306) Ilan, Y. A.; Rabani, J.; Czapski, G. *Biochim. Biophys. Acta* **1976**, *446*, 277.
(307) Sutton, H. L.; Roberts, P. B.; Winterbourn, C. C. *Biochem. J.* **1976**, *155*, 503.
(308) Debey, P.; Land, E. J.; Santus, R.; Swallow, A. J. *Biochem. Biophys. Res. Commun.* **1979**, *86*, 953.
(309) Taniguchi, T.; Hirata, F.; Hayaishi, O. *J. Biol. Chem.* **1977**, *252*, 2774.
(310) Sono, M. *J. Biol. Chem.* **1989**. *264*, 1616.
(311) Chance, B.; Sies, H.; Boveris, A. *Physiol. Rev.* **1979**, *59*, 527.
(312) Fridovich, I. *Annu. Rev. Pharmacol. Toxicol.* **1983**, *23*, 239.
(313) Badwey, J. A.; Karnovsky, M. L. *Annu. Rev. Biochem.* **1980**, *49*, 695.
(314) Chanock,S. J.; Benna, J. EI.; Smith, R. M.; Babior, B. M. *J. Biol. Chem.* **1994**. *269*, 24519.

(315) Sono, M.; Taniguchi, T.; Watanabe, Y.; Hayaishi, O. *J. Biol. Chem*. **1980**, *255*, 1339.
(316) Ishimura, Y.; Nozaki, M.; Hayaishi, O.; Nakamura, T.; Tamura, M.; Yamazaki, I. *J. Biol. Chem*. **1970**, *245*, 3693.
(317) Uchida, K. Shimizu, T.; Makino, R.; Sakaguchi, K.; Iizuka, T.; Ishimura, Y.; Nozawa, T.; Hatano, M. *J. Biol. Chem*. **1983**, *258*, 2519.
(318) Sono, M.; Dawson, J. H. *Biochim. Biophys. Acta* **1984**, *789*, 170.
(319) Henry, Y.; Ishimura, Y.; Peisach, J. *J. Biol. Chem*. **1976**, *251*, 1578.
(320) Makino, R.; Sakaguchi, K.; Iizuka, T.; Ishimura, Y. *J. Biol. Chem*. **1980**, *255*, 11883.
(321) Morishima, I. In ref 292, pp 479−484.
(322) Sono, M. *Biochemistry* **1990**, *29*, 1451.
(323) Sono, M. *Biochemistry* **1986**, *25*, 6089.
(324) Cady, S. G.; Sono, M. *Arch. Biochem. Biophys*. **1991**, *291*, 326.
(325) Saito, I.; Matsuura, T.; Nakagawa, M.; Hino, T. *Acc. Chem. Res*. **1977**, *10*, 346.
(326) Cady, S. G. Effects of Tryptophan Analogs on the Catalytic Activity and Binding Activity of Indoleamine 2,3-Dioxygenase. Ph.D. Thesis, University of South Carolina, Columbia, SC, 1989.
(327) Sono, M.; Cady, S. G., unpublished data.
(328) Yagil, G. *Tetrahedron* **1967**, *23*, 2855.
(329) Leeds, J. M.; Brown, P. J.; McGeehan, G. M.; Brown, F. K.; Wiseman, J. S. *J. Biol. Chem*. **1993**, *268*, 17781.
(330) (a) Que, L., Jr. *J. Chem. Educ*. **1985**, *62*, 938. (b) Arciero, D. M.; Lipscomb, J. D. *J. Biol. Chem*. **1986**, *261*, 2170.
(331) Vanneste, W. H.; Zuberbühler, A. In: ref 2, Chapter 9, pp 371−404.
(332) (a) Feig, A. L.; Lippard, S. J. *Chem. Rev*. **1994**, *94*, 759. (b) Wallar, B. J.; Lipscomb, J. D. *Chem. Rev*., **1996**, *96*, 2625 (this issue).
(333) Hamilton, G. A. *Adv. Enzymol*. **1969**, *32*, 55.
(334) Nakagawa, M.; Watanabe, H.; Kodata, S.; Okajima, H.; Hino, T.; Flippen, J. L.; Witkop, B. *Proc. Natl. Acad. Sci. U.S.A*. **1977**, *74*, 4730.
(335) Fraser, M. S.; Hamilton, G. A. *J. Am. Chem. Soc*. **1982**, *104*, 4203.
(336) Muto, S.; Bruice, T. C. *J. Am. Chem. Soc*. **1980**, *102*, 7379.
(337) DeFelippis, M. R.; Murthy, C. P.; Faraggi, M.; Klapper, M. H. *Biochemistry* **1989**, *28*, 4847.
(338) Tsang, P. K. S.; Sawyer, D. T. *Inorg. Chem*. **1990**, *29*, 2848.
(339) Nishinaga, A.; Ohara, H.; Tomita, H.; Matsuura, T. *Tetrahedron Lett*. **1983**, *24*, 213.
(340) Uchida, K.; Soda, M.; Naito, S.; Ohnishi, T.; Tamaru, K. *Chem. Lett*. **1978**, 471.
(341) Dufour, M. N.; Crumbliss, A. L.; Johnston, G.; Gaudemer, A. *J. Mol. Catal*. **1980**, *7*, 277.
(342) Ohkubo, K.; Sagawa, T.; Ishida, H. *Inorg. Chem*. **1992**, *31*, 2682.
(343) Yoshida, Z.; Sugimoto, H.; Ogoshi, H. In *Biomimetic Chemistry*, Advances in Chemistry Series, No. 191; Dolphin, D., McKenna, C., Murakami, Y., Tabushi, I., Eds.; American Chemical Society: Washington, DC, 1980; pp 307−326.
(344) Tajima, K.; Yoshino, M.; Mikami, K.; Edo, T.; Ishizu, K.; Ohya-Nishiguchi, H. *Inorg. Chim. Acta* **1990**, *172*, 83.

CR9500500